



LIBRARY  
Michigan State  
University

This is to certify that the  
thesis entitled

CATALYTIC HYDROGENATION OF 2,5-PIPERAZINEDIONE TO  
PIPERAZINE

presented by

Andrea Sue Molengraft

has been accepted towards fulfillment  
of the requirements for the

M.S. degree in Chemistry

  
Major Professor's Signature

28 April 2006  
Date

*MSU is an Affirmative Action/Equal Opportunity Institution*

**PLACE IN RETURN BOX** to remove this checkout from your record.  
**TO AVOID FINES** return on or before date due.  
**MAY BE RECALLED** with earlier due date if requested.

DATE DUE	DATE DUE	DATE DUE

**CATALYTIC HYDROGENATION OF 2,5-PIPERAZINEDIONE TO PIPERAZINE**

**By**

**Andrea Sue Molengraft**

**A THESIS**

**Submitted to  
Michigan State University  
in partial fulfillment of the requirements  
for the degree of**

**MASTER OF SCIENCE**

**Department of Chemistry**

**2006**



## ABSTRACT

### CATALYTIC HYDROGENATION OF 2,5-PIPERAZINEDIONE TO PIPERAZINE

By

Andrea Sue Molengraft

Catalytic hydrogenation of nearly all the carbonyl functional groups is well established and widely practiced with one exception: the amide moiety. Stable, ubiquitous in nature, and easily synthesized, amides' value as chemical intermediates would increase if a general, practical catalytic hydrogenation which preserved the C-N bond were available. As an underutilized biomass fraction, proteinaceous substrates are a particular interesting class of polyamides to explore; the resulting amine products could have a wide variety of potential applications as pH adjusters, surfactants, detergent additives, metal ion scavengers, or chiral building blocks for pharmaceutical synthesis. Water, the native environment of peptidic materials, presents any hydrogenation must compete with C-N cleavage via hydrolysis. We aimed to develop '*green*' selective heterogeneous aqueous-phase catalytic amide reduction. The cyclic anhydride of glycine, 2,5-piperazinedione, was used as a model peptidic amide substrate. The reaction was optimized using a systematic experimental design, the Box-Behnken model. At optimal conditions (1800 psi H<sub>2</sub>, 90°C, 3 g 5% Ru/C), 2,5-piperazinedione was reduced to 37% piperazine at 24 hrs. Glycylglycine, glycine and ethanolamine formed in 10, 1 and 2% yield, respectively. Development of this '*green*' process, and the formation of polyamido and polyamino alcohol polymers from polypeptides opens the door to chemical upgrading of new renewables-based feedstock fraction, the proteinaceous component, for economical production of value-added products.

**To Mom and Dad**

## **ACKNOWLEDGMENTS**

I would like to express my gratitude to my major professor, Dr. James Jackson, for his knowledge and support throughout my studies at Michigan State University.

I am also grateful to my committee members for their prolonged support. I would like to acknowledge Dr. Dennis Miller for all his support and enthusiasm for this project, especially for his guidance with the project, use of the equipment in his laboratory, and help with data analyses and interpretation. Thank you to Drs. Baker and Walker for their support and interest of this project and serving as committee members. I also want to express my thanks to Drs. Simona Marincean and Mikhail Redko for their guidance in the laboratory as well. I would also like to thank past and present colleagues in my laboratory, for all their support in the lab.

## TABLE OF CONTENTS

<b>LIST OF FIGURES .....</b>	<b>vii</b>
<b>LIST OF TABLES .....</b>	<b>x</b>
<b>INTRODUCTION .....</b>	<b>1</b>
<b>CHAPTER ONE LITERATURE REVIEW .....</b>	<b>4</b>
1.1 Carboxamide Group.....	4
1.2 Amide Reactivity .....	5
1.2.1 Classical amide reduction using complex metal hydrides .....	7
1.2.1.1 LiAlH <sub>4</sub> .....	8
1.2.1.2 BH <sub>3</sub> .....	10
1.2.1.3 NaBH <sub>4</sub> .....	14
1.2.2 Catalytic Hydrogenation .....	24
1.2.2.1 Mechanisms for Catalytic Hydrogenation .....	30
1.2.2.2 Bimetallic Catalyst Systems .....	32
1.3 Relevant Laboratory Studies.....	36
1.3.1 Catalytic Hydrogenation of Amino Acids .....	36
1.3.1.1 L-Alanine .....	36
1.3.1.2 Glycylglycine.....	37
1.3.1.2.1 Hydrolysis of Glycylglycine .....	40
<b>CHAPTER TWO ANALYTICAL METHOD DEVELOPMENT.....</b>	<b>42</b>
2.1 Introduction.....	42
2.2 Experimental Procedures .....	44
2.2.1 Materials .....	44
2.2.2 Methods.....	45
2.3 Results & Discussion .....	46
<b>CHAPTER THREE.....</b>	<b>50</b>
<b>CATALYTIC HYDROGENATION OF AMIDES TO AMINES .....</b>	<b>50</b>
3.1 Introduction.....	50
3.2 Experimental Procedures .....	55
3.2.1 Materials .....	55
3.2.2 Methods.....	56
3.3 Results & Discussion .....	58
3.3.1 Box-Behnken Model.....	58
3.3.1.1 Effect of Temperature .....	59
3.3.1.2 Effect of Pressure.....	60

3.3.1.3 Effect of Catalyst Loading.....	60
3.3.2 Beyond the Boundaries of Box-Behnken Model .....	73
3.3.3 Control Experiments .....	79
3.3.4 Reaction pathways for 2,5-piperazinedione hydrogenation to piperazine .....	85
<b>CHAPTER FOUR.....</b>	<b>92</b>
<b>SUMMARY AND CONCLUSIONS .....</b>	<b>92</b>
<b>CHAPTER FIVE .....</b>	<b>93</b>
<b>FUTURE RESEARCH.....</b>	<b>93</b>
<b>LIST OF REFERENCES .....</b>	<b>95</b>

## LIST OF FIGURES

Figure 1.1 Resonance structures of amide .....	4
Figure 1.2 Mechanism of amide reduction with a metal (M) hydride .....	5
Figure 1.3 Possible hydrogenolysis sites .....	6
Figure 1.4 Hydrogenolysis of an amide forming an amine and water .....	6
Figure 1.5 Hydrogenolysis of the carbon-nitrogen bond of amides .....	6
Figure 1.6 Hydrolysis of an amide to a carboxylic acid and an amine under aqueous conditions .....	7
Figure 1.7 Secondary product formation from amide aminolysis or amine alkylation .....	7
Figure 1.8 Reduction of triisopropylamide and benzamide to a primary amine via a nitrile intermediate .....	9
Figure 1.9 Proposed mechanism of amide reduction to a nitrile with $\text{LiAlH}_4$ .....	9
Figure 1.10 Reduction of N,N-diethylpivalamide and N,N-diisopropylbenzamide to their corresponding amines with $\text{BH}_3/\text{THF}$ (0-25°C) .....	10
Figure 1.11 Amine yields from amide reduction with $\text{BH}_3/\text{THF}$ (0-25°C) .....	11
Figure 1.12 Relative rate of reduction of $\alpha$ substituted N,N-dimethylamides with $\text{BH}_3/\text{THF}$ (25°C) .....	11
Figure 1.13 Rate of reduction of N substituted N,N-dialkylbutyramides with $\text{BH}_3/\text{THF}$ at 25°C .....	12
Figure 1.14 Rates of reduction of substituted N,N-dimethylbenzamides with $\text{BH}_3/\text{THF}$ at 25°C .....	12
Figure 1.15 Representative selective amide reduction in the presence of an ester ( $\text{BH}_3/\text{THF}$ (0-25°C)) .....	13
Figure 1.16 Reduction of methyl hippurate with $\text{BH}_3/\text{THF}$ (0-25°C) .....	14
Figure 1.17 Proposed intermediate of the coordinate covalent bond of an ester oxygen with boron .....	14
Figure 1.18 Amine yield from the reduction of amides with $\text{NaBH}_3(\text{OCOR})$ in THF or dioxane .....	16
Figure 1.19 Thioamide reduction to an amine with $\text{Et}_3\text{O}^+\text{BF}_4^-/\text{CH}_2\text{Cl}_2$ and $\text{NaBH}_4/\text{MeOH}$ .....	16
Figure 1.20 Amine yields from the reduction of its thioamide with $\text{Et}_3\text{O}^+\text{BF}_4^-/\text{CH}_2\text{Cl}_2$ and $\text{NaBH}_4/\text{MeOH}$ .....	17
Figure 1.21 Reduction of an amide to an amine via direct formation of an imino ether fluoborate intermediate .....	18
Figure 1.22 Mechanism of reduction of imino ether fluoborate intermediate to an amine with $\text{BH}_4^-$ .....	18
Figure 1.23 Reaction sequence of an amide or lactam reduction to an amine via an imino derivative .....	19
Figure 1.24 Selective reduction of amides over olefin, nitrile and esters groups with 1) $\text{POCl}_3/\text{glyme}$ and 2) $\text{NaBH}_4/\text{EtOH}$ .....	19
Figure 1.25 Amine yields from their corresponding amide reduced with $\text{POCl}_3/\text{glyme}$ and $\text{NaBH}_4/\text{EtOH}$ .....	20
Figure 1.26 Amide reduction to an amine via a Vilsmeier intermediate .....	21
Figure 1.27 Lactam reduction to an amine with $\text{NaAlH}_2(\text{OCH}_2\text{CH}_2\text{OCH}_3)_2$ in benzene (100°C) .....	22

Figure 1.28 Amides reduced with $\text{NaBH}_4/\text{CoCl}_2$ in dioxane or methanol (100°C) .....	22
Figure 1.29 Proposed mechanism of amide reduction with $\text{NaBH}_4/\text{glyme}$ .....	23
Figure 1.30 Amides reduced using Na metal/ <i>n</i> -propanol .....	24
Figure 1.31 First reported hydrogenation of an amide by Mailhe .....	24
Figure 1.32 Hydrogenation of benzamide over Ni (1500 psi $\text{H}_2$ , 200°C) .....	25
Figure 1.33 Amides reduced over $2\text{CuO}\cdot\text{Cr}_2\text{O}_3/\text{dioxane}$ (1470-4400 psi $\text{H}_2$ , 175-250°C) .....	26
Figure 1.34 Ester reduction over $2\text{CuO}\cdot\text{Cr}_2\text{O}_3/\text{dioxane}$ (1470-4400 psi $\text{H}_2$ , 200-260°C) in the presence of an amide .....	28
Figure 1.35 Lactam hydrogenation over $2\text{CuO}\cdot\text{Cr}_2\text{O}_3/\text{dioxane}$ (1470-4400 psi $\text{H}_2$ , 200-260°C) .....	29
Figure 1.36 Hydrogenation of quinolones over $2\text{CuO}\cdot\text{Cr}_2\text{O}_3/\text{dioxane}$ (1470-4400 psi $\text{H}_2$ , 200-260°C) .....	29
Figure 1.37 Transalkylation of an amine with alcohol over $2\text{CuO}\cdot\text{Cr}_2\text{O}_3/\text{H}_2$ .....	30
Figure 1.38 Formation of ether and ammonia via an amino alcohol over $2\text{CuO}\cdot\text{Cr}_2\text{O}_3/\text{H}_2$ .....	30
Figure 1.39 Side reaction forming a secondary amine via an imine intermediate over $2\text{CuO}\cdot\text{Cr}_2\text{O}_3/\text{H}_2$ .....	31
Figure 1.40 Secondary amine formation via nitrile over $2\text{CuO}\cdot\text{Cr}_2\text{O}_3/\text{H}_2$ .....	31
Figure 1.41 Nitrile hydrogenation over Ni (R)/ $\text{NH}_3$ (125°C) to an amine .....	32
Figure 1.42 Transalkylation of tertiary amides with alcohols to form amines over copper-chromium barium oxide (I)/dioxane (4500-12000 psi $\text{H}_2$ , 250°C) .....	32
Figure 1.43 Proposed catalytic cycle of an amide reacting with dialkylsilane .....	35
Figure 1.44 Reaction pathway of L-alanine to L-alaninol hydrogenation .....	36
Figure 1.45 Catalytic hydrogenation of glycylglycine with $\text{H}_3\text{PO}_4/\text{H}_2\text{O}$ (1000 psi $\text{H}_2$ , 100°C, 1 g 5% Ru/C) .....	37
Figure 1.46 Catalytic hydrogenation (1000 psi $\text{H}_2$ , 100°C, 5% Ru/C) of glycylglycine ( $\text{ZnHPO}_4/\text{H}_2\text{O}$ ) and glycinamide ( $\text{Ca}(\text{H}_2\text{PO}_4)_2/\text{H}_2\text{O}$ ) .....	38
Figure 1.47 Catalytic hydrogenation of 2,5-piperazinedione with $\text{H}_3\text{PO}_4/\text{H}_2\text{O}$ (1000 psi $\text{H}_2$ , 100°C, 1 g 5% Ru/C) .....	39
Figure 1.48 Equilibrium between 2,5-piperazinedione and glycylglycine at 25°C .....	40
Figure 2.1 Amino acids and corresponding amines of interest .....	43
Figure 2.2 Sample chromatogram of amides, corresponding amines, and aminoalcohols .....	47
Figure 2.3 Sample Chromatogram of amino acid separation .....	49
Figure 3.1 Catalytic hydrogenation of glycylglycine and 2,5-piperazinedione with $\text{H}_3\text{PO}_4/\text{H}_2\text{O}$ (1000psi $\text{H}_2$ , 100°C, 1 g 5% Ru/C) .....	51
Figure 3.2 Possible reaction pathways of 2,5-piperazinedione .....	52
Figure 3.3 Box-Behnken Model .....	54
Figure 3.4 Regression analysis of predicted %yield versus experimental % yield .....	59
Figure 3.5 The effect of temperature (90, 110 and 130°C), on yield (A) and conversion (B) of piperazine from 2,5-piperazinedione at 1500 psi $\text{H}_2$ , 3 g 5% Ru/C .....	63
Figure 3.6 The effect of pressure (500, 1500, and 1800 psi $\text{H}_2$ ) on % yield of piperazine from 2,5-piperazinedione at 110°C, 3g 5% Ru/C .....	65
Figure 3.7 Product yields from the conversion of 2,5-piperazinedione at (A) 1000 (B) 1500 and (C) 1800 psi $\text{H}_2$ , 90°C, 3g 5% Ru/C .....	67

Figure 3.8 The effect of catalyst loading (A) 0.3 g, (B) 1 g, (C) 3 g 5% Ru/C on all product yields at 1500 psi H <sub>2</sub> , 130°C .....	69
Figure 3.9 The effect increased catalyst loading on product yields on from (A) 3 g 5% Ru/C to (B) 6 g 5% Ru/C at 1500 psi H <sub>2</sub> , 110°C .....	71
Figure 3.10 Representative chromatogram series of 2,5-piperazinedione hydrogenation to piperazine at 1800 psi H <sub>2</sub> , 90°C, 3 g 5% Ru/C .....	76
Figure 3.11 Effect of temperature on % yield at 1500 psi H <sub>2</sub> , 3 g 5% Ru/C .....	77
Figure 3.12 Effect of temperature on % yield at 1800 psi H <sub>2</sub> , 3 g 5% Ru/C .....	78
Figure 3.13 Product formation from control experiments .....	80
Figure 3.14 Change of pH over time from the conversion of 2,5-piperazinedione to piperazine at 1800 psi, 90°C, 3g 5% Ru/C.....	81
Figure 3.15 The effect of catalyst loading on initial % conversion of 2,5-piperazinedione at 1500 psi H <sub>2</sub> , 130°C, with 0.3, 1, and 3 g 5% Ru/C .....	83
Figure 3.16 The effect of catalyst loading on initial % conversion of 2,5-piperazinedione (0.1 and 0.05M) at 1500 psi H <sub>2</sub> , 110°C, with 3 and 6 g 5% Ru/C .....	83
Figure 3.17 Modeling of proposed mechanism for amide hydrogenation in gas phase and in solution.....	89
Figure 3.18 Predicted reaction pathways for hydrogenation of 2,5-piperazinedione .....	90
Figure 3.19 Predicted reaction pathways for hydrolysis of 2,5-piperazinedione .....	91



## LIST OF TABLES

Table 3.1 Percent yield of all products for the reduction of 2,5-piperazinedione at 6 hrs	62
Table 3.2 Percent yield of all products for the reduction of 2,5-piperazinedione at 24 hrs.	75

## INTRODUCTION

The amide functionality in organic chemistry is one of the more intriguing functional groups to work with, and must first be understood in order to discuss its reductions. This functional group's polarity, stability, and planar geometry are usually explained in terms of resonance delocalization of *pi* electrons among the amide's N, C, and O atoms. When not decorated with hydrophobic alkyl groups, amides can hydrogen bond as both donors and acceptors, enabling their diverse roles in biological structures and reactions. As for their reactivity, like most polar moieties, amides are both nucleophilic (at O or N) and electrophilic (at the carbonyl C).

In this study we illustrate a systematic experimental design to facilitate the catalytic hydrogenation of amides. Even though the primary methods of amide reduction are through the classic use of hydride reagents in organic solvents, later studies proved by catalytic hydrogenation was also effective. Traditional amide reductions using nucleophilic hydride donor reagents such as  $\text{LiAlH}_4$  in organic solvents exploit the latter reactivity, ultimately reducing the carbonyl center to a methylene via imine or iminium intermediate species. But another widely used amide reductant, the strong Lewis acid  $\text{BH}_3$ , exploits the amide's reactivity as a nucleophile. Though effective, these stoichiometric reactions have poor atom economy, form undesired byproducts, solvent and work-up waste. Even the few known catalytic reductions, mainly transition metal-based, involve reactive compounds that require handling in aprotic organic solvents, a setting that is not ideal for the amide's intrinsic hydrophilic nature.

This report describes work toward “green” reduction of amides. The “holy grail,”

direct aqueous-phase catalytic hydrogenation, would maximize atom economy by avoiding reagent and protecting group byproducts and by minimizing reaction steps and organic solvent streams. Such a process would offer new opportunities for agriculture via formation of value-added chemicals from underutilized crop byproducts. Specifically, after separation from the carbohydrate and oil fractions, a crop's peptide and protein fractions could serve as starting materials for substituted polyamido and polyamino alcohol polymers. Such compounds have a wide range of potential applications as pH adjusters, surfactants, detergent additives, metal ion scavengers, gas scrubbers, support materials, or chiral building blocks and auxiliaries for pharmaceutical synthesis.

Despite the challenges of working under aqueous conditions with amides, we believe a systematic, mechanistic study will extend our understanding of the carbonyl reduction and minimize the use of organic solvents. The cyclic dipeptide 2,5-piperazinedione was chosen as a model substrate. The “*green*” heterogeneous aqueous-phase catalytic hydrogenation was optimized via a parametric study at modest temperatures (90-130°C) and pressures (500-1500 psi H<sub>2</sub>) using a 5% Ru/C catalyst originally found to be optimal for carboxylic acid reduction. To evaluate reaction results, a direct analytical HPLC method was first developed to quantify all possible reaction products (amino alcohols, amines, amino acids, alcohols and amides).

This thesis is organized into five chapters. The following chapter provides an overview of the literature for this study. The subsequent chapters each cover a specific objective and were prepared as manuscripts for publication preparation. Chapter 2 is devoted to the first objective, i.e., analytical method development and Chapter 3

describes the parametric study for amide hydrogenation. Overall conclusions and suggestions for future research are also provided in Chapters 4 and 5.

## CHAPTER ONE

### LITERATURE REVIEW

#### 1.1 Carboxamide Group

The carboxamide group, simply termed amide, is one of the more complex functionalities in organic chemistry. Amides are relatively weak bases with  $pK_a$  values ~10-15 units lower than the corresponding amines. Protonation occurs at the carbonyl oxygen, because (a) the oxygen is more negatively charged than the nitrogen, and (b)  $\pi$  delocalization is retained in the O-protonated form, whereas N-protonation forces  $\pi$  localization on the carbon oxygen double bond. The delocalization of the  $\pi$  electrons along the O-C-N chain moderates both the carbonyl reactivity and nucleophilic properties of the amide group (Figure 1.1).

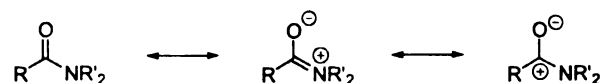


Figure 1.1 Resonance structures of amide

Like most polar moieties, amides are both nucleophilic (at O or N) and electrophilic (at the carbonyl C).<sup>1</sup> Nucleophilic addition to the carbonyl carbon requires activation of the carbonyl either by protonation of the carbonyl oxygen or O-coordination with an electron-deficient species, such as an organometallic reagent.

This report pays particular attention to the selective reduction of the carbonyl of the amide, in the presence of other reducible functional groups.

## 1.2 Amide Reactivity

The overall reactivity of amides depends on the substitution of the amides themselves and activation of the carbonyl carbon. Metal hydrides are classically used for the reduction of amides to amines. Figure 1.2 shows the scheme proposed by Brown and Heim summarizing the reaction paths of amide reduction with a metal hydride. They propose that a tetrahedral intermediate is initially formed, which can further react by either carbon-oxygen (C-O) or carbon-nitrogen (C-N) bond cleavage. Nucleophilic attack by the hydride reagent on the C-O bond can form the amine directly, or attack on the C-N bond with subsequent hydrolysis can form the alcohol. Cleavage of the tetrahedral intermediate's C-N bond can also form an amine and an aldehyde which can be further reduced to the alcohol.<sup>1,2,3</sup> Sterically demanding substituents on N tend to favor C-N bond rupture products.

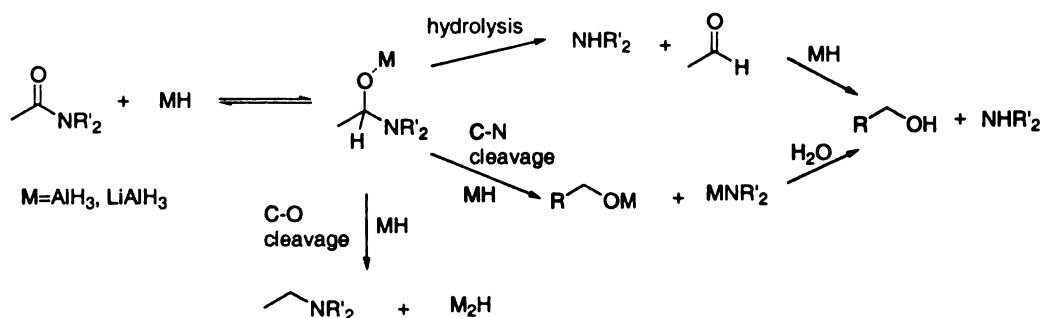


Figure 1.2 Mechanism of amide reduction with a metal (M) hydride

Catalytic hydrogenation, another possible method for amide reduction, is the primary focus for this project. Adkins and co-workers describe the possible reactions that can take place during catalytic hydrogenation of amides.<sup>4</sup> First, there are three possible linkages in which hydrogenolysis can occur on an amide (Figure 1.3).

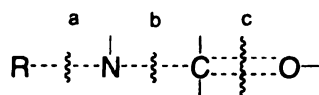


Figure 1.3 Possible hydrogenolysis sites

In the presence of hydrogen, complete cleavage of the C-O (c) double bond results in the formation of the corresponding amine (primary, secondary or tertiary) and water. Further cleavage of the C-N bond (b) of the amine product, would result in another amine and water (Figure 1.4).

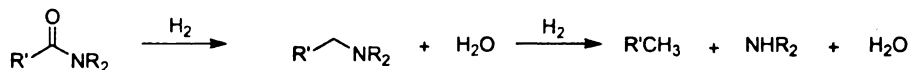


Figure 1.4 Hydrogenolysis of an amide forming an amine and water

When ethanol was used as a solvent during amide hydrogenation, cleavage of the amide C-N (b), resulted in the formation of an alcohol and an ammonia (Figure 1.5).<sup>4-6</sup> The alcohol formed in this process is believed to be the product of hydrogenation of an intermediate ester.



Figure 1.5 Hydrogenolysis of the carbon-nitrogen bond of amides

It is known that amides react with several nucleophilic species; for example, amines, alcohols, hydroxylamines, carboxylic acids etc. Most relevant to this project, is

amide hydrolysis to its parent carboxylic acid and amine fragments under aqueous conditions (Figure 1.6).<sup>7</sup>

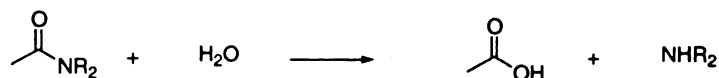


Figure 1.6 Hydrolysis of an amide to a carboxylic acid and an amine under aqueous conditions

In addition to hydrolysis, other possible secondary reactions, such as aminolysis of the amide or amine alkylation by an alcohol, should be noted (Figure 1.7).

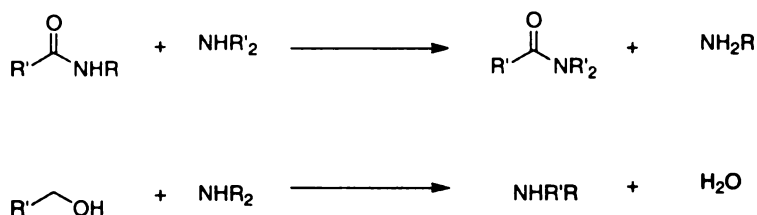


Figure 1.7 Secondary product formation from amide aminolysis or amine alkylation

### 1.2.1 Classical amide reduction using complex metal hydrides

The classical approach for the reduction of an amide to its corresponding amine is the use of various hydride reagents and solvents. Examples include lithium,<sup>2,8</sup> sodium, and potassium, and aluminum hydrides, tetrahydrido aluminates and diborane.<sup>3,9,10</sup> Well established reductions of amides have been reported using  $\text{NaBH}_4/\text{TFA}$ ,<sup>11</sup>  $\text{NaBH}_4/\text{glyme}$ ,<sup>12</sup>  $\text{NaBH}_4/\text{CH}_3\text{SO}_2\text{OH}$  in DMSO,<sup>13</sup> and  $\text{POCl}_3/\text{NaBH}_4$ .<sup>14</sup> However, the choice of reducing agent depends on the functional groups present. Since amides are the least electrophilic of the carbonyl functionalities, it is not surprising that nucleophilic



hydride reagents are generally not selective for amides, preferring to reduce better electrophiles first. When used alone,  $\text{NaBH}_4$  reduces aldehydes, ketones, acid chlorides, nitriles, nitro or halogenated organic molecules and amides.<sup>1,12</sup>  $\text{LiAlH}_4$  is considered a more active hydride donor and is often used over  $\text{NaBH}_4$ , but it also reduces ketones, esters, and even carboxylic acids in preference to amides.<sup>12</sup> Consequently, electrophilic borane complexes are more often used than nucleophilic hydrides. These reagents exhibit amide selectivity, and are easy to use, but  $\text{C}=\text{C}$  double bonds are also susceptible to reduction.<sup>2, 14</sup> Mixed systems, such as sodium borohydride-cobalt chloride have been used to successfully reduce nitriles, amides and nitro compounds to their corresponding primary amines in both hydroxylic and non-hydroxylic solvents.<sup>15</sup>

#### *1.2.1.1 $\text{LiAlH}_4$*

Kuehne and Shannon reported that the reduction of amides and lactams with  $\text{LiAlH}_4$  proceeds with much difficulty, due to the formation of insoluble complexes.<sup>14</sup> Brown and Heim reported that such reactions are often incomplete and side reactions take place resulting in C-N cleavage to the corresponding alcohol.<sup>3</sup> However, Newman and Fukunaga<sup>8</sup> carried out amide reductions using  $\text{LiAlH}_4/\text{THF}$  or ether (reflux or room temperature) with ease. They suggested that the reduction of amides to primary amines proceeds via a base-induced dehydration of the amide to a nitrile, which is then reduced to the amine. This is different from Adkins'<sup>4</sup> original proposal, and was confirmed by detecting the nitrile intermediate and hydrogen evolution from two sterically different compounds, triisopropylacetamide and benzamide. The reduction of triisopropylacetoneitrile to the amine was found to be quite slow, but gave almost

quantitative yield, whereas the reduction of benzonitrile was very fast with only trace amounts detected (Figure 1.8).

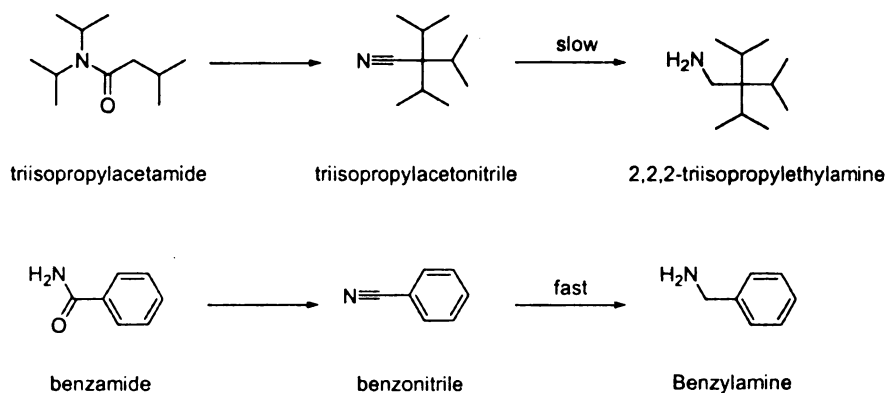


Figure 1.8 Reduction of triisopropylamide and benzamide to a primary amine via a nitrile intermediate

For the above reductions, a few possible mechanisms were considered. The amide can undergo nucleophilic attack by a hydride ion or form an amide salt by an acid-base reaction. The amide salt can further react through another acid-base reaction forming a double salt, with the evolution of two equivalents of  $\text{H}_2$ . The authors believe the amide forms the double salt to yield a nitrile (Figure 1.9). The other possibility is that the amide salt can be reductively attacked to form an aldehyde-ammonia intermediate, which is then dehydrated forming an aldimine salt.

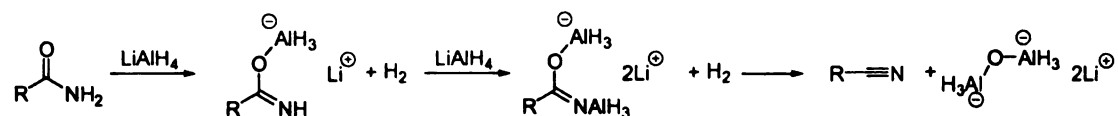


Figure 1.9 Proposed mechanism of amide reduction to a nitrile with  $\text{LiAlH}_4$

### 1.2.1.2 $BH_3$

Borane complexes are often used over  $LiAlH_4$  due to their electrophilic nature and mild reducing conditions which are rapid, quantitative, and clean. Selectively for amides over nitro, halogen, ester, sulfone and carbamate groups is often achieved using borane complexes.

As mentioned above, the reduction of primary, secondary and tertiary amides (both aliphatic and aromatic) derivatives in the presence of other less reactive functional groups was achieved using  $BH_3/THF$  from 0-25°C.<sup>3,9,10</sup> Early studies by Brown and Heim<sup>9</sup> reported the ease of using borane over  $LiAlH_4$ , with yields of 94 and 98% for the reduction of N,N-diethylpivalamide to N,N-diethylnopentylamine and N,N-diisopropylbenzamide to N,N-diisopropylbenzylamine, respectively (Figure 1.10).

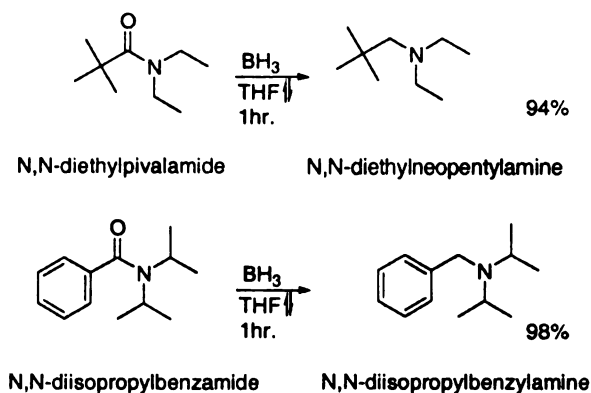


Figure 1.10 Reduction of N,N-diethylpivalamide and N,N-diisopropylbenzamide to their corresponding amines with  $BH_3/THF$  (0-25°C)

Additional reductions by Brown and Heim<sup>9</sup> were carried out with  $BH_3$  (refluxing THF) for 1hr to give the amines shown in Figure 1.11. Under these conditions, the primary amides, hexanamide and benzamide, were both reduced to their corresponding

amines in 87% yield. Secondary amines, N-methylhexanamide and N-methylpivalamide, were converted in 98 and 83% yields. The selective reduction of the amide carbonyl of N,N-dimethyl-*p*-nitrobenzylamide, was obtained in 97% yield.

The authors concluded that primary amides rapidly form a complex with borane, but are reduced slowly, compared to secondary and tertiary amides. Primary aliphatic amides were also reduced faster than primary aromatic amides. The authors rationalized the outcome in terms of H<sub>2</sub> evolution from the amide-borane complex, to form a poorly reactive iminoxyborane species.

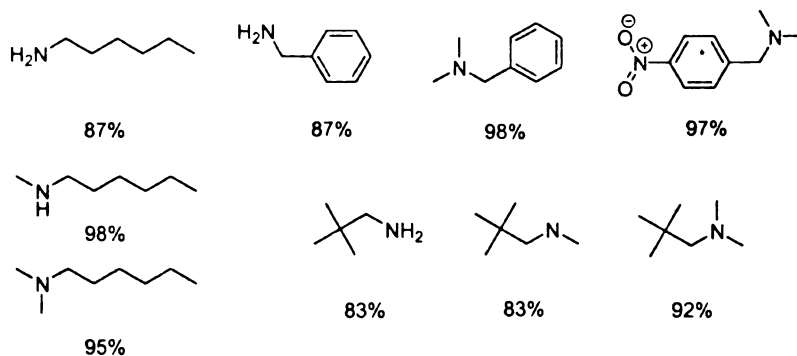


Figure 1.11 Amine yields from amide reduction with BH<sub>3</sub>/THF (0-25°C)

In later studies by Brown and Heim,<sup>3</sup> steric and electronic effects were evaluated and reaction rate measurements showed that increasing branching on the α-carbon increases the rate of reduction. They also concluded that aliphatic amides are reduced faster than aromatic amides (Figure 1.12).

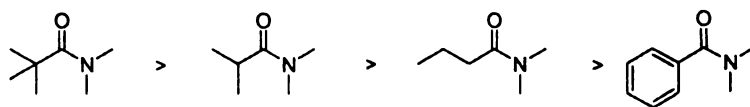


Figure 1.12 Relative rate of reduction of α substituted N,N-dimethylamides with BH<sub>3</sub>/THF (25°C)

Faster reduction rates were found with N,N-diethylbutyramide and N-butyrylpyrrolidine compared to N,N-dimethylbutyramide and N,N-diisopropylbutyramide (Figure 1.13), due to steric effects of the substituents on nitrogen.

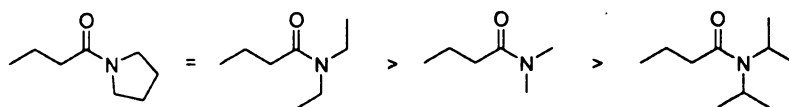


Figure 1.13 Rate of reduction of N substituted N,N-dialkylbutyramides with  $\text{BH}_3/\text{THF}$  at  $25^\circ\text{C}$

Polar substituents on N,N-dimethylbenzamide did not influence the rate of reduction. However, *ortho* substitution of the benzamide did slow the reaction rate significantly, suggesting difficulty in forming the tetrahedral intermediate due to steric effects (Figure 1.14).

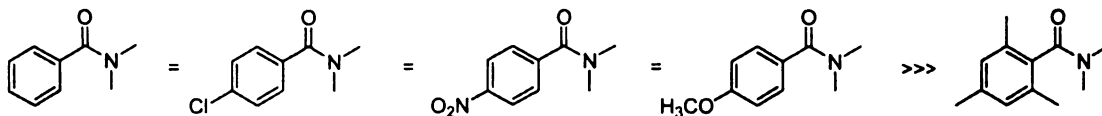


Figure 1.14 Rates of reduction of substituted N,N-dimethylbenzamides with  $\text{BH}_3/\text{THF}$  at  $25^\circ\text{C}$

Though amides are typically less reactive than esters toward nucleophilic reductants,  $\text{BH}_3/\text{THF}$  effected selective reduction of a primary and secondary amides in the presence of an ester as shown by Kornet and others<sup>10</sup> (Figure 1.15). Despite the close proximity of the amide and the ester in ethyl N,N-diethyloxamate, the amide was

selectivity reduced to N,N-diethylaminoacetate (94%) and 5% of the amino alcohol. Ethyl N,N-diethylsuccinamate gave the selectively reduced product, ethyl 4-diethylaminobutanoate in only 36% yield. The reduction of a benzylic amide, *para* substituted with a methyl ester gave a 66% yield of the amino ester. The higher yield of the amine is believed due to the slower reaction rate of esters adjacent to aromatic systems.

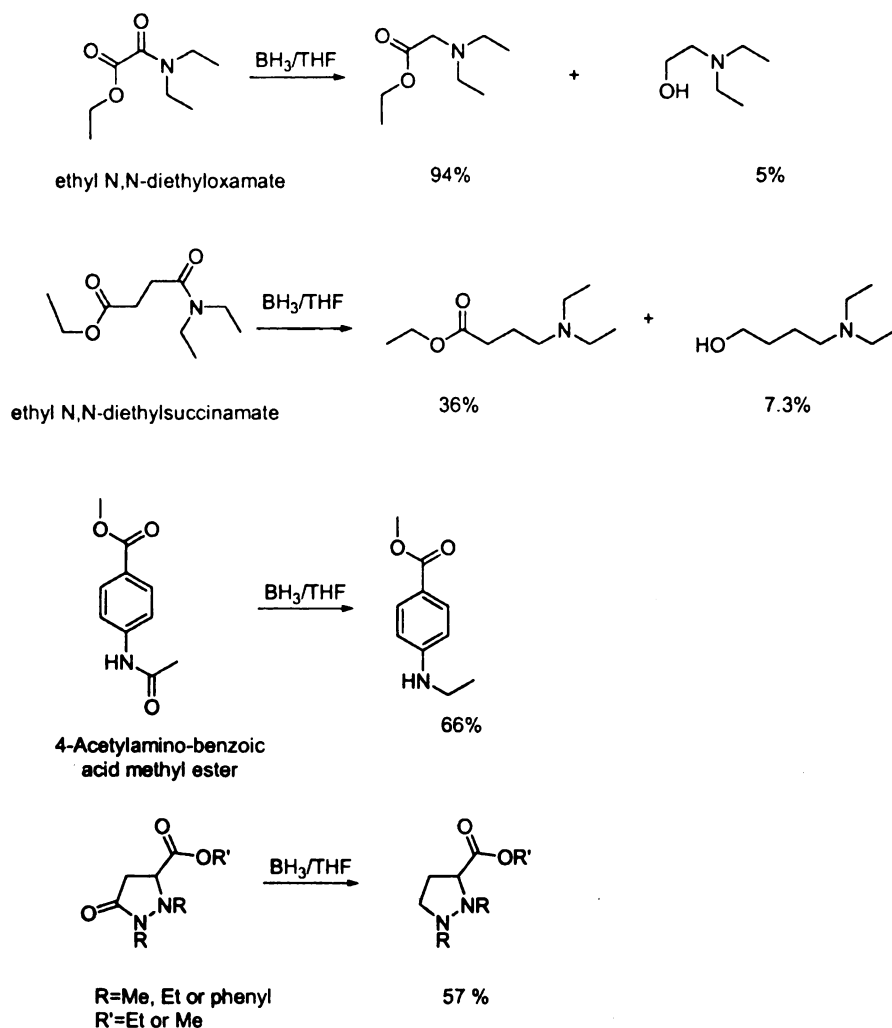


Figure 1.15 Representative selective amide reduction in the presence of an ester ( $\text{BH}_3/\text{THF}$  (0-25°C))

The reduction of methyl hippurate gave a mixture of products consisting of 2-benzylaminoethanol (85%), methyl 2-benzylaminoacetate (11%) and 4% of an unidentified product (Figure 1.16). The authors believe a cyclic intermediate is formed in which the ester carbonyl oxygen forms a coordinate covalent bond with boron, activating the carbonyl of the ester (Figure 1.17) which results in the higher yield of the amino alcohol.

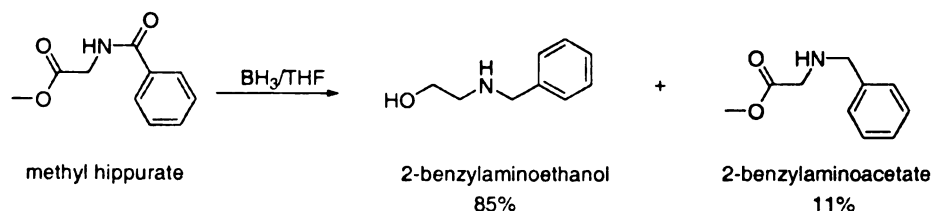


Figure 1.16 Reduction of methyl hippurate with  $\text{BH}_3/\text{THF}$  (0-25°C)

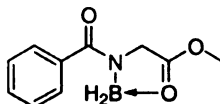


Figure 1.17 Proposed intermediate of the coordinate covalent bond of an ester oxygen with boron

#### 1.2.1.3 $\text{NaBH}_4$

Selective reduction of an amide to an amine has been reported using various combinations of reagents with  $\text{NaBH}_4$ . Examples including  $\text{NaBH}_4/\text{CH}_3\text{SO}_2\text{OH}$ ,<sup>13</sup>  $\text{Et}_3\text{O}^+\text{BF}_4^-/\text{NaBH}_4$ ,<sup>16,17</sup>  $\text{POCl}_3/\text{NaBH}_4$ ,<sup>14</sup>  $\text{PCl}_5/\text{NaBH}_4$ ,<sup>18</sup>  $\text{NaBH}_4/\text{glyme}$ ,<sup>12</sup> and  $\text{P}_4\text{S}_{10}/\text{Raney Ni}$ <sup>19</sup> will be discussed. Other systems such as  $\text{NaBH}_4/\text{CoCl}_2$ ,<sup>15</sup> and  $\text{PCl}_5/\text{NaBH}_4$ ,<sup>18</sup> have been used to successfully reduce nitriles, amides and nitro compounds to their corresponding primary amines in both hydroxylic and non-hydroxylic solvents.

Wann and others<sup>13</sup> carried out similar reductions to those reported by Brown and Heim,<sup>3</sup> but with  $\text{NaBH}_4/\text{CH}_3\text{SO}_2\text{OH}$  in DMSO. They reported that excess  $\text{NaBH}_4$  increased product yields which ranged from 60-88% for primary benzylic amides. This combination of reagents, however, is not necessary selective for amides, and was shown to also reduce carboxylic acids, esters and  $\text{C}=\text{C}$  double bonds. Carbon-halogen bonds were undisturbed under these conditions. Esters are typically reduced much slower than carboxylic acids under  $\text{BH}_3/\text{THF}$  conditions, but were equally reduced under the present conditions. No reduction occurred if either the ester or acid carbonyl group was adjacent to an aromatic ring. The only conclusions made were that the reduction of the amide was carried out by activation of the carbonyl group with the acid, followed by nucleophilic attack by the hydridic protons of  $\text{BH}_4^-$ .

Umino and others<sup>11</sup> reported a simple, highly selective reagent used to reduce both primary and secondary amides to their corresponding amines.<sup>11</sup> Using sodium acyloxyborohydrides  $\text{NaBH}_3(\text{OCOR})$  in either THF or dioxane, provided the amine salt in 82-90% yield. Tertiary amines were reduced only in 20% yield. Figure 1.18 shows the amines studied and their corresponding yields.



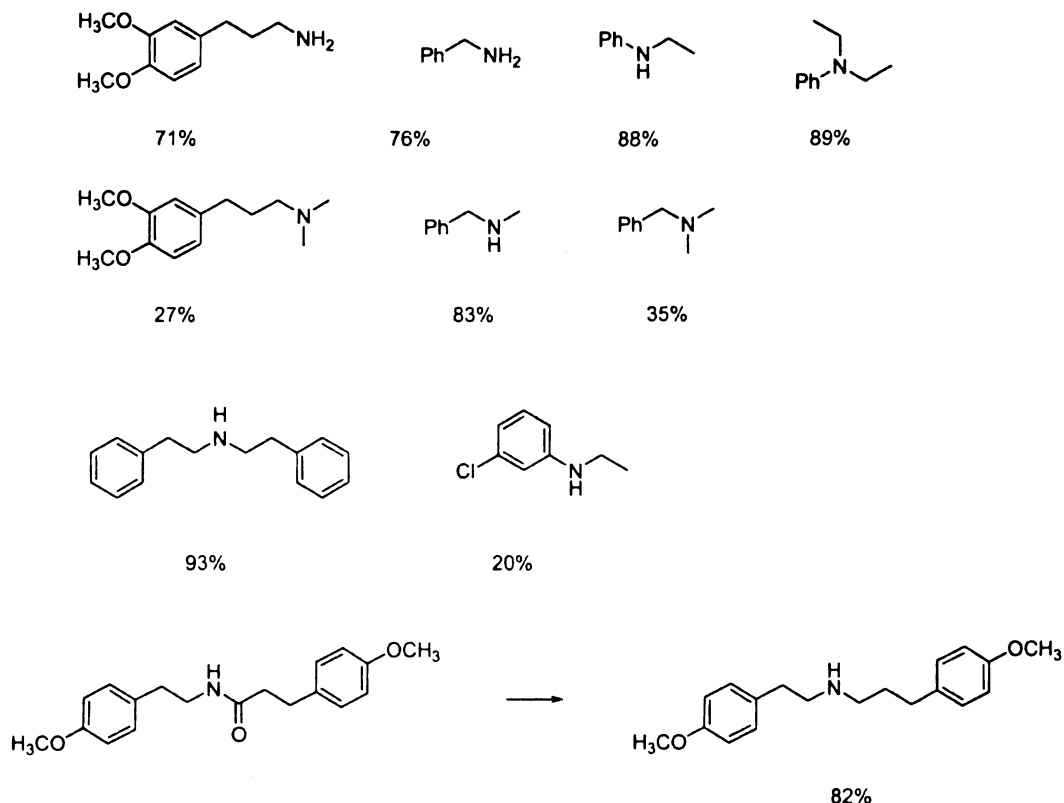


Figure 1.18 Amine yield from the reduction of amides with  $\text{NaBH}_3(\text{OCOR})$  in THF or dioxane

Raucher and Klein found that thioamides are more reactive than their corresponding amides toward alkylation with  $\text{Et}_3\text{O}^+\text{BF}_4^-/\text{CH}_2\text{Cl}_2$ , which can then be reduced to an amine with  $\text{NaBH}_4/\text{MeOH}$ .<sup>16</sup> A variety of amides, primary, secondary, tertiary, benzamides, acetanilides, and lactams, were reduced to their amines via the thioamide intermediate in this manner (Figure 1.19).

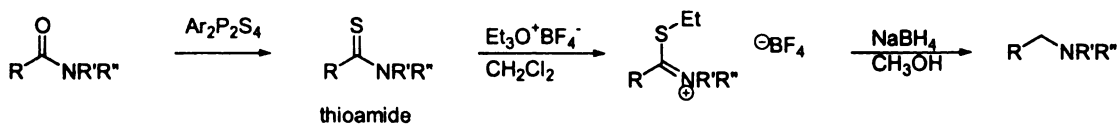


Figure 1.19 Thioamide reduction to an amine with  $\text{Et}_3\text{O}^+\text{BF}_4^-/\text{CH}_2\text{Cl}_2$  and  $\text{NaBH}_4/\text{MeOH}$

The procedure was found to be selective for the thioamide over conjugate double bonds, esters, nitro groups and sulfonamides. Reactions typically ran 30-60 min. at ambient temperature, with yields ranging from 70-100% (Figure 1.20).

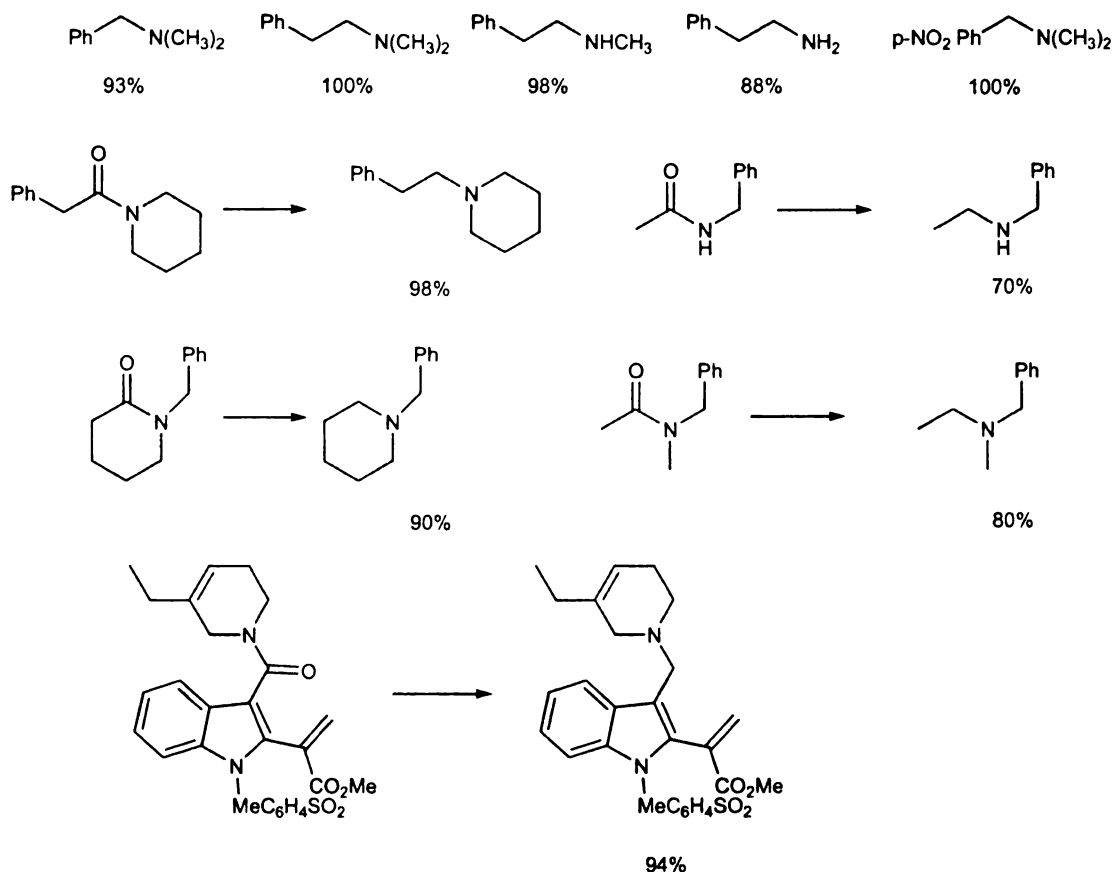


Figure 1.20 Amine yields from the reduction of its thioamide with  $\text{Et}_3\text{O}^+\text{BF}_4^-/\text{CH}_2\text{Cl}_2$  and  $\text{NaBH}_4/\text{MeOH}$

Borsh ran similar reductions of secondary amides using  $\text{Et}_3\text{O}^+\text{BF}_4^-/\text{NaBH}_4$  in ethanol but directly formed the iminium ether tetrafluoroborate intermediate (20hrs, 25°C), which was reduced (20hrs. 25°C) to the amine in essentially quantitative yield (Figure 1.21).<sup>17</sup>

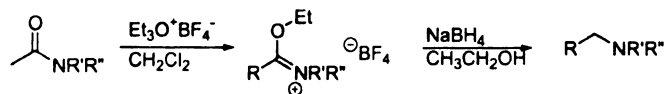


Figure 1.21 Reduction of an amide to an amine via direct formation of an imino ether fluoborate intermediate

A two step mechanism was suggested as shown for N-ethylbenzamide in Figure 1.22, for secondary and tertiary amides, lactams, and ethers. Primary amides were not reduced under these conditions, but instead underwent a dehydration type reaction to form a nitrile by eliminating ethanol.



Figure 1.22 Mechanism of reduction of imino ether fluoborate intermediate to an amine with BH<sub>4</sub><sup>-</sup>

Selective reduction of N-mono- and disubstituted amides and lactams with preservation of ester, nitrile and olefinic groups was achieved using POCl<sub>3</sub>/glyme and NaBH<sub>4</sub> at room temperature, 15-60 min., as reported by Kuehne and Shannon.<sup>14</sup> These studies are similar in selectivity to those by Kornet and others using BH<sub>3</sub>/THF (0-25°C), for the selective reduction of amides in the presence of esters. Kuehne and Shannon proposed that diborane is generated with the addition of NaBH<sub>4</sub> to the imino intermediate. Figure 1.23 shows the reaction sequence of an amide or lactam to an imino intermediate. Either the O-phosphoryl derivative or the corresponding imino chloride can be formed in the reaction medium. In order to avoid the formation of diborane and

still achieve direct reduction of the amide,  $\text{NaBH}_4$  was added as an ethanolic solution to the imino derivative. Figure 1.24 shows the reactions in which the amide was selectively reduced.

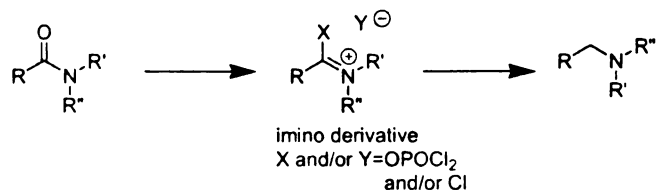


Figure 1.23 Reaction sequence of an amide or lactam reduction to an amine via an imino derivative

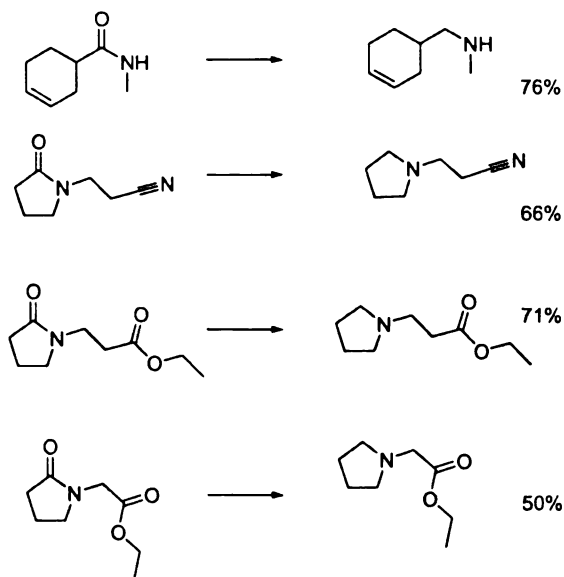


Figure 1.24 Selective reduction of amides over olefin, nitrile and esters groups with 1) $\text{POCl}_3$ /glyme and 2) $\text{NaBH}_4$ /EtOH

Steric and electronic effects on reaction rates were also studied (Figure 1.25). The authors found that  $\alpha$  substitution decreases reaction rate, and secondary amides react faster than tertiary amides. In particular, aliphatic amides reacted faster than benzamides, which reacted faster than anilides. The addition of a base, pyridine, increased the rate of the formation of the imino derivative, especially among amides with no  $\alpha$  proton.

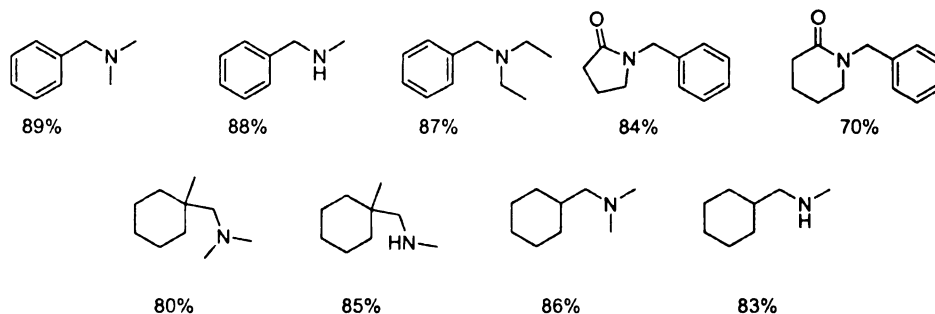


Figure 1.25 Amine yields from their corresponding amide reduced with  $\text{POCl}_3$ /glyme and  $\text{NaBH}_4$ /EtOH

In a different study by Rahman and others, the  $\alpha$  carbon of amides or imides was activated via a Vilsmeier complex, and reduced to an amine with  $\text{NaBH}_4$ /EtOH.<sup>18</sup> Isolated yields ranged from 75-90% for secondary and tertiary amides and primary amides formed the corresponding nitrile quantitatively (Figure 1.26).

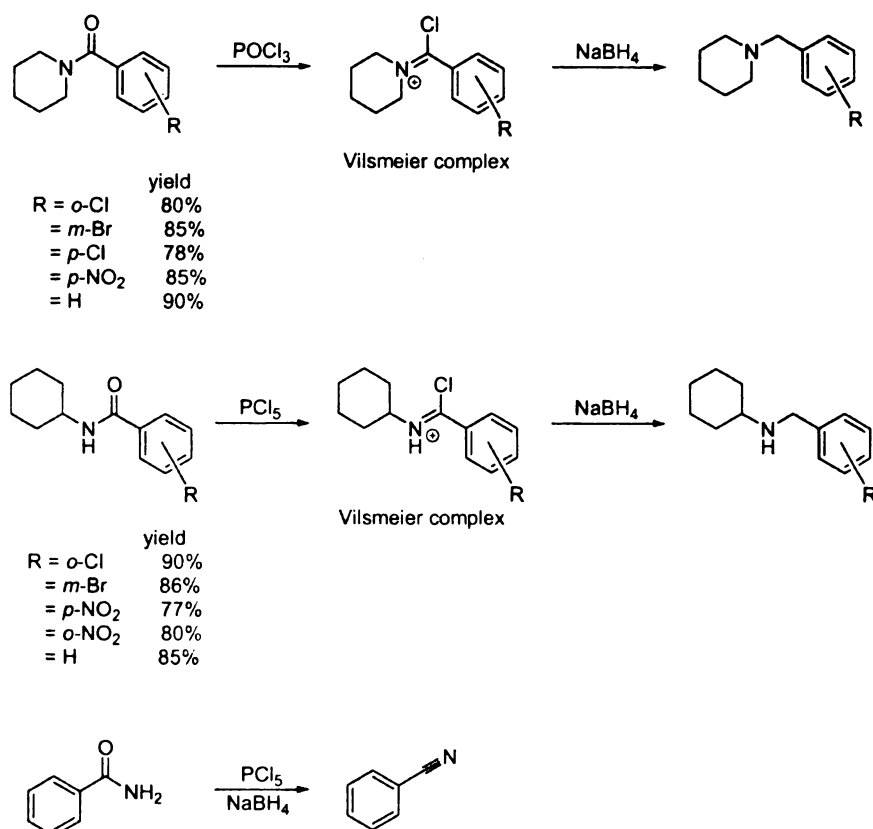


Figure 1.26 Amide reduction to an amine via a Vilsmeier intermediate

Bazant and others reported reduction of lactams, aldehydes, ketones, oximes, acid anhydrides, lactones, and imides using  $\text{NaAlH}_2(\text{OCH}_2\text{CH}_2\text{OCH}_3)_2$  in benzene ( $100^\circ\text{C}$ ).<sup>20</sup> Of particular interest,  $\epsilon$ -caprolactam was reduced to hexamethylenimine in 82% yield and N-methylsuccinimide was reduced to N-methylpyrrolidine in 92% yield (Figure 1.27). No chemoselectivity studies were carried out.

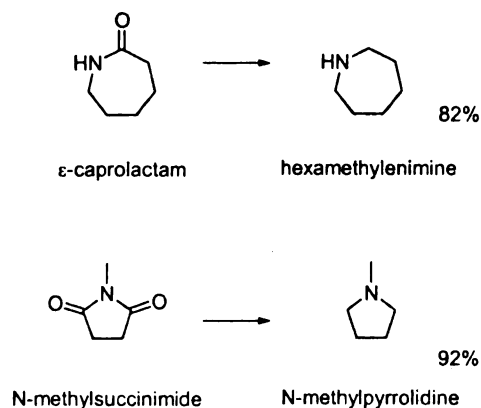


Figure 1.27 Lactam reduction to an amine with  $\text{NaAlH}_2(\text{OCH}_2\text{CH}_2\text{OCH}_3)_2$  in benzene ( $100^\circ\text{C}$ )

Sato and others reported the reduction of nitro compounds, nitriles and amides in dioxane ( $100^\circ\text{C}$ ) or methanol ( $30^\circ\text{C}$ ), with  $\text{NaBH}_4/\text{CoCl}_2$ .<sup>15</sup> Nitro compounds require higher reaction temperatures than nitriles, and primary amides reacted much faster than secondary amides. Figure 1.28 shows the amides reduced; tertiary amides were unreactive under these conditions.

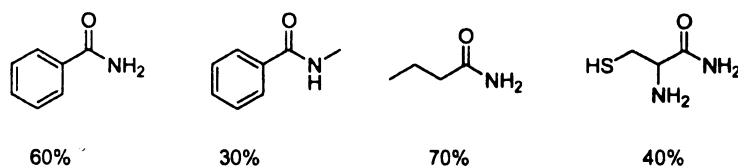


Figure 1.28 Amides reduced with  $\text{NaBH}_4/\text{CoCl}_2$  in dioxane or methanol ( $100^\circ\text{C}$ )

Zhu and others<sup>12</sup> reported the reduction of primary aromatic amides using  $\text{NaBH}_4$ /diglyme at high temperature. They found that amides (primary and secondary) were first dehydrated to their nitriles with evolution of one mole  $\text{H}_2$  upon treatment with  $\text{NaBH}_4$ /diglyme at  $162^\circ\text{C}$ . The nitriles were reduced to the amines with the addition of  $\text{LiCl}$ . Their conclusions are similar to Newman and Fukunaga's ( $\text{LiAlH}_4/\text{THF}$ ),<sup>8</sup> with

amide reduction proceeding through a nitrile intermediate. The mechanism proposed by Zhu and others is shown in Figure 1.29.

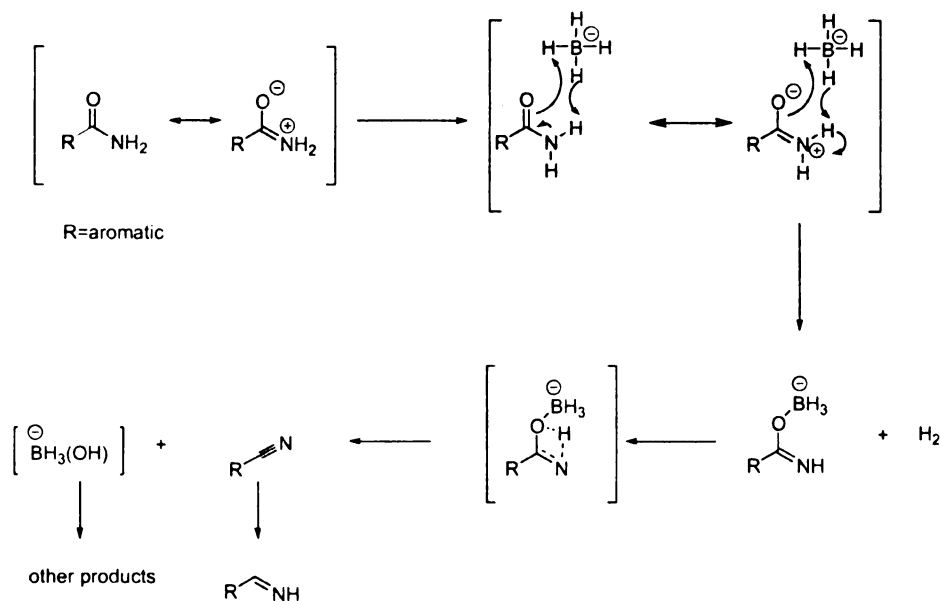


Figure 1.29 Proposed mechanism of amide reduction with  $\text{NaBH}_4/\text{glyme}$

Bhandari and others<sup>21</sup> reported the reduction of lactams to their corresponding amines by Na metal/*n*-propanol (reflux, 1hr.). Yields ranged from 70% for a five membered ring to 72 and 65% for six and seven membered rings, respectively (Figure 1.30). When  $\text{LiAlH}_4$  was used, yields decreased 5-10%, and no reduction was achieved with either  $\text{H}_2/\text{Pd}$  or  $\text{H}_2/\text{Ni}$  (R).



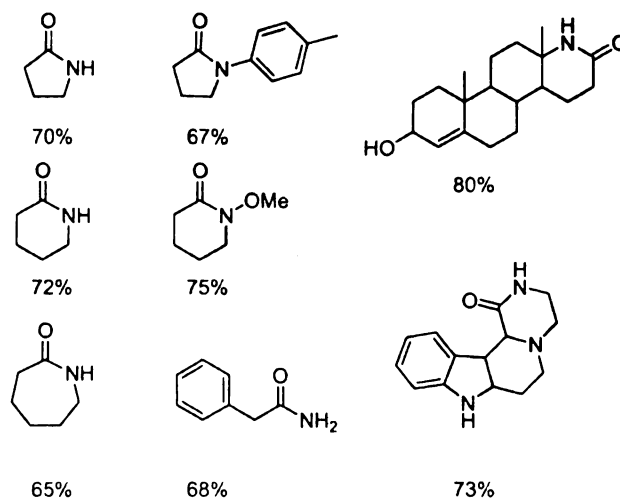


Figure 1.30 Amides reduced using Na metal/*n*-propanol

### 1.2.2 Catalytic Hydrogenation

As cited in Adkins and Wojcik,<sup>22</sup> and as early as 1906, Mailhe and others had reported the hydrogenation of acetamide and propionamide to ethyl and dimethyl amines, and dipropylamines, respectively, in the vapor phase over a nickel catalyst (Figure 1.31). No additional reaction conditions, yields or purities were reported. These experiments by Mailhe, unfortunately, have never been reproduced with yields higher than 1%.<sup>4</sup>

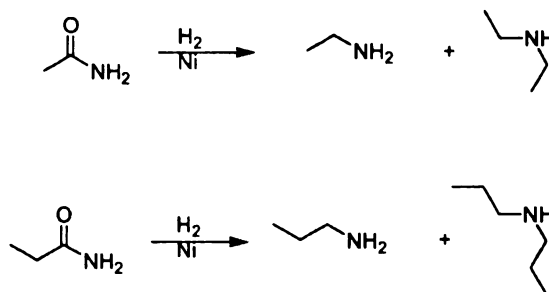


Figure 1.31 First reported hydrogenation of an amide by Mailhe

Beginning in the 1930's additional cases of catalytic hydrogenation of amides to amines were published. Winans and Adkins<sup>6</sup> first reported the catalytic hydrogenation of a number of nitrogen compounds over nickel. As shown in Figure 1.32, hydrogenation converts benzamide to a mixture of the primary amine, benzyl amine, and its dimer, dibenzylamine. It is believed that the conversion of benzamide involves an imine intermediate which converts to the primary amine in the presence of an anhydrous solvent.<sup>6</sup>

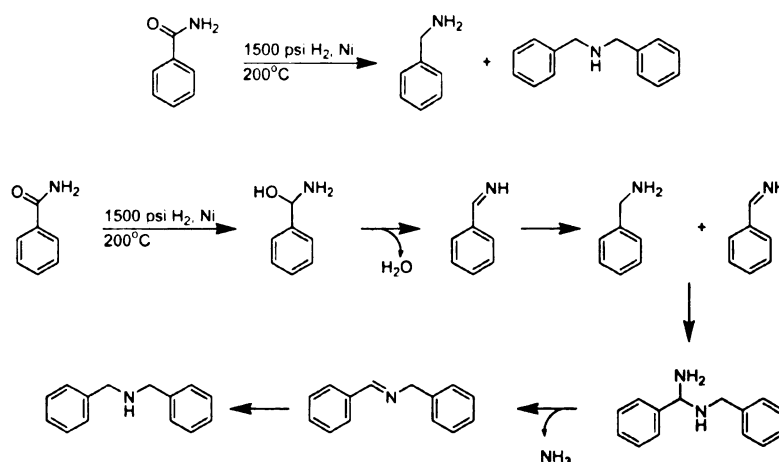


Figure 1.32 Hydrogenation of benzamide over Ni (1500 psi H<sub>2</sub>, 200°C)

Adkins and co-workers continued to explore hydrogenation experiments in which an amide was reacted exclusively with hydrogen<sup>22</sup> over copper chromite catalysts.<sup>4, 5, 23-25</sup> Wojcik and Adkins<sup>4</sup> found that reductions using H<sub>2</sub> were incomplete when performed under aqueous conditions due to the hydrolysis of the starting amide to form an acid and ammonia. The formation of ammonia is undesirable since it may deactivate most catalysts. Alternative reaction conditions using dioxane were chosen to reduce

hydrolysis, over  $2\text{CuO}\cdot\text{Cr}_2\text{O}_3$  under 1470-4400 psi  $\text{H}_2$  at 175-250°C.<sup>22</sup> In the work of Wojcik and Adkins,<sup>4</sup> both carbon-oxygen and carbon-nitrogen hydrogenolysis were observed. Primary amides of lauric, heptanoic and tetrahydrofuranic acids gave an average yield of 88.5% to their corresponding amine plus water, and yields for the substituted amides were lower ranging from 54-72% (Figure 1.33). Secondary cleavage products from nitrogen-carbon bond hydrogenolysis formed predominantly with secondary and tertiary amines.

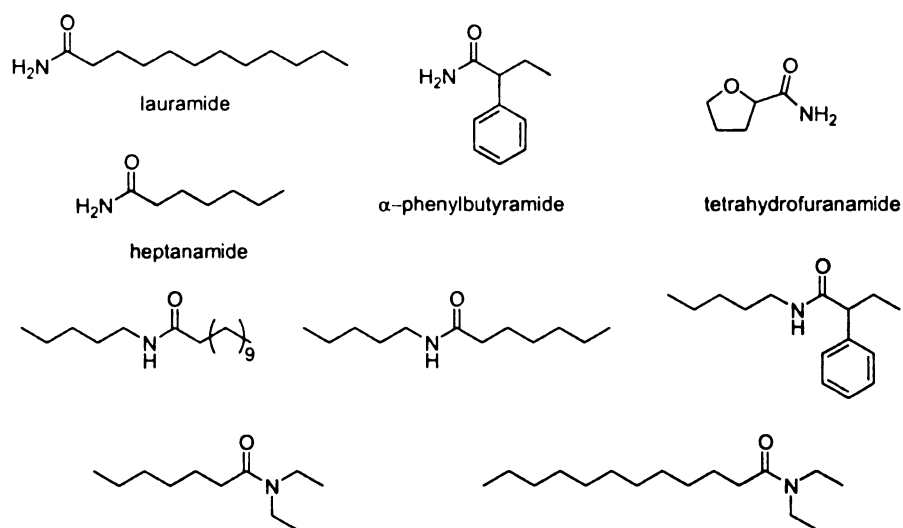


Figure 1.33 Amides reduced over  $2\text{CuO}\cdot\text{Cr}_2\text{O}_3$ /dioxane (1470-4400 psi  $\text{H}_2$ , 175-250°C)

D'Ianni and Adkins<sup>23</sup> looked specifically at the effect of hydroxyl group position of amide hydrogenation over  $2\text{CuO}\cdot\text{Cr}_2\text{O}_3$  at 250-260°C (4 hrs.) and over Raney Ni at 225°C (5-8 hrs.) in dioxane. Raney Ni showed no activity for most of the amides studied, whereas  $2\text{CuO}\cdot\text{Cr}_2\text{O}_3$  gave appreciable yields. Five hydroxyamides were studied, with the hydroxyl group placed in the  $\alpha$ ,  $\beta$ ,  $\gamma$ ,  $\delta$ ,  $\epsilon$  positions with respect to the amide. The corresponding hydroxyamines were formed in yields of 51, 0, 79, 76, and 60%,

respectively, over  $2\text{CuO}\cdot\text{Cr}_2\text{O}_3$ . The low yield of the  $\beta$ -hydroxybutyramide producing the hydrogenolysis product (78% alkylpiperidine) was predicted as seen in previous experiments with oxygen and nitrogen  $\beta$  to each other. Another type of hydrogenolysis of the C-N bond was also observed producing glycol in each of the reaction mixtures of the five hydroxyamides. The authors believe the hydroxylamine is formed by the interaction of the amine and glycol.

Surprisingly, hydrogenation of  $\beta$ -hydroxybutyramide over Ni (R) yielded 86% 4-amino-butan-2-ol. The rate of the Ni-catalyzed reaction of hydroxyamides was higher than for amides with no hydroxyl group. This was shown by competitive hydrogenation of caproamide and  $\delta$ -hydroxycaproamide. After 8 hrs, 83% of caproamide was still present, compared to only 14%  $\delta$ -hydroxycaproamide. In the case of hydroxydiamides and lactams, mixtures of cleavage products were formed over  $2\text{CuO}\cdot\text{Cr}_2\text{O}_3$ .

Sauer and Adkins also reported the hydrogenation of several amino or carbethoxy pyrrolidones, piperidones, or quinolones over  $2\text{CuO}\cdot\text{Cr}_2\text{O}_3$ /dioxane, 1470-4400 psi  $\text{H}_2$ , at elevated temperatures of 200-260°C.<sup>25</sup> The focus of their experiments was to compare the relative reactivity of amido and carbethoxy pyrrolidones, piperidones, or quinolones. Three competing reactions were described: the reduction of an ester to a hydroxyl methyl group, reduction of an amide carbonyl to a methylene group, and hydrolysis of a hydroxyl to methyl. In the case of pyrrolidones, the esters of 5-carbethoxypyrroline-2 and 5-amylcarbamylypyrrolidone-2 were reduced to their alcohols in 93 and 68% yield, respectively with no reaction occurring at the amide carbonyl (Figure 1.34). When comparing  $\beta$ -carbethoxypyrrolidones, the ester carbonyl was again preferentially

hydrogenated to the hydroxyl group (50% yield) over the amide. Extending the time of the reaction did allow the carbonyl of the lactam to be hydrogenated to methylene.

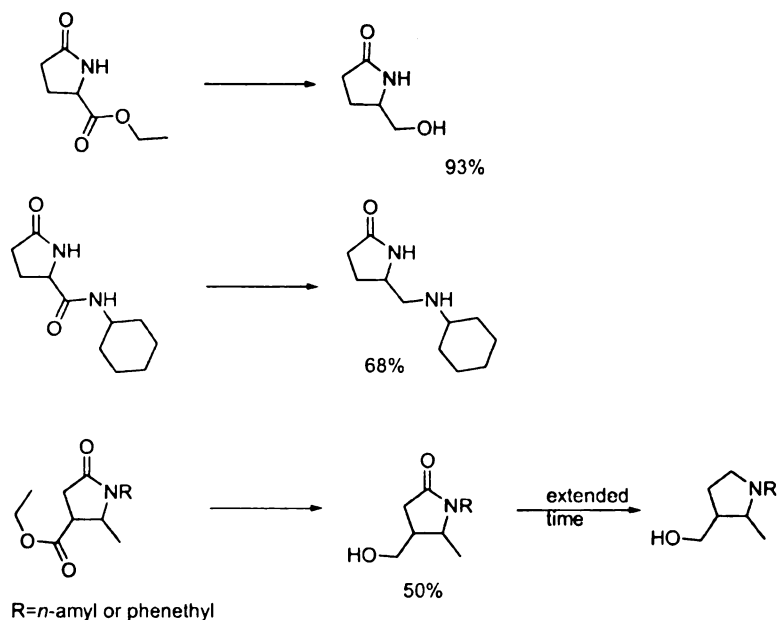


Figure 1.34 Ester reduction over  $2\text{CuO}\cdot\text{Cr}_2\text{O}_3/\text{dioxane}$  (1470-4400 psi  $\text{H}_2$ , 200-260°C) in the presence of an amide

$\beta$ -carbethoxypiperidones also reacted in which the ester hydrogenated first to the hydroxyl (24%), then to the fully reduced cyclic amine (Figure 1.35). In the case of a diamide, the lactam carbonyl hydrogenated first, followed by reduction of the side chain amide with subsequent cleavage to the hydroxyl group.

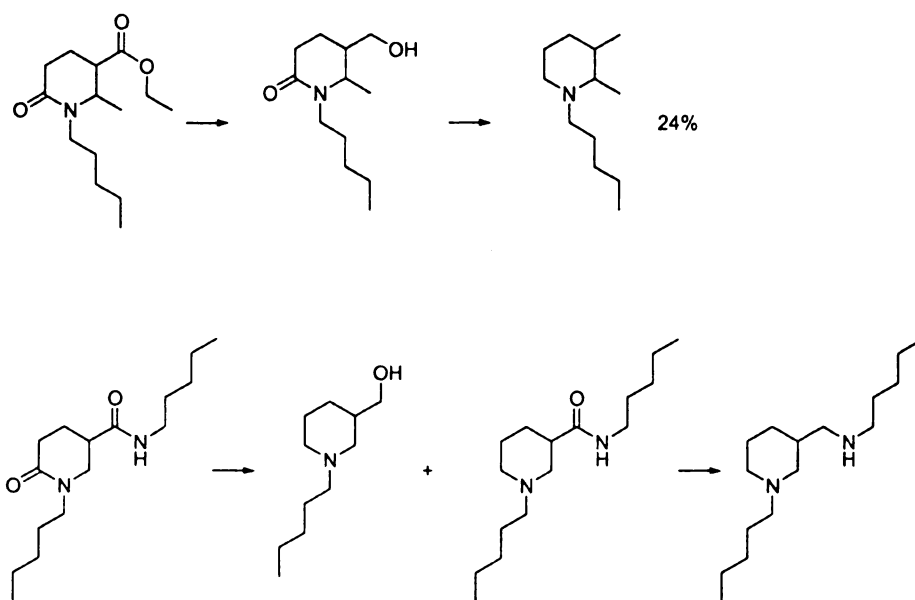


Figure 1.35 Lactam hydrogenation over  $2\text{CuO}\cdot\text{Cr}_2\text{O}_3/\text{dioxane}$  (1470-4400 psi  $\text{H}_2$ , 200-260°C)

Hydrogenation of quinolones occurs at the amide and ester groups forming the primary alcohol (24%), which is then converted to a methyl group (29%). When the ester was  $\beta$ - from the nitrogen, it was cleaved by hydrogenolysis or retroaldol, and the carbonyl amide was reduced to the amine (85%) (Figure 1.36).

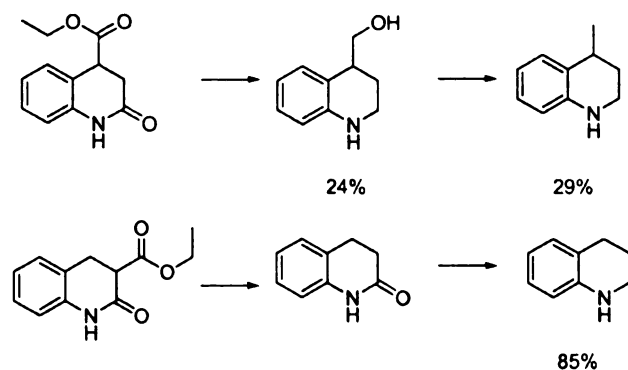


Figure 1.36 Hydrogenation of quinolones over  $2\text{CuO}\cdot\text{Cr}_2\text{O}_3/\text{dioxane}$  (1470-4400 psi  $\text{H}_2$ , 200-260°C)

### 1.2.2.1 Mechanisms for Catalytic Hydrogenation

The transalkylation of secondary and tertiary amines with alcohols over copper-chromium catalysts was investigated by Adkins and coworkers.<sup>24, 26</sup> They determined that the catalyst dehydrogenates the alcohol to an aldehyde or ketone, which reacted with the amine to form a gem-amino alcohol, which was then hydrogenated to the amine (Figure 1.37), presumably via an imine intermediate.

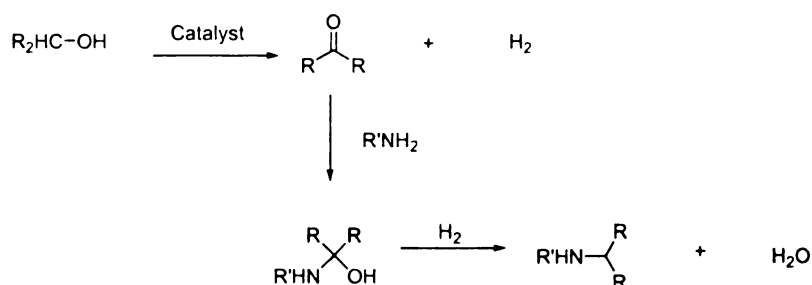


Figure 1.37 Transalkylation of an amine with alcohol over 2CuO·Cr<sub>2</sub>O<sub>3</sub>/H<sub>2</sub>

It is also possible to dehydrogenate the starting amine, which reacts with the alcohol to form an amino alcohol, then cleaves into an ether and ammonia (Figure 1.38).

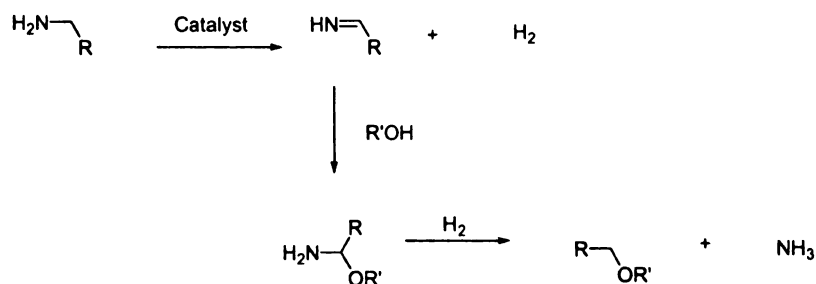


Figure 1.38 Formation of ether and ammonia via an amino alcohol over 2CuO·Cr<sub>2</sub>O<sub>3</sub>/H<sub>2</sub>

A possible side reaction, alkyl group exchange among amines, may occur via the following route (Figure 1.39) which starts with the initial dehydrogenation of the amine to an imine intermediate, followed by amine addition across the C=N double bond.

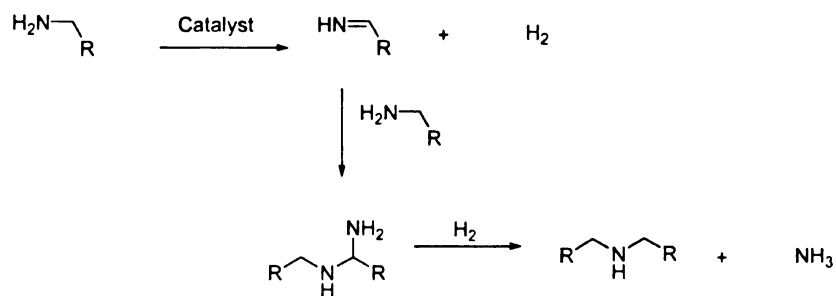


Figure 1.39 Side reaction forming a secondary amine via an imine intermediate over  $2\text{CuO}\cdot\text{Cr}_2\text{O}_3/\text{H}_2$

The formation of secondary amines through a nitrile intermediate, which is reduced to an imine (Figure 1.40), was also considered.

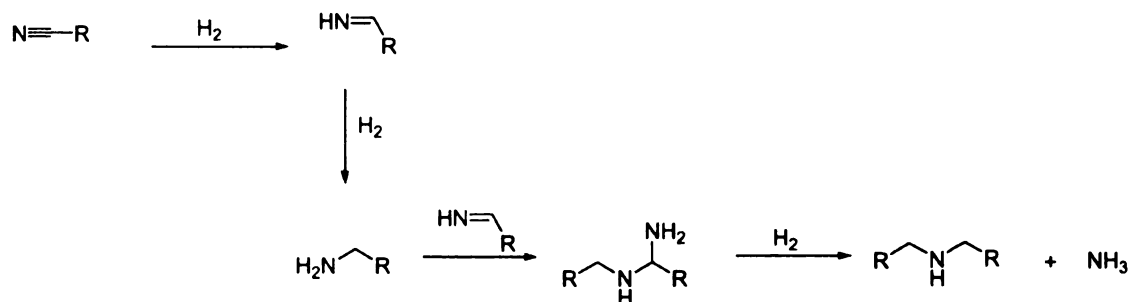


Figure 1.40 Secondary amine formation via nitrile over  $2\text{CuO}\cdot\text{Cr}_2\text{O}_3/\text{H}_2$

To test the reactivity of nitriles, *n*-butyl cyanide and *n*-hexyl cyanide were hydrogenated in ammonia over Raney nickel at 125°C. The primary amines formed in 90-95%, and the secondary amines formed in less than 5% (Figure 1.41).<sup>26</sup>



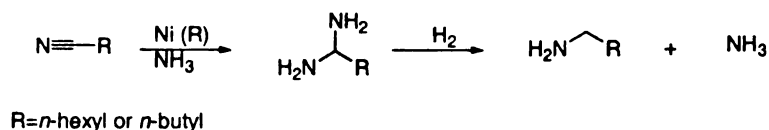


Figure 1.41 Nitrile hydrogenation over Ni (R)/NH<sub>3</sub> (125°C) to an amine

The transalkylation of tertiary amides with alcohols to form amines over copper-chromium barium oxide (I)/dioxane was investigated by Schneider and others (Figure 1.42).<sup>24</sup> The major product formed during the reduction of lauramide was the alcohol, carried out under 4500-12000 psi H<sub>2</sub> (250°C). Decreased temperatures (175°C) favored alcohol formation. When an alcohol was used as the solvent, an intermediate ester was converted into an amine as the major product under the hydrogenation conditions stated. Water as a solvent deactivated the catalyst, and little hydrogenation took place.

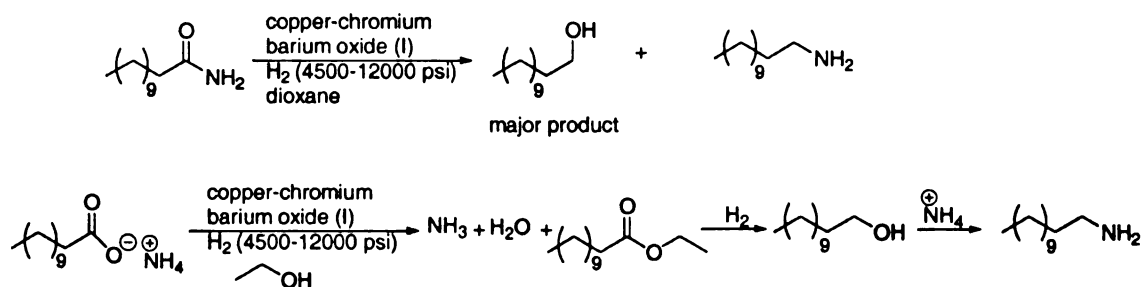


Figure 1.42 Transalkylation of tertiary amides with alcohols to form amines over copper-chromium barium oxide (I)/dioxane (4500-12000 psi H<sub>2</sub>, 250°C)

#### 1.2.2.2 Bimetallic Catalyst Systems

The use of bimetallic catalyst systems has proven to be advantageous, enabling selectivity for amide reduction and less harsh conditions (lower pressures and temperatures), then with simpler catalyst systems.

The bimetallic catalytic hydrogenation of amide derivatives was carried by Hirosawa and others, concluding that synergistic effects of metals are quite useful, and can be carried out under relatively mild reaction conditions, 1500 psi H<sub>2</sub> (170°C) in 1,2-dimethoxyethane (DME).<sup>27</sup> Metals from Groups 8 to 10, late transition metals Rh<sub>6</sub>(CO)<sub>16</sub> or Ru<sub>3</sub>(CO)<sub>12</sub>, and Group 6 or 7 early transition metal complexes, Re<sub>2</sub>(CO)<sub>10</sub>, W(CO)<sub>6</sub>, or Mo(CO)<sub>6</sub> were found to catalyze reduction of N-acetylpiperidine to N-ethylpiperidine in yields ranging from 50-98%. Alone, Rh<sub>6</sub>(CO)<sub>16</sub> afforded 19% yield of N-ethylpiperidine. The most effective combinations were rhodium-rhenium (96%), rhodium-molybdenum (98%), and ruthenium-rhenium (96%). Synergistic effects of rhenium, molybdenum, or tungsten with rhodium or ruthenium were observed in both homo- and heterogeneous systems. Several amides were examined over Rh<sub>6</sub>(CO)<sub>16</sub>-Re<sub>2</sub>(CO)<sub>10</sub> metal complexes at varied catalyst loading ratios. Tertiary amides were reduced with amine yields ranging from 70-92%. Increased catalyst loading and reaction time showed increased yields. Secondary amides were reduced to their corresponding amines with yields ranging from 82-90%, with 3% mol catalyst loading at 170-180°C. Primary amides, on the other hand, were converted to the secondary amine.

When evaluating the reactivity of bimetallic catalysts on lactams, it was found that ring size affects reactivity. Slightly higher reaction temperatures were needed for  $\delta$ -valerolactam than for  $\epsilon$ -caprolactam, (160 versus 180°C) and  $\omega$ -heptalactam required higher catalyst loading (3 mol% versus 1 mol %) than  $\delta$ -valerolactam and  $\epsilon$ -caprolactam. Substitution at the nitrogen atom of the lactam decreased overall activity. These bimetallic systems have been shown to be effective toward the hydrogenation of carboxylic acids, but not esters. Selectivity studies have not been carried out as of yet.

Kuwano and others described a rhodium complex catalyzed reaction with  $\text{Ph}_2\text{SiH}_2$  for the selective reduction of tertiary amides at room temperature in THF.<sup>28</sup> N,N-dibenzylacetamide was reduced to dibenzylethylamine with various rhodium metal complexes.  $\text{RhH}(\text{CO})(\text{PPh}_3)_3/\text{Ph}_2\text{SiH}_2$  gave a 94% yield, and  $\text{RhH}(\text{PPh}_3)_4/\text{Ph}_2\text{SiH}_2$  (93%). Rhodium complexes without a hydride ligand,  $[\text{Rh}(\text{COD})_2]^{-2}\text{BF}_4\text{PPh}_3$ ,  $\text{RhCl}(\text{PPh}_3)_3$  and  $\text{RhCl}_3 \cdot \text{H}_2\text{O}$ , all in  $\text{Ph}_2\text{SiH}_2$ , gave yields of 86, 93, and 93% respectively, but were very slow. When the hydride equivalent was varied,  $\text{Ph}_2\text{SiH}_2$ ,  $\text{PhSiH}_3$  and  $\text{Ph}_3\text{SiH}$  with  $\text{RhH}(\text{CO})(\text{PPh}_3)_3$  gave yields varying from 49, 90, and 0%, respectively. Even when sterically hindered amides were employed, amine yields were still high. However, reaction rate slowed down.

Chemoselectivity studies of amide reduction was carried out as well. It was found that  $\text{RhH}(\text{CO})(\text{PPh}_3)_3$  catalyzed reductions with  $\text{Ph}_2\text{SiH}_2$  selectively reducing amides to their amines without reacting with bromo, ester or epoxy groups. Amides with either double or triple bonds, and  $\alpha$ -active methylenes gave mixtures of products.

The proposed mechanism by Kuwano of the reduction of an amide with the dialkylsilane is shown in Figure 1.43.

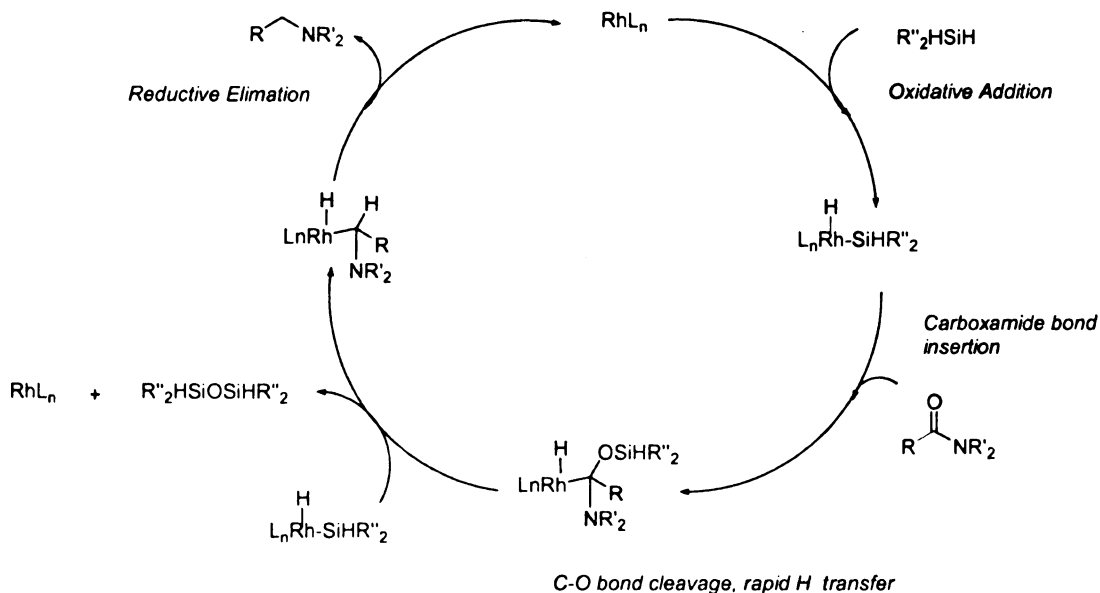


Figure 1.43 Proposed catalytic cycle of an amide reacting with dialkylsilane

Later studies by Igarashi and others reported metal complex catalyzed amide reductions with hydrosilane ( $\text{H}_2\text{SiPh}_2$  or  $\text{H}_3\text{SiPh}$ ) to be an effective means of producing tertiary, secondary and primary amines at elevated temperatures.<sup>29</sup> Monohydrosilanes were used as the reducing agent for N-acetylpiperidine with a variety of Group 7-10 transition metals (Mn, Re, Ru, Os, Rh, Ir, Pd and Pt). Highest yields were found using  $\text{HSiEt}_3/\text{Os}_3(\text{CO})_{12}/\text{Et}_2\text{NH}$  (99.8%),  $\text{HSiMe}_2\text{Ph}/\text{RuCl}_2(\text{CO})_2(\text{PPh}_3)_2/\text{EtI}$  (90.2%),  $\text{HSiMe}_2(\text{OEt})/\text{RuCl}_2(\text{CO})_2(\text{PPh}_3)_2$  (93.1%),  $\text{HSiMe}(\text{OEt})_2/\text{RuCl}_2(\text{CO})_2(\text{PPh}_3)_2$  (90.8%), and  $\text{HSiMe}(\text{OEt})_3/[\text{RuCl}_2(\text{CO})_3]_2/\text{EtI}/\text{Et}_2\text{NH}$  (86.1%) at  $100^\circ\text{C}$ , in toluene. A variety of lactams were also reduced in yields ranging from 86-99%.

### 1.3 Relevant Laboratory Studies

In our laboratory, working under alternative 'green' conditions plays a major role. In particular, reactions compatible with biomass-based substrates are desired, to open paths to value-added based products as an alternative to petroleum based products. The catalytic hydrogenation of organic acids to their corresponding alcohols has been studied quite extensively under aqueous conditions over ruthenium catalysts. More recently hydrogenation of sugars, and now amides, has also been carried out.

#### 1.3.1 Catalytic Hydrogenation of Amino Acids

##### 1.3.1.1 L-Alanine

Studies by Jere and others<sup>30,31</sup> evaluated the catalytic hydrogenation of L-alanine to L-alaninol over 5% Ru/C (1000 psi H<sub>2</sub>, 100°C) in excess H<sub>3</sub>PO<sub>4</sub>/H<sub>2</sub>O. In these studies, it was found that the stereochemistry at the  $\alpha$ -carbon was retained. Reduction selectivities and enantiometric excesses for L-alaninol were found >95%, and >99%, respectively. The presence of acid was found to be necessary in order for hydrogenation to take place; presumably the acid keeps the amino acid carboxylate in its fully protonated form. Together with isotopic labeling and kinetics data, the following mechanism of hydrogenation of L-alanine to L-alaninol was proposed (Figure 1.44).

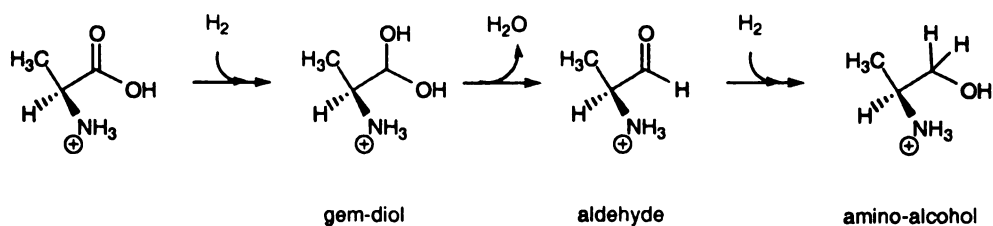


Figure 1.44 Reaction pathway of L-alanine to L-alaninol hydrogenation

### 1.3.1.2 Glycylglycine

From the work by Jere and others, the next step was to run these reactions on peptides. The simplest peptide, glycylglycine, was explored briefly in our laboratory under the same conditions: 5% Ru/C (1000 psi H<sub>2</sub>, 100°C) in excess H<sub>3</sub>PO<sub>4</sub>/H<sub>2</sub>O.<sup>32</sup> Isolated yields of the resulting products were detected using NMR, which show that the reaction mixture consisted of the starting material (50%), 2% of its cyclic anhydride (2,5-piperazinedione), hydrolysis product (glycine, 25%), and the product of glycine hydrogenation (ethanolamine, 20%) (Figure 1.45).

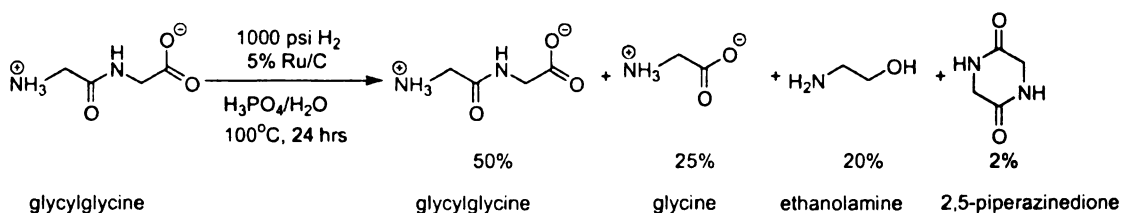


Figure 1.45 Catalytic hydrogenation of glycylglycine with H<sub>3</sub>PO<sub>4</sub>/H<sub>2</sub>O (1000 psi H<sub>2</sub>, 100°C, 1 g 5% Ru/C)

Subsequent studies were carried out to stabilize the intermediate and prevent hydrolysis using metal complexes. Glycylglycine under hydrogenation conditions of 1000 psi H<sub>2</sub> (100°C), in the presence of the mildly acidic zinc phosphate (ZnHPO<sub>4</sub>)/H<sub>2</sub>O gave similar results as previously mentioned recovering 49% of the starting material, 1.5% 2,5-piperazinedione, 34% ethylamine, 24% glycine and 20% ethanolamine at 24 hours. Glycinamide was reacted over 5% Ru/C (1000 psi H<sub>2</sub> 100°C) with Ca(H<sub>2</sub>PO<sub>4</sub>)<sub>2</sub>/H<sub>2</sub>O, producing 72% ethanolamine, 14% ethylenediamine, 9% glycine and

2% ethylamine (Figure 1.46). Although the desired ethylenediamine product was produced, the reaction was still predominantly going through hydrolysis.

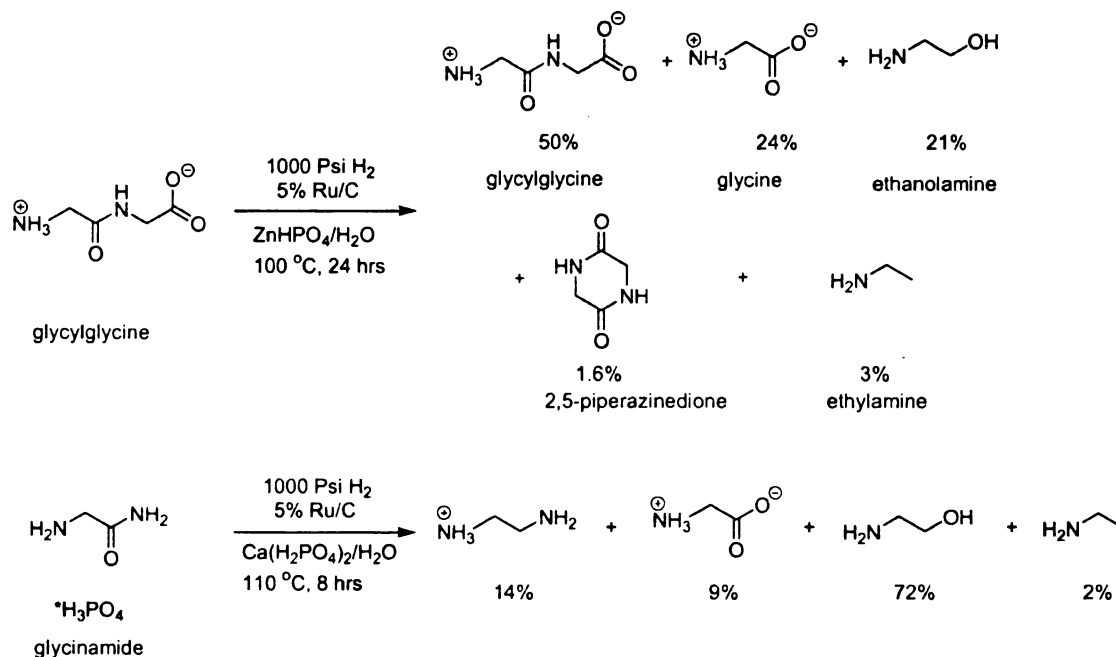


Figure 1.46 Catalytic hydrogenation (1000 psi H<sub>2</sub>, 100°C, 5% Ru/C) of glycyglycine (ZnHPO<sub>4</sub>/H<sub>2</sub>O) and glycylglycine (Ca(H<sub>2</sub>PO<sub>4</sub>)<sub>2</sub>/H<sub>2</sub>O)

Next, hydrogenation of glycyglycine in the presence of Zn[HN(C<sub>2</sub>H<sub>4</sub>NH<sub>2</sub>)<sub>2</sub>][HN(CH<sub>2</sub>COO)<sub>2</sub>] and Ca(H<sub>2</sub>PO<sub>4</sub>)<sub>2</sub>, was carried out at 130°C, 500 psi H<sub>2</sub> for 42 hrs. At 23 hrs, NMR analysis showed only slight conversion to the alcohol, glycyaminoethanol among a complicated mix of products with overlapping peaks.

In another attempt to prevent hydrolysis, the solvent was changed to a non-aqueous system. In the studies by Redko,<sup>32</sup> the ionic liquid (Me<sub>3</sub>N-HCOOH) was chosen assuming formic acid could play a role as the reducing agent, and still be separated easily from the final product. However, it can also react with primary and secondary amines forming an amide. It can also serve as a buffer preventing protonation of the

oligopeptide; thus preventing hydrogenation. Glycylglycine and  $\text{Me}_3\text{N-HCOOH}$  were refluxed for 4 hours at which time catalyst (5% Ru/C) was added and the reaction ran an additional 4 hours. Results by NMR showed partial conversion to 2,5-piperazinedione and glycine, but no hydrogenation products.

Polyphosphoric acid ( $\text{H}_6\text{P}_4\text{O}_{13}$ ) was also studied as a dehydrating agent to prevent hydrolysis of glycylglycine and also acidic enough to protonate the amide and accelerate the reaction. Under hydrogenation conditions of 660 psi  $\text{H}_2$ ,  $100^\circ\text{C}$ , 5% Ru/C, the reaction was run for 45 hrs. The only product detected using NMR and confirmed by HPLC was 2,5-piperazinedione.

Subsequent studies with 2,5-piperazinedione, under similar acidic conditions gave primarily the desired cyclic reduction product piperazine (25%), ethanolamine (30%), and ethylenediamine (20%) (Figure 1.47).

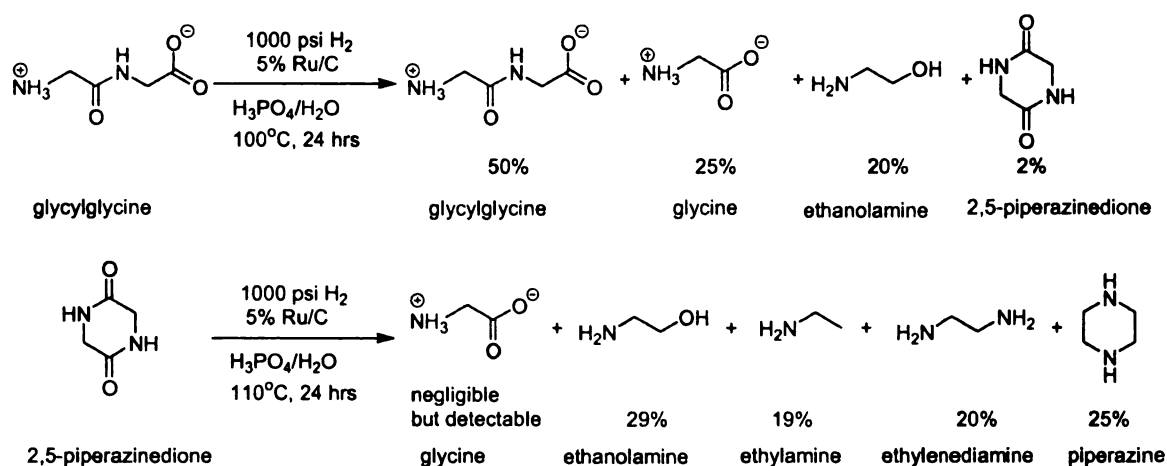


Figure 1.47 Catalytic hydrogenation of 2,5-piperazinedione with  $\text{H}_3\text{PO}_4/\text{H}_2\text{O}$  (1000 psi  $\text{H}_2$ ,  $100^\circ\text{C}$ , 1 g 5% Ru/C)



#### 1.3.1.2.1 Hydrolysis of Glycylglycine

One of the biggest challenges in Redko's studies was the hydrolysis of the amide under aqueous conditions. Mechanistic studies in the area of peptide hydrolysis have been found to very complicated due to the simultaneous reactions occurring in solution. Hydrolysis of the peptide bond, internal aminolysis, cyclization of the dipeptide to the diketopiperazine, and decomposition of product amino acids must be considered. Recent studies<sup>33-36</sup> by Steinberg and Radzicka describe the rate constants and mechanistic theory of peptide hydrolysis and diketopiperazine formation.

The results indicate equilibrium between glycylglycine and 2,5-piperazinedione, which occurs more rapidly than the hydrolysis to glycine in neutral solutions at 25°C (Figure 1.48).<sup>33-36</sup> The hydrolysis rate of peptide bonds is slow at ambient temperatures and the formation of the diketopiperazine is the major product at increased temperatures. The decomposition of tripeptides by Steinberg<sup>34</sup> supported the formation of the diketopiperazine as the major product during the decomposition of peptides, via the internal aminolysis reaction.

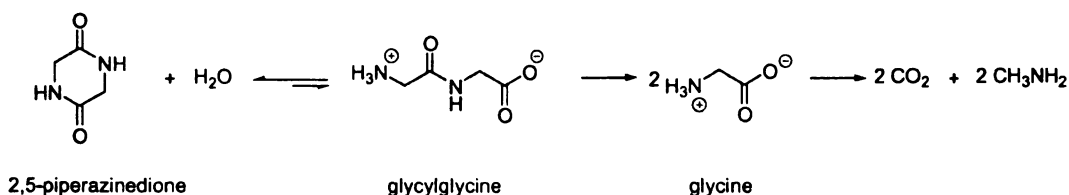


Figure 1.48 Equilibrium between 2,5-piperazinedione and glycylglycine at 25°C

One of the other most challenging portions of Redko's studies proved to be the limitations of product analysis. Quantitative NMR analysis was limited,<sup>32</sup> by the presence of paramagnetic metal ion impurities leached from the stainless steel reactor. In

addition, the NMR spectra of the compounds studied have many overlapping proton peaks making it difficult to distinguish among products. The presence of acid in solution was found to corrode the reactor, increasing dissolved metal ion concentrations and increasing difficulty with product analysis. In response to the difficult product analysis of amide hydrogenation, a direct method was solely needed. Such a method, which analyzes all possible hydrogenation and hydrolysis products quantitatively using High Performance Liquid Chromatography (HPLC) was developed, and the subject of the next chapter.

## **CHAPTER TWO**

### **ANALYTICAL METHOD DEVELOPMENT**

#### *2.1 Introduction*

The preliminary portion of this project was to develop a single quantitative method using High Performance Liquid Chromatography (HPLC) for the routine determination of specific amides, polyamides, their corresponding amines, and other related compounds (Figure 2.1) which may be present under the planned aqueous-phase catalytic hydrogenation conditions. High Performance Liquid Chromatography is often used because of its high sensitivity, reproducibility, and rapid analysis. However, the broad range of polarity and charge among the compounds analyzed in this work makes direct HPLC quantization difficult both in terms of separations and detector type. Simple amines and amino acids, typically present in their ionic or zwitterionic forms, are often analyzed by a combination of either pre- or postcolumn derivatization and reverse-phase column chromatography, with ultra violet (UV) or fluorescence detection. However, derivatization fails for most uncharged amides or carboxylic acids; and consequently limits its use in this work. Ionic species, on the other hand, under aqueous conditions are quantified using ion-chromatography. This type of separation is ideal for quantifying the amine products of interest and the other related side products.

With the above complexity in mind, mixed-mode separation was chosen to identify and quantify the compounds of interest. The mixed-mode column selected is specific for retaining basic compounds by a cation-exchange mechanism while retaining neutral compounds in a reverse-phase mechanism. In this particular case, the net charge of the compounds must be manipulated to allow for complete baseline separation of the

compounds of interest (Figure 2.2). This is done by simply changing the pH of the mobile phase under gradient conditions, and therefore limits the use of refractive index

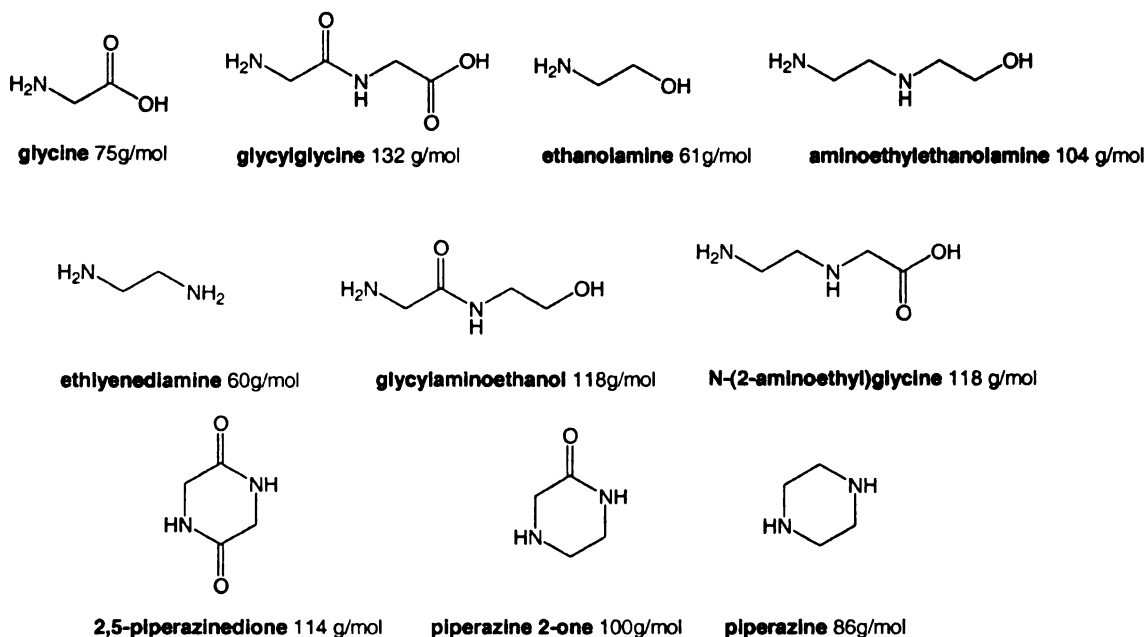


Figure 2.1 Amino acids and corresponding amines of interest

(RI) detection. As a result, the evaporative light-scattering detection (ELSD), a technique almost as versatile and general as RI was selected. This type of detector functions on the differences in volatility between the solvent and the sample. The key operation is the nebulization of volatile effluent from the column into a fine mist. The mist is carried through a heated drift tube which evaporates the mobile phase, leaving behind only non-volatile solute particles. The solute particles are carried at high speed through a beam of light; an off-axis photomultiplier then detects the scattered light. The amount of light scattered is dependent upon size and number of particles and is proportional to

concentration. The key is that all solutes must have a lower volatility than the mobile phase.

## *2.2 Experimental Procedures*

### *2.2.1 Materials*

Complete separation and quantitative analysis of all samples was performed on a Primesep<sup>®</sup> 100 mixed-mode column (3.2x150 mm, particle/pore: 5 $\mu$ m/100Å) (SIELC Technologies, Chicago, IL). A guard column (3.2x10 mm, particle/pore: 5 $\mu$ m/100Å) was also in place prior to the analytical column (SIELC Technologies, Chicago, IL). Acetonitrile used to make the mobile phase was HPLC grade, (Sigma-Alrich, St. Louis, MO). Trifluoroacetic acid (TFA) (99%) (Sigma-Alrich, St. Louis, MO) was stored under dry house nitrogen following each use. A Milli-Q ultrapure water purification system (Millipore, Billerica, MA) was used as the sole source of water. Additional filtration of the mobile phase upon entering the instrument was carried out using a Corning top filter nylon membrane (70mm membrane diameter, pore size 0.20 $\mu$ m) (Fisher Scientific, Pittsburgh, PA).

The chemical standards, glycine, glycyglycine, and 2,5-piperazinedione were purchased from Sigma-Alrich (St. Louis, MO), piperazine from Lancaster Synthesis Inc., (Pelham, NH), piperazine-2-one from Alfa-Aesar, (Ward Hill, MA), and N-(2-aminoethyl)glycine from Toronto Research Chemicals Inc. (North York, Ontario, Canada). Glycylaminoethanol is not commercially available.

All chromatography was performed using a Waters 600E HPLC pump (Waters, Milford, MA). Both UV 490E (Waters, Milford, MA), and ELSD 800 (Alltech, Chicago, IL) detection were carried out. The ELSD was used for all quantification and the UV

was used to monitor the gradient flow and equilibration confirmation. The evaporation tube temperature was set at 60°C and the nebulizer inlet gas (N<sub>2</sub>) pressure set at 3.00 bar.

All data acquisition and analyses were carried out using Star Chromatography Workstation (Version 6.20) (Varian Inc., Palo Alto, CA).

### 2.2.2 Methods

Running conditions of the mobile phase consisted of 10% acetonitrile in water with a TFA buffer gradient from 0.05% to 0.5% at a constant flowrate of 1mL/min. The HPLC was set at initial gradient conditions (10% acetonitrile in water, 0.05% TFA, (reservoir A)) for approximately one hour to allow the column to equilibrate. The gradient elution began with reservoir A at injection and proceeded from 0% to 100% reservoir B (10% acetonitrile in water, 0.5% TFA) over 7.5 min. Reservoir B was held for 5 min and then the gradient returned to initial conditions (reservoir A) over 3 min and held until the column equilibrated, approximately 10 minutes. Small peaks (< 10mV) at 9.5 and 14 min are systematic peaks resulting from the change in acid concentration and do not interfere with the compounds of interest. Mobile phase and water were injected as standards to account for any additional peak area interference. Control samples of water were run in the reactor and analyzed to identify any metal peaks present in the HPLC.

*Important Note:* For this experimental design, it was concluded that the source of water must be chosen carefully. By using an ion-exchange exchange column with such low sensitivity, any unpurified water increased baseline noise. The Milli-Q ultrapure water was found to keep the most stable baseline and reproducible results. Proper storage of TFA under nitrogen storage was also found essential for reproducible results. Lastly,

it is highly suggested to prepare fresh mobile phase just prior to use, but always keep the pump running.

*Calibration Setup:* Calibration curves were prepared from a mixed standard sample set, by using the dilutions (0.003, 0.005, and 0.007M) from a prepared stock solution (0.01M). One sample set consisted of 2,5-piperazinedione, ethanolamine, and piperazine. The second set consisted of glycine, glycylglycine and piperazine-2-one. The stock solutions and each subsequent dilution were prepared using water.

Four point (0.003, 0.005, 0.007 and 0.010M) linear calibration curves were used for the quantification of products in the parametric study. An initial single calibration method was created and used in all experimental analyses for the parametric study. Mixed standard solutions of the compounds, prepared initially and kept at 0°C, were injected each day to check for system performance and sample stability.

For the desorption study, four point (0.003, 0.005, 0.007 and 0.010M) quadratic calibration curves were used for all analysis. A new calibration method was created for each individual study, with standards prepared fresh each day.

### *2.3 Results & Discussion*

The analytical method development for the detection and quantification of amides, amines, amino alcohols, and amino acids proved to be challenging, yet necessary. The method developed is a direct method, with no derivatization needed, which detects all the compounds of interest for this study in less than 25 min. Nearly complete baseline separation is shown in a sample chromatogram (Figure 2.2) of a mixed standard at 0.007M. Retention times (min.) are as follows: 2,5-piperazinedione 1.0,

glycine 3.2, glycylglycine 4.3, ethanolamine 4.7, piperazine-2-one 5.2, N-(2-aminoethyl)glycine 9.2, ethylenediamine 10.2, AEEA 10.6, and piperazine 10.8. All peaks on the chromatogram have been accounted for. A small peak (<10mV) is present just prior to glycylglycine at 4.2 min. This was concluded to be the detection of metals from the reactor, an interpretation supported by 1) the observation of this peak in HPLC analyses of water that been heated in the Parr reactor with catalyst and hydrogen alone, but no substrate, and 2) the absence of observable  $^1\text{H}$  NMR peaks, other than that for HOD, in the blank sample.

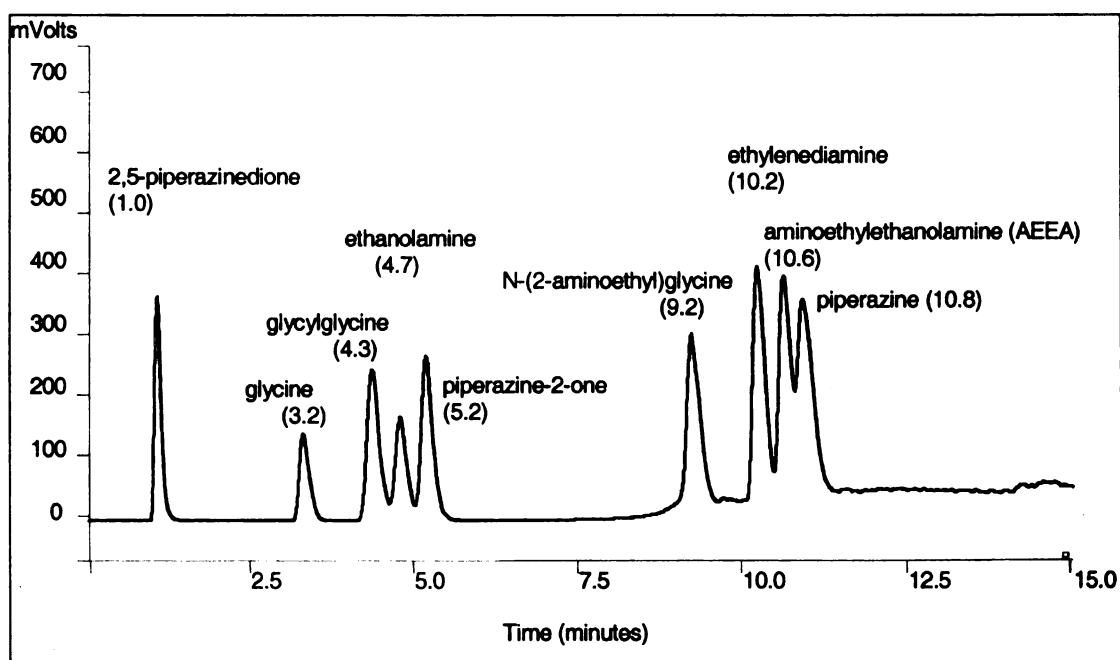


Figure 2.2 Sample chromatogram of amides, corresponding amines, and aminoalcohols

The initial calibration method created used a linear fit. However, over time (7 months) the ELSD response at lower concentrations (0.003 and 0.005M) was found to be non-linear. At these low concentrations the analyte may not form droplets readily, and



thus may produce a weak signal resulting in a non-linear response. A non-linear calibration curve (quadratic fit) might be better for future experimental analyses.

In addition, the standard solutions used for the analysis of the parametric study were unstable over time, even when refrigerated. In standard set 1, the concentration of the 2,5-piperazinedione slowly decreased, and glycylglycine was observed and its concentration increased slowly. The concentrations of ethanolamine, piperazine (set 1), glycine, glycylglycine, and piperazine-2-one (set 2) stayed constant. There was no indication of 2,5-piperazinedione formation in set 2. Therefore, it is suggested that standard mixes be prepared daily for any quantitative analysis.

Figure 2.3 shows a sample chromatogram of the separation of a selection of amino acids under the same HPLC running conditions as stated previously. Full separation of asparagine, proline, valine, cysteine, isoleucine and arginine was achieved. Glycine, glutamine and threonine co-elute at 2.7 min, while lysine and histidine co-elute at 8.8 min. Serine was not detected under these conditions. Further evaluation and manipulation of this method is underway to further separate all amino acids.

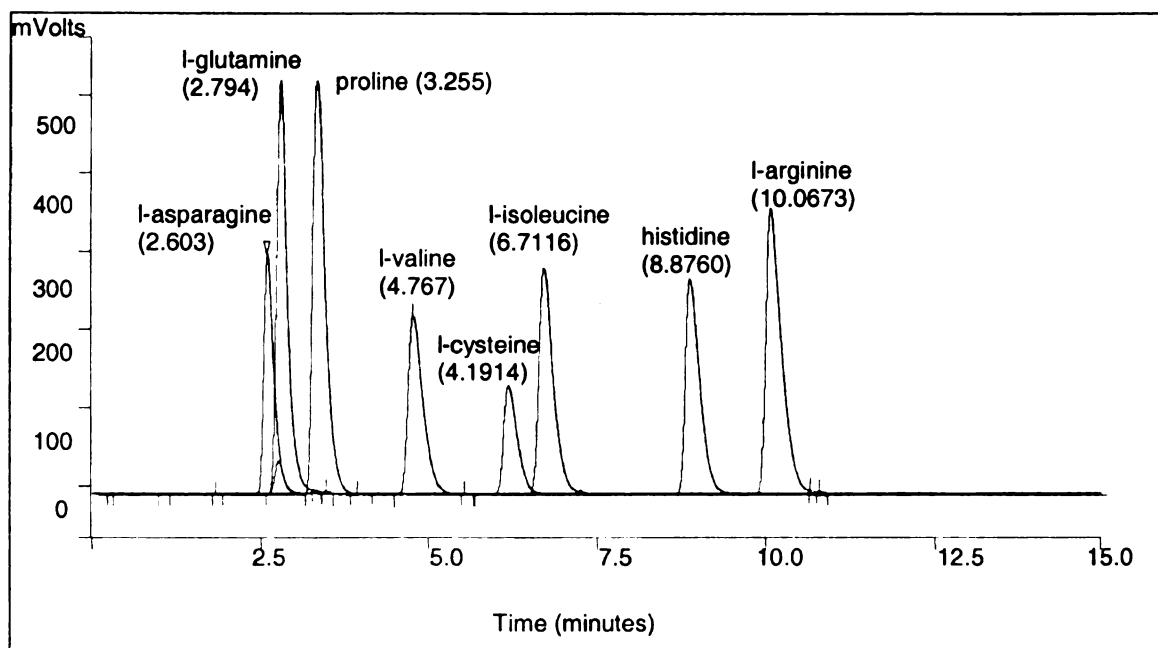


Figure 2.3 Sample Chromatogram of amino acid separation

## CHAPTER THREE

### CATALYTIC HYDROGENATION OF AMIDES TO AMINES

#### 3.1 Introduction

The primary goal of this project is to optimize heterogeneous catalytic reduction of an amide under aqueous conditions. It is the latter aspect of such a '*green*' process that poses the greatest technical challenge. Amide hydrolysis in water may be competitive with or faster than hydrogenation of the amide group itself.<sup>7</sup> Thus, the targeted amines are formed within a mixture of products also comprising amino acids, which themselves can be reduced to the corresponding amino alcohols. Such a reduction of a monomeric amino acid, L-alanine, has been explored in great detail in our laboratory. Under hydrogenation conditions (1000 psi H<sub>2</sub>, 100°C, 5% Ru/C in excess acid) L-alanine was reduced to 2-aminol-1-propanol in 91% yield. In these studies, it was found that the stereochemistry at the  $\alpha$ -carbon was retained. Selectivities and enantiometric excesses for L-alaninol were found >95%, and >99%, respectively.<sup>30, 31</sup> These studies confirmed that the carboxylic acid must be protonated to undergo complete reduction, as expected from simple thermochemical and pK<sub>a</sub> arguments.

From the work by Jere and others, the next step was to attempt hydrogenation of peptides. Hydrogenation of the simplest peptide, glycylglycine, was explored briefly in our laboratory<sup>32</sup> under the same conditions, (1000 psi H<sub>2</sub>, 100°C, 5% Ru/C in excess acid). As summarized in Chapter 1, a mixture of products was seen via <sup>1</sup>H NMR detection, showing 50% of unreacted starting material, 2% of its cyclic anhydride, 2,5-piperazinedione, hydrolysis to glycine (25%), and hydrogenation to ethanolamine (20%).

Subsequent studies with 2,5-piperazinedione, under similar acidic conditions gave 25% of the cyclic reduction product, piperazine, 29% ethanolamine, and 20% each of ethylenediamine and ethylamine (Figure 3.1).

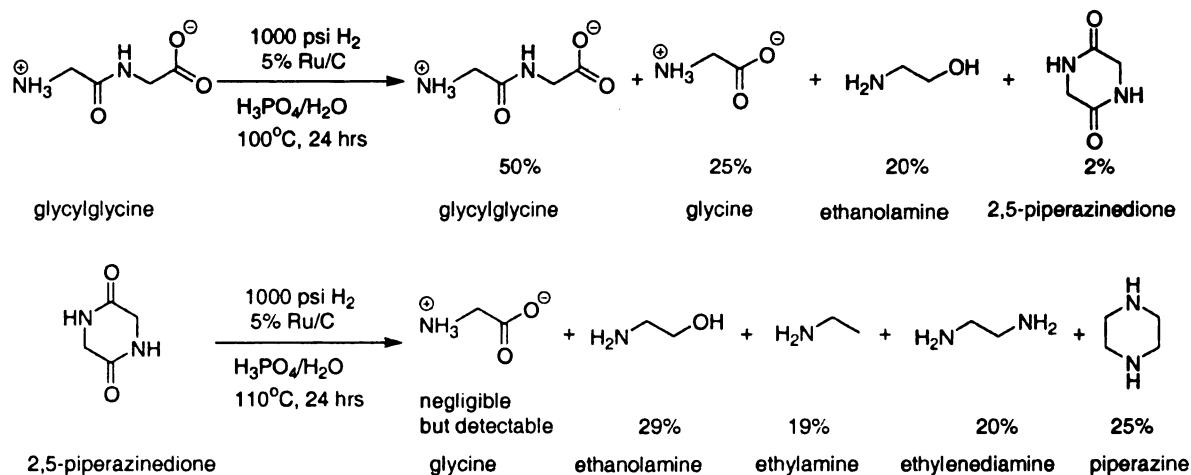


Figure 3.1 Catalytic hydrogenation of glycylglycine and 2,5-piperazinedione with H<sub>3</sub>PO<sub>4</sub>/H<sub>2</sub>O (1000psi H<sub>2</sub>, 100°C, 1 g 5% Ru/C)

In order to understand and control these competing hydrolysis and hydrogenation reactions further, a systematic experimental design was used to optimize conditions for aqueous amide reduction. The starting material chosen in this study, 2,5-piperazinedione, is a cyclic dipeptide formed from two residues of glycine, the simplest amino acid.

Figure 3.2 shows possible pathways for 2,5-piperazinedione conversion under hydrogenation conditions. The desired route is sequential hydrogenation of 2,5-piperazinedione via the piperazine-2-one intermediate to piperazine. Competing hydrolysis leads to ring opening of 2,5-piperazinedione to glycylglycine, a reversible process that favors the cyclic form at higher temperatures.<sup>33-36</sup> Glycylglycine itself undergoes further hydrolysis to glycine monomers. Glycylglycine may also undergo reduction in two ways: (1) at the amide, to form N-(2-aminoethyl)glycine, and (2) at the

carboxylate, to form glycylaminoethanol; the combination of these two reduction modes would form N-(2-aminoethyl)ethanolamine. Finally, as found by Jere, monomeric glycine may be reduced to ethanolamine. However, this reduction and presumably the one in (1) above require the protonated form of the carboxylate moiety; in the absence of added acid, carboxylate reduction should be minimal.<sup>30,31</sup> Thus, the main products downstream from 2,5-piperazinedione hydrolysis should simply be glycylglycine and glycine.

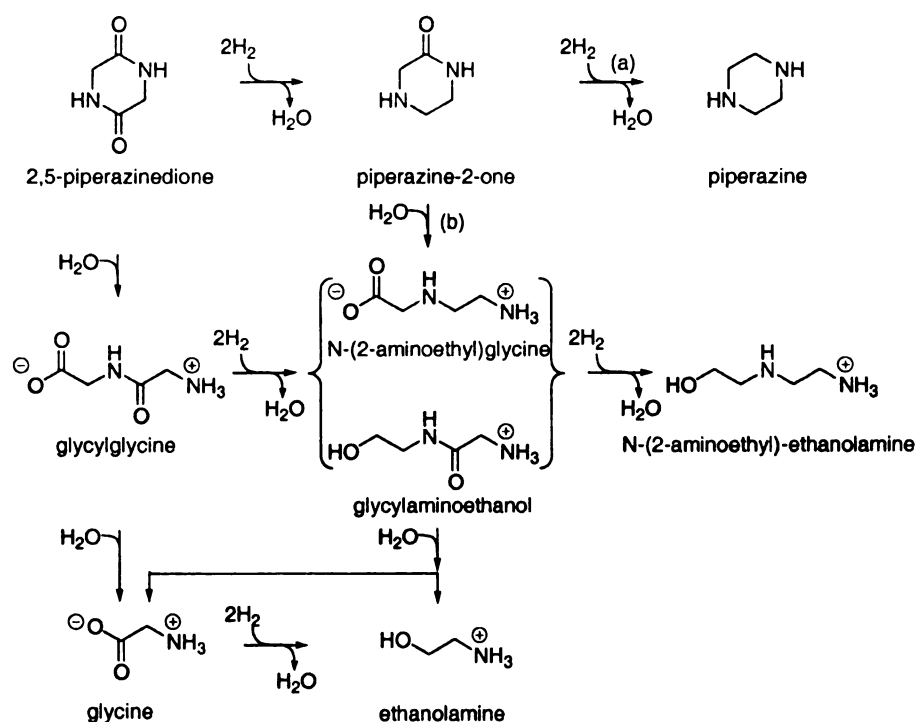


Figure 3.2 Possible reaction pathways of 2,5-piperazinedione

Despite the apparent simplicity of the scheme in Figure 3.2, several of the products may be formed via multiple paths, and even in processes not explicitly represented here. There are two modes of cleavage of the inferred 1,1-aminoalcohol intermediate formed by addition of  $\text{H}_2$  across the  $\text{C}=\text{O}$  moiety of an amide. The desired

path (a) releases water and forms the imine whose subsequent hydrogenation leads to the target amine. Path (b), however, is a C-N bond cleavage process, which produces the aldehyde and liberates the amine (or ammonia) that was bound in the amide.

One of the most challenging aspects of our preliminary amide studies was product analysis. Quantitative NMR analysis was limited,<sup>32</sup> by the presence of paramagnetic metal ion impurities leached from the stainless steel reactor. In addition, the NMR spectra of the compounds studied have many overlapping proton peaks making it difficult to distinguish among products. In response to the difficulties of NMR-based product analysis of amide hydrogenation, a direct method, High Performance Liquid Chromatography (HPLC), was developed to analyze all possible hydrogenation and hydrolysis products quantitatively (See Chapter 2).

Control of selectivity is critical to the success of any practical process. Among these many possible pathways, a multiparameter reaction optimization was set up using a Box-Behnken experimental design. In this approach, reaction variables are systematically varied between selected boundary values. The treatment combinations are at the midpoints of edges of the process space and at the center. The geometry of this design can be envisioned as a sphere occupying a cube, with the center (0,0,0) reactions at values corresponding together with a base set of conditions. This suggests the surface of the sphere within the process space protrudes through each face with the surface of the sphere tangential to the midpoint of each edge of the space. These designs are rotatable and require 3 levels of each factor. For this experiment, three reaction conditions were chosen; temperature, pressure, and catalyst loading ( $x_1, x_2, x_3$ ) as independent variables, respectively. The following parameter set points were used: Temperature: 90, 110, and

130°C; Hydrogen pressure: 500, 1000, and 1500 psi; Catalyst loading: 0.3, 1, and 3 g (dry weight basis) of 5% Ru/C.

Results from this survey of parameters space (e.g. yields, selectivities, reaction time to completion, costs, etc.) are then fit to an idealized empirical quadratic functional form which describes their local dependence on reaction conditions and reveals trends in product yields and optimum values. Figure 3.3 shows a representation of the Box-Behnken design. From these results, evaluations of the product yield, selectivity and conversion functions were carried out and the optimal conditions determined.

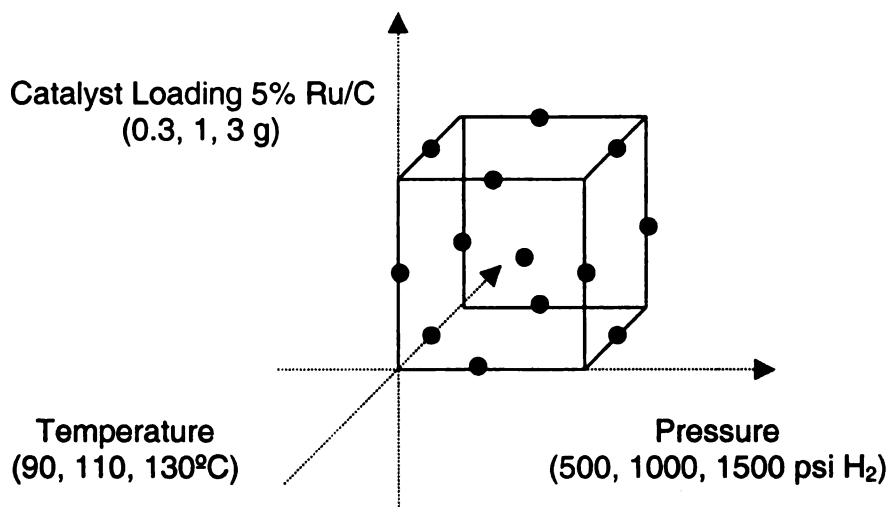


Figure 3.3 Box-Behnken Model

### *3.2 Experimental Procedures*

#### *3.2.1 Materials*

The starting substrate, 2,5-piperazinedione, celite, sodium hydroxide (NaOH) and analysis standards, glycine, and glycyglycine were purchased from Sigma-Alrich (St. Louis, MO), piperazine from Lancaster Synthesis Inc., (Pelham, NH), piperazine-2-one from Alfa-Aesar, (Ward Hill, MA), and N-(2-aminoethyl)glycine from Toronto Research Chemicals Inc. (North York, Ontario, Canada). Glycylaminoethanol is not commercially available.

A Milli-Q ultrapure water purification system (Millipore, Billerica, MA) was used as the sole source of water. Whatman #1 filter (42.5-mm cut to 15-mm) were purchased from (Whatman Co., Maidstone, England). Ultra high purity H<sub>2</sub> (AGA 99.999%) was used without further purification.

Syringe filters (Millex-GV 0.22  $\mu$ m PVDF 33 mm non-sterile, Millipore, Billerica, MA) were used to filter all samples from the reactor prior to analysis using the HPLC. The catalyst used in these experiments was 5% ruthenium metal on activated carbon support (5% Ru/C) (Johnson Matthey-Tennessee, Sevierville, TN). All pH measurements were taken on a digital Chemcadet pH meter (Model 5984-50) (Cole-Palmer Instruments Co., Chicago, IL).

All reactions were carried out in a 300 mL batch reactor (Series 4560, Parr Instrument Company, Moline, Illinois) made of 316 stainless steel, equipped with a magnetic driven impeller, liquid sampling condenser, gas sampling vent for real-time analysis, and a heating mantle for controlling the temperature of reactor ( $\pm 1^\circ\text{C}$ ).



### 3.2.2 Methods

*Catalyst Reduction:* Prior to the start of each reaction, the catalyst (2.0136g wet basis is equal to 1.000g dry basis) was reduced under the following conditions. The appropriate amount of catalyst was placed into the reactor, which was then sealed, purged three times with hydrogen, and finally pressurized to 200 psi H<sub>2</sub>. The temperature was then set to 250°C. The reduction was carried out overnight for an average of 14 hrs, at which time the reactor was cooled to room temperature and the remaining hydrogen was vented.

*Sample preparation:* All reactions were carried out using freshly prepared 0.1M substrate (2,5-piperazinedione) loading, dissolved in water. At room temperature, the reactor vessel was charged with the starting substrate, and purged with hydrogen (200-300 psi) three times. The reactor temperature was set to the desired temperature (90, 110, or 130°C). Once the reactor reached the desired temperature, the vessel was pressurized with H<sub>2</sub> to the desired pressure (500, 1000, 1500 or 1800 psi), and the stirring set to 1000 rpm. A portion of the charged substrate (~2 mL) always remained in the sidearm of the charge vessel and was used as a control for the initial concentration of substrate, which did not come in contact with either hydrogen or catalyst.

Samples (~2mL) were taken through the sampling condenser attached to the reactor at zero minutes, defined as the time in which hydrogen is introduced into the system at the desired temperature, every fifteen minutes up to one hour, and every hour thereafter up to either six or twenty four hrs. Each sample taken from the reactor was filtered using a syringe filter to remove suspended catalyst particles, had its pH recorded, was diluted (20-fold) to lie within the center of the calibration curve, and analyzed

immediately by HPLC (See Chapter 2). No calibration for ethylenediamine or AEEA was performed so only qualitative results are reported.

*Product Evaluation:* For each individual experiment, reaction conversion (Eq. 1), selectivity (Eq. 2) and product yields (Eq. 3) were calculated using the following equations:

$$\% \text{ conversion} = \frac{\text{moles of reactant consumed}}{\text{moles reactant fed}} \times 100 \quad (\text{Eq. 1})$$

$$\% \text{ selectivity} = \frac{\text{moles of product of interest}}{\text{moles reacted}} = \frac{\% \text{ conversion}}{\% \text{ yield}} \times \frac{1}{100} \quad (\text{Eq. 2})$$

$$\% \text{ yield} = \frac{\text{moles of product formed}}{\text{moles reactant fed}} \times 100 \quad (\text{Eq. 3})$$

Equation 4 was used for regression analysis;

$$Y = b_0 + b_1x_1 + b_2x_2 + b_3x_3 + b_{12}x_1x_2 + b_{13}x_1x_3 + b_{23}x_2x_3 + b_{11}x_1^2 + b_{22}x_2^2 + b_{33}x_3^2 \quad (\text{Eq. 4})$$

where Y=yield,  $x_1$ =pressure,  $x_2$ =temperature and  $x_3$ =catalyst loading

*Control Experiments:* Control experiments were carried out to verify the effect of reaction parameters and intermediate product fate. A typical reaction with 2,5-piperazinedione (0.1M) in the absence of *either* hydrogen or catalyst was carried out. The reactions run in the absence of hydrogen were run with helium (1000 psi). The catalyst was reduced as previously stated with hydrogen, but purged with helium before charging with starting material.

Glycylglycine, piperazine-2-one and piperazine were run individually under the following hydrogenation conditions: 1000 psi  $H_2$ , 110°C, 1 g 5% Ru/C with 0.1M

substrate loading for six hrs. Glycylglycine and piperazine were also run with 3 g 5% Ru/C loading.

*Desorption of products:* Using a Pasteur pipette, (3-5 mL at a time), the entire reaction solution was slowly introduced into a half inch glass column with a fitted frit, layered with filter paper (Whatman #1) glass wool and Celite (~1.5 g). House N<sub>2</sub> was used to push the remaining liquid through the column. Once all the catalyst was filtered through the reaction solution, the column was eluted with hot water (90-95°C) (two times the volume of reaction solution), followed by 1M NaOH, (volume equivalent to the reaction volume). All filtrate fractions were clear, and therefore not filtered. Filtrate fractions from the initial filtration and hot water washes were diluted (20x) with water. Base washes were diluted (20x) with 10% acetonitrile (0.05% TFA) (mobile phase). Each fraction was analyzed immediately using HPLC.

### *3.3 Results & Discussion*

#### *3.3.1 Box-Behnken Model*

Following completion of the experiments based on the Box-Behnken model, regression analysis predicted increased pressure, temperature and catalyst loading as the optimal conditions for high yield of piperazine. This prediction is based from the center of the cube using 1000 psi H<sub>2</sub>, 110°C and 1 g catalyst loading (5% Ru/C) as the base conditions. For maximum yield at six hrs, the predicted conditions were 1000 psi H<sub>2</sub>, 111°C, and 2.7 g 5% Ru/C for 10% piperazine yield or at 1800 psi H<sub>2</sub>, 114°C, 3.8 g 5% Ru/C, 29% piperazine yield. Figure 3.4 shows the plot of experimental yield versus predicted yield at six hrs, (80% R<sup>2</sup> value).

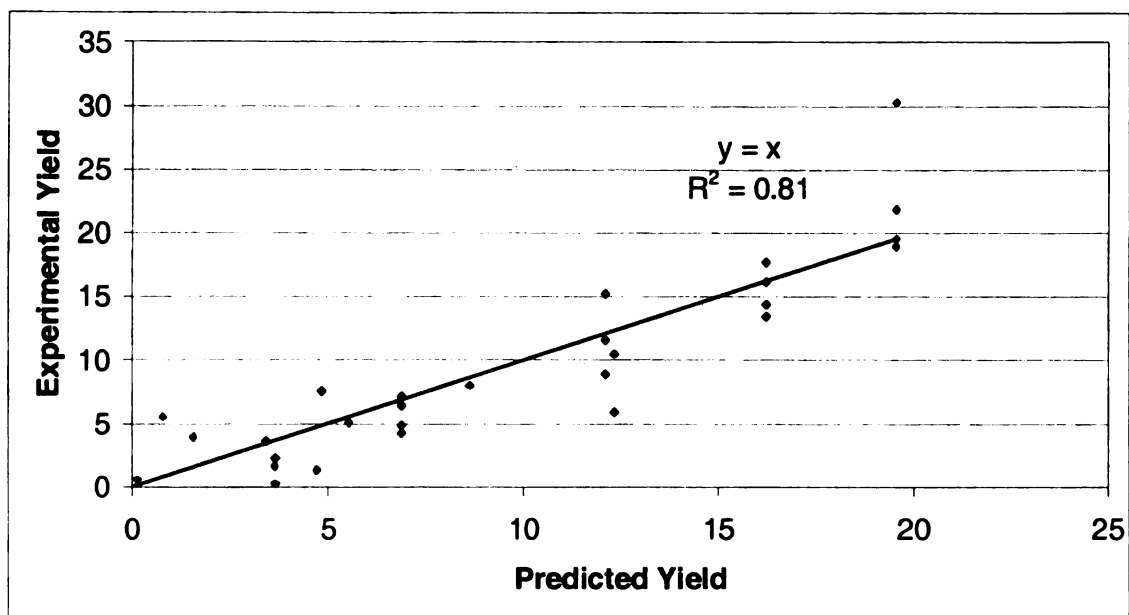


Figure 3.4 Regression analysis of predicted %yield versus experimental % yield

Experimental yields from the Box-Behnken model indicated lower temperature with higher pressure and catalyst loading increased product yield. Results of the experiments conducted using the Box-Behnken model at six hrs are shown in Table 3.1. Optimizing for piperazine selectivity rather than yield may have been a better choice, even if reaction rate decreased. Therefore, additional experiments were carried out beyond the experimental design of the Box-Behnken model to verify the true optima along with the predicted trend of laboratory data.

#### 3.3.1.1 Effect of Temperature

The effect of temperature at 1500 psi H<sub>2</sub> and 3 g Ru/C is shown in entries 12, 14 & 17 (Table 3.1, Figure 3.5 A). As the temperature is increased from 90 to 110°C, the yield of piperazine increases from 8 to 23%. Increasing temperature from 110 to 130°C decreases the yield to 15%. The effect of temperature on the rate of conversion is shown in Figure 3.5 B. Overall, increased temperature increases the rate of conversion.

### 3.3.1.2 Effect of Pressure

The experimental results from the Box-Behnken model at six hrs show that increasing pressure may not necessarily increase yield (Table 3.1, Entries 14 and 19, Figure 3.6). At both 1500 and 1800 psi H<sub>2</sub>, 110°C, 3 g 5% Ru/C, only 23% piperazine forms. Figure 3.7 shows the effect of pressure (1000, 1500 and 1800 psi H<sub>2</sub>) on all product yields at 90°C, 3 g 5% Ru/C. At 1000 and 1500 psi H<sub>2</sub>, piperazine-2-one has the highest yield overall, 6% at six hrs. At 1800 psi H<sub>2</sub>, piperazine yield is equal to piperazine-2-one at 4 hrs. but continues to increase, as piperazine-2-one yield decreases, reflecting hydrogenation of piperazine-2-one to piperazine. At 1000 and 1500 psi H<sub>2</sub>, glycylglycine forms at the same rate of piperazine-2-one, but at elevated pressure (1800 psi H<sub>2</sub>), glycineglycine continues to form at 5 hrs. whereas piperazine-2-one yield starts to decrease. In addition, ethanolamine is detected (2%) only at the elevated pressure.

### 3.3.1.3 Effect of Catalyst Loading

Increased catalyst loading increased product yields at six hrs. For example, piperazine yield increased from <1 (0.3 g Ru/C) to 7.5% (3 g 5% Ru/C) at 1000 psi H<sub>2</sub>, 90°C, and from 3.6 (1 g 5% Ru/C) to 8.2% (3 g Ru/C) at 1500 psi H<sub>2</sub>, 90°C (Table 3.1, Entries 5 & 6 and 11 & 12 respectively). Entries 13, 16 and 17, (Figure 3.8 A, B, and C) show an increase in piperazine yield from 8 to 12 to 16% as catalyst loading is increased from 0.3, to 1 and then 3 g 5% Ru/C at 1500 psi H<sub>2</sub>, 130°C. All intermediate product yields are shown; at higher catalyst loading, piperazine is primarily formed, whereas glycylglycine is the primary product formed at the lower catalyst loadings.

Further increases in catalyst loading from 3 g to 6 g 5% Ru/C, do not show an increase in piperazine yield, but similar trends in product formation, at a slower rate (Figure 3.9). Piperazine-2-one, on the otherhand, did form faster with increased catalyst loading (12% with 6 g 5% Ru/C) versus <10% with 3 g 5% Ru/C. With the increased catalyst loading piperazine-2-one yield drops rapidly at 2 hrs., whereas with 3 g 5% Ru/C the amount of piperazine-2-one yield is steady

Table 3.1

Reaction Conditions					Experimental % yield (6 hrs)						
entry	P (psi)	H <sub>2</sub>	T (°C)	Ru/C (g)	G	GG	EA	P2	P	% Selectivity P (% conversion PD)	Material Balance
1	500		90	1	0	1.8	0	2.7	<1	2.0 (28)	77
2 <sup>a</sup>	500		110	0.3	0	4.0	0	<1	1.0	4.7 (24)	81
3	500		110	3	0	12.0	0	9.3	5.1	5.7 (89)	37
4	500		130	1	1	18.5	0	7.0	5.5	7.5 (74)	58
5	1000		90	0.3	0	1.0	0	1.0	<1	1.2 (15)	88
6	1000		90	3	0	7.0	0	7.8	7.5	12.7 (60)	63
7	1000		110	0.3	0	6.0	0	3.6	1.7	4.9 (33)	78
8	1000		130	0.3	<1	14.9	<1	5.8	4.0	6.4 (62)	64
9 <sup>c</sup>	1000		110	1	0	9.8	0	7.0	7.2	9.9 (58)	67
10	1000		130	3	4.0	4.0	<1	0	1.4	1.4 (100)	10
11	1500		90	1	0	4.7	0	5.5	3.6	9.7 (37)	77
12 <sup>a</sup>	1500		90	3	<1	7.7	<1	7.7	8.2	9.8 (83)	41
13	1500		130	0.3	<1	16.6	<1	7.4	8.0	14.8 (54)	79
14 <sup>c</sup>	1500		110	3	<1	16.3	<1	4.6	22.7	22.8 (100)	47
15	1500		110	6	<1	10.8	<1	3.4	20.0	20.6 (100)	36
16 <sup>b</sup>	1500		130	1	3.0	19.0	<1	7.3	12.0	12.2 (98)	44
17 <sup>c</sup>	1500		130	3	<1	5.4	<1	<1	15.4	15.4 (100)	25
18 <sup>b</sup>	1800		90	3	0	8.2	0	6.1	12.7	13.9 (90)	37
19 <sup>a</sup>	1800		110	3	<1	13.6	<1	4.4	23.6	23.8 (100)	43

Table 3.1 Percent yield of all products for the reduction of 2,5-piperazinedione at 6 hrs

All reactions were run at the stated reaction conditions using 0.1M 2,5-piperazinedione (PD); G=glycine, GG=glycylglycine, EA=ethanolamine, P2=piperazine-2-one, P=piperazine

Results are expressed as <sup>a</sup> duplicate, <sup>b</sup> triplicate, or <sup>c</sup> quadruplicate measurements

Figure 3.5 The effect of temperature (90, 110 and 130°C), on yield (A) and conversion (B) of piperazine from 2,5-piperazinedione at 1500 psi H<sub>2</sub>, 3 g 5% Ru/C

Results are expressed as the average of duplicate (90°C) and quadruplicate (110 and 130°C) measurements. Error bars correspond to  $\pm$  SD

90°C (—■—), 110°C (—◆—), 130°C (—▲—)



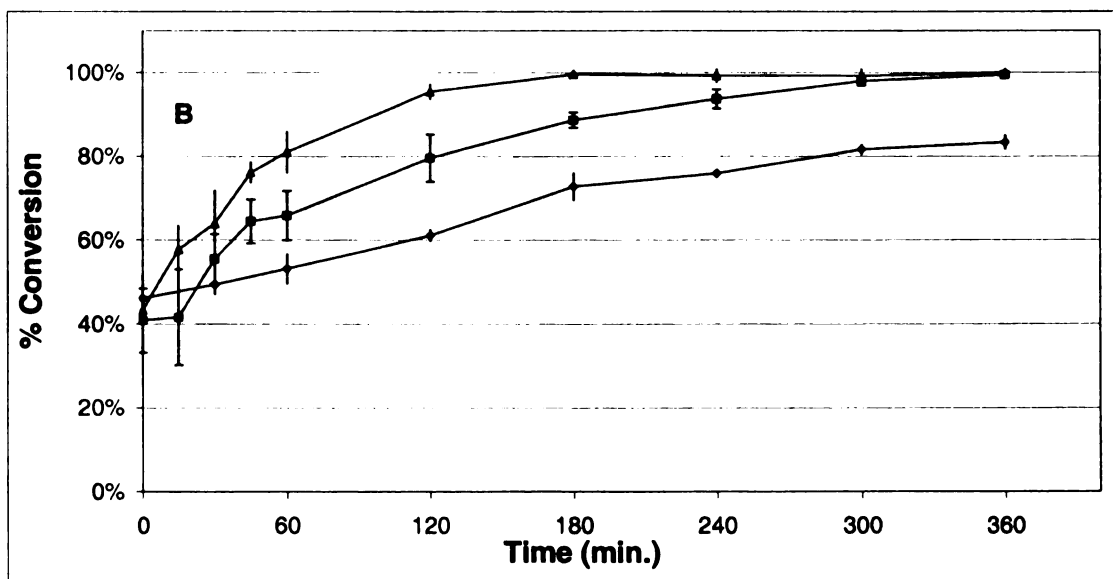
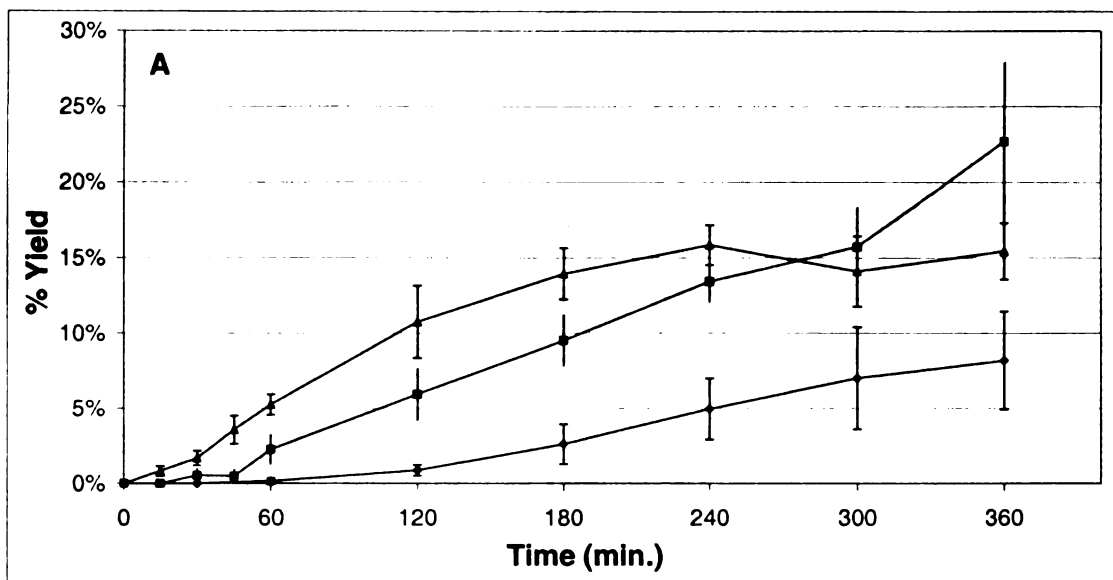


Figure 3.5

Figure 3.6 The effect of pressure (500, 1500, and 1800 psi H<sub>2</sub>) on % yield of piperazine from 2,5-piperazinedione at 110°C, 3g 5% Ru/C

Results 1500 psi H<sub>2</sub> are expressed at the average of quadruplicate measurements, and 1800 psi are the average of duplicate measurements. Error bars correspond to  $\pm$  SD

500 (—◆—), 1500 (—■—), and 1800 (—▲—) psi H<sub>2</sub>

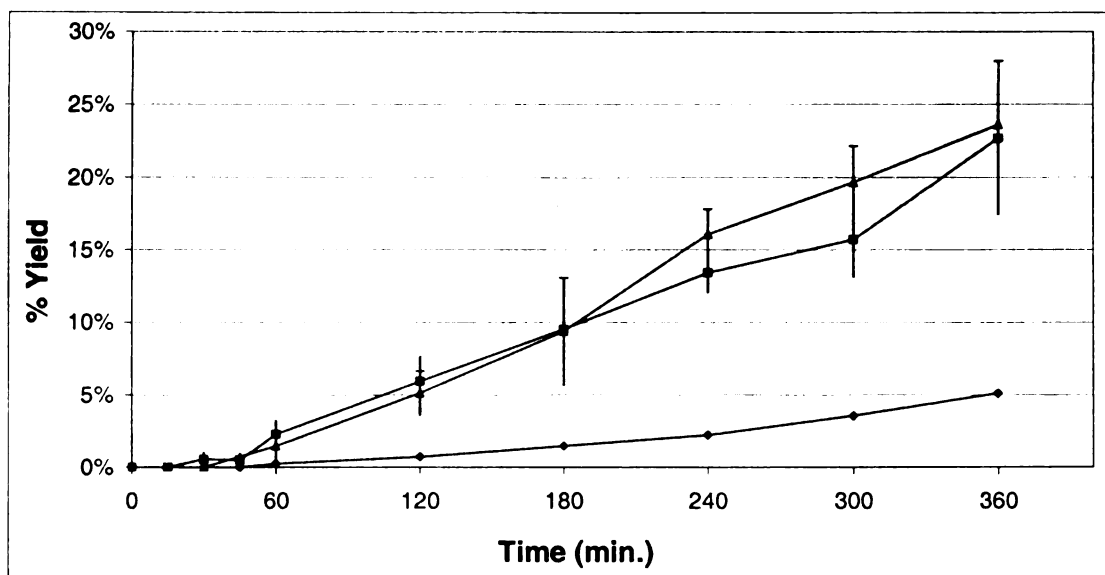


Figure 3.6

Figure 3.7 Product yields from the conversion of 2,5-piperazinedione at (A) 1000 (B) 1500 and (C) 1800 psi H<sub>2</sub>, 90°C, 3g 5% Ru/C

Results are expressed as the average of (B) duplicate and (C) triplicate measurements; Error bars correspond to  $\pm$  SD. ((A) n=1)

piperazine (—◆—), piperazine-2-one (—■—), glycylglycine (—✕—), glycine (—✱—), ethanolamine (—▲—)

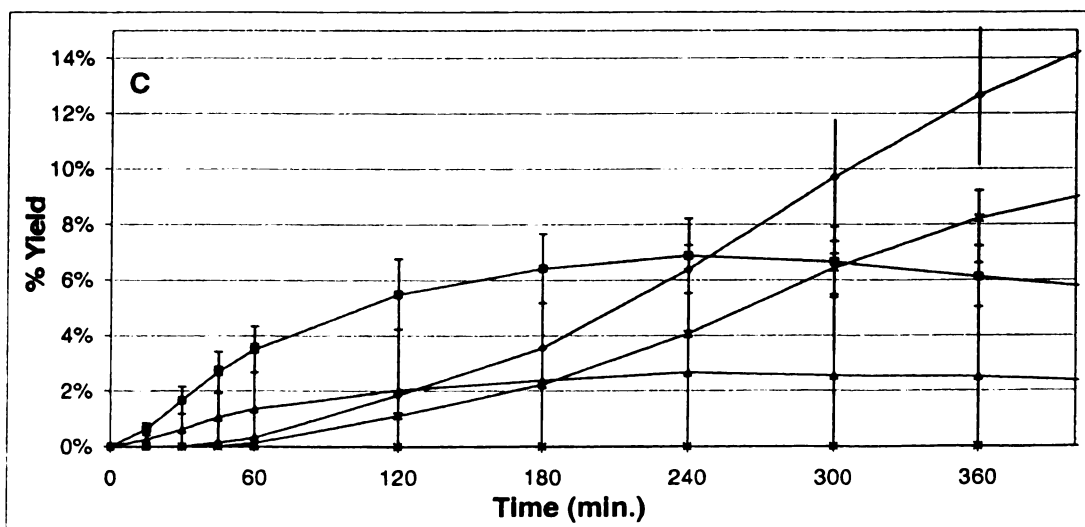
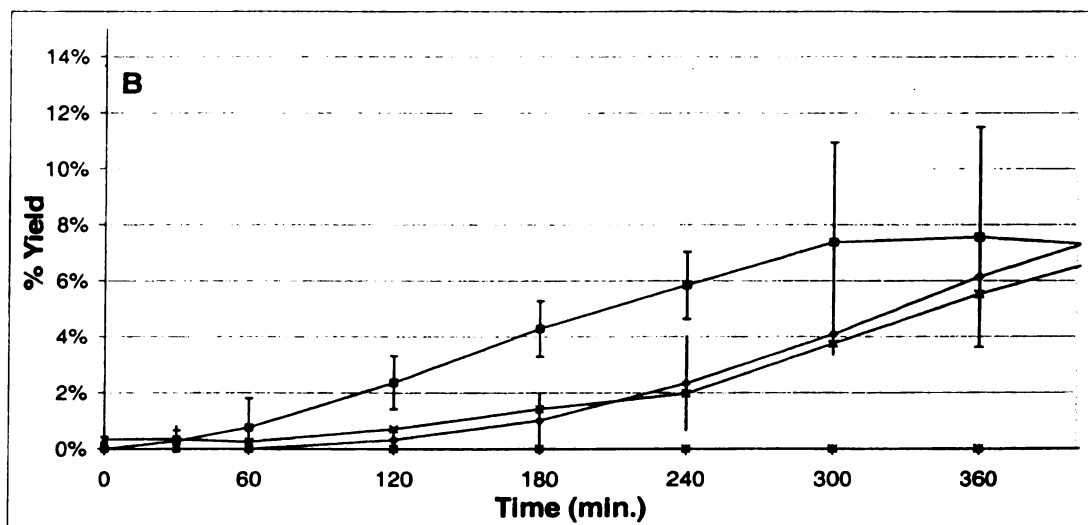
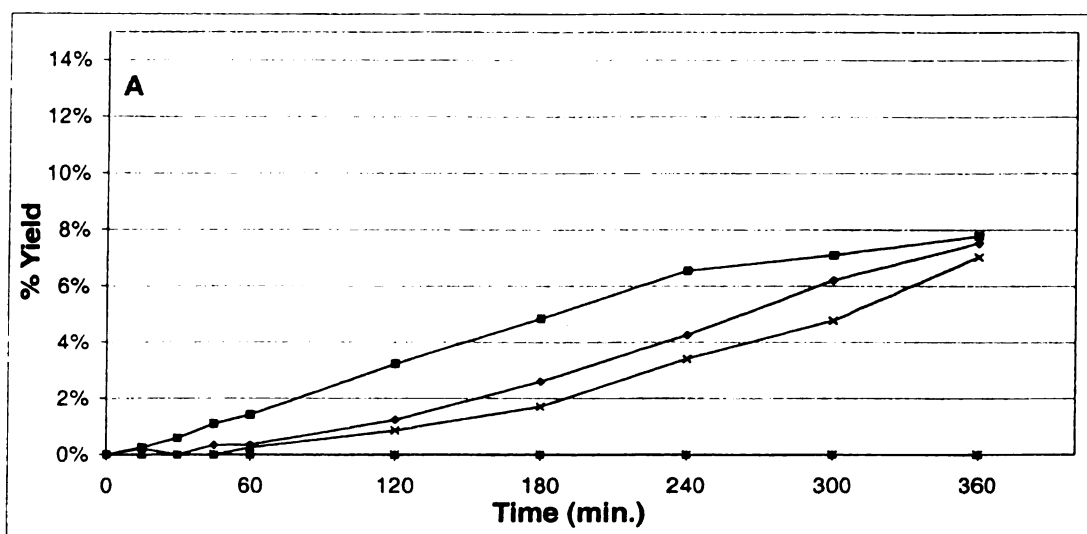


Figure 3.7

Figure 3.8 The effect of catalyst loading (A) 0.3 g, (B) 1 g, (C) 3 g 5% Ru/C on all product yields at 1500 psi H<sub>2</sub>, 130°C

Results are expressed as the average of (B) triplicate and (C) quadruplicate measurements; Error bars correspond to  $\pm$  SD. ((A) n=1)

piperazine (—◆—), piperazine-2-one (—■—), glycylglycine (—✕—), glycine (—✱—), ethanolamine (—▲—)

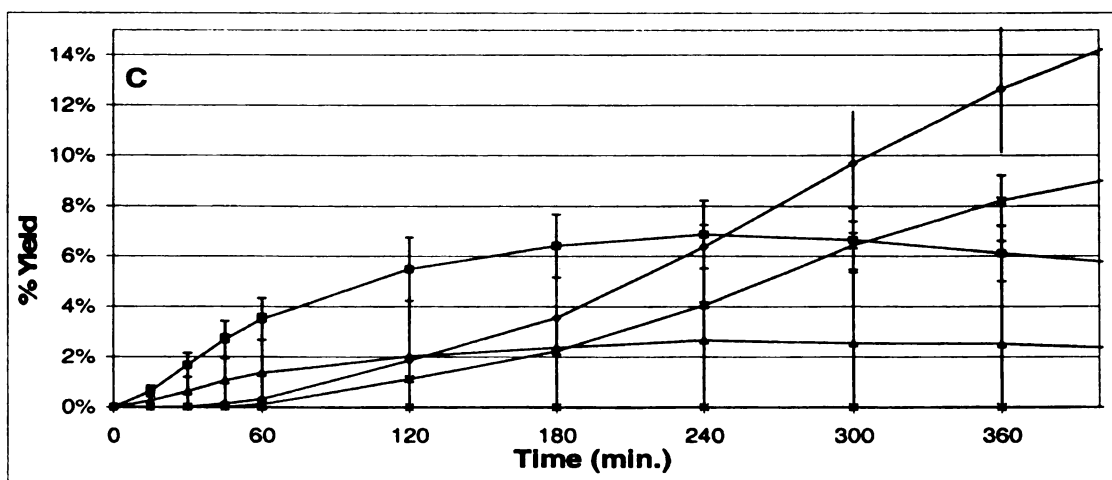
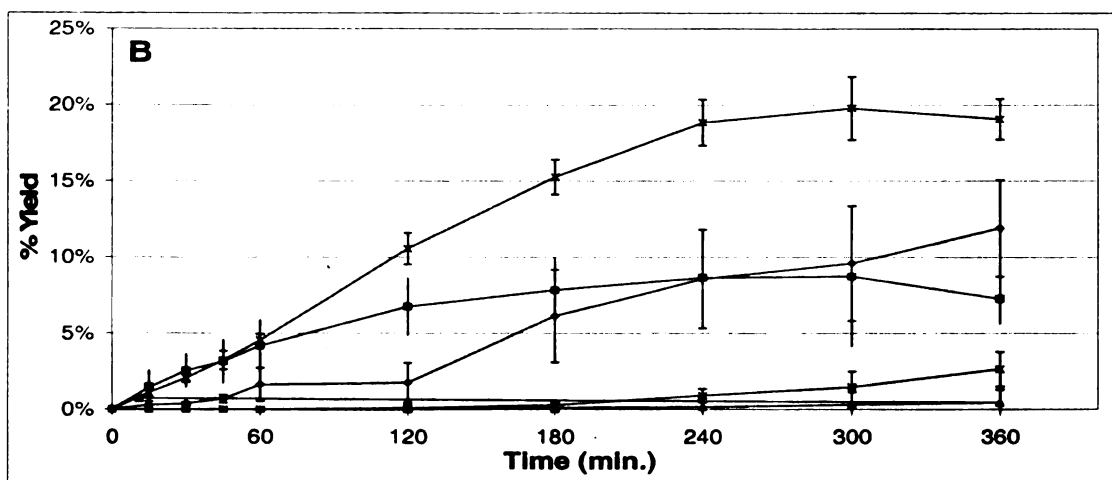
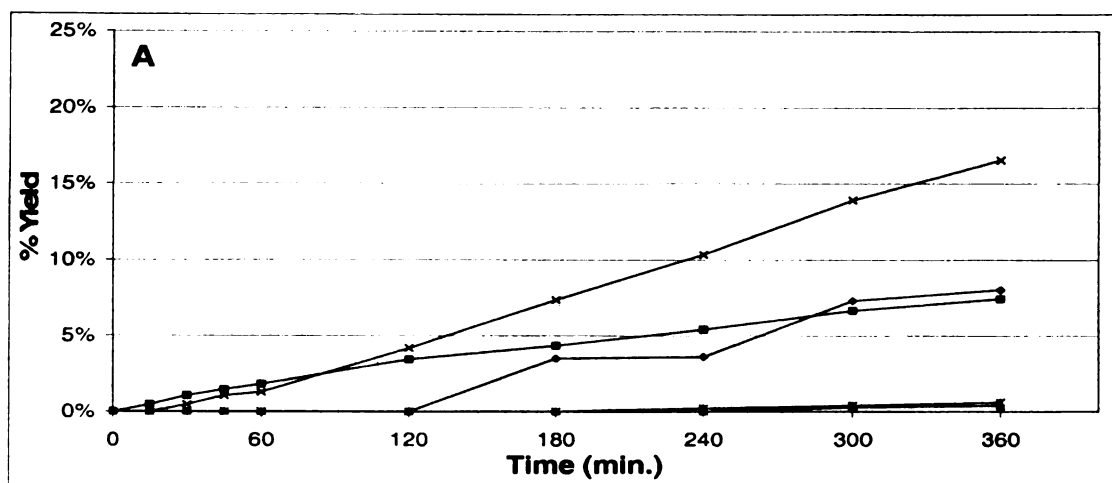


Figure 3.8

Figure 3.9 The effect increased catalyst loading on product yields on from (A) 3 g 5% Ru/C to (B) 6 g 5% Ru/C at 1500 psi H<sub>2</sub>, 110°C

(A) Results are expressed as the average of quadruplicate measurements; Error bars correspond to  $\pm$  SD. ((B) n=1)

piperazine (—◆—), piperazine-2-one (—■—), glycylglycine (—✕—), glycine (—✱—), ethanolamine (—▲—)



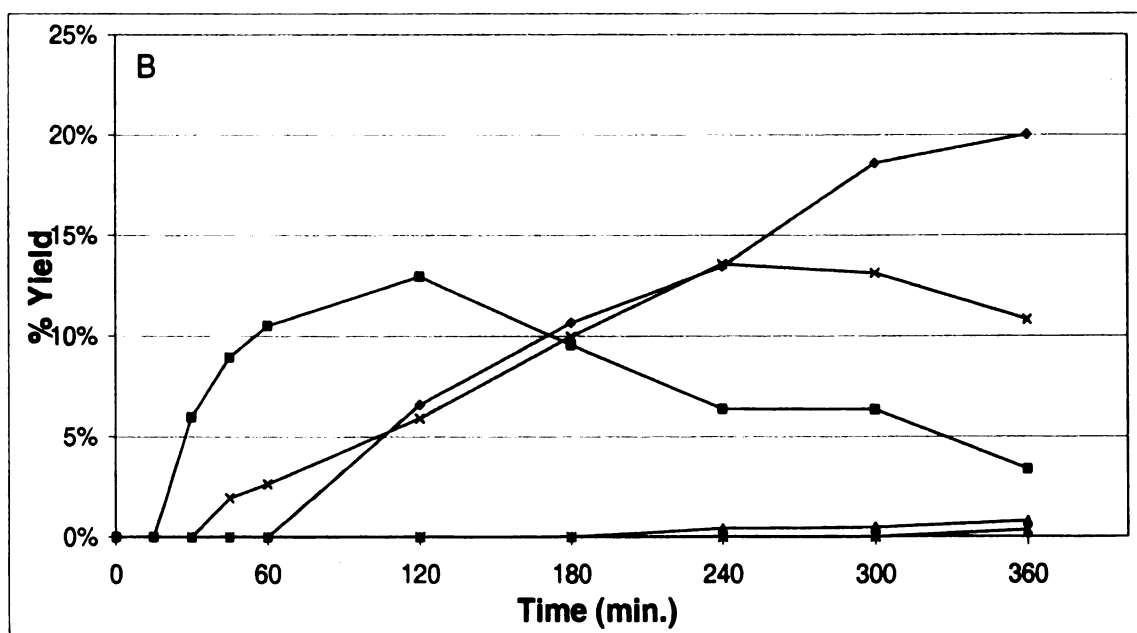
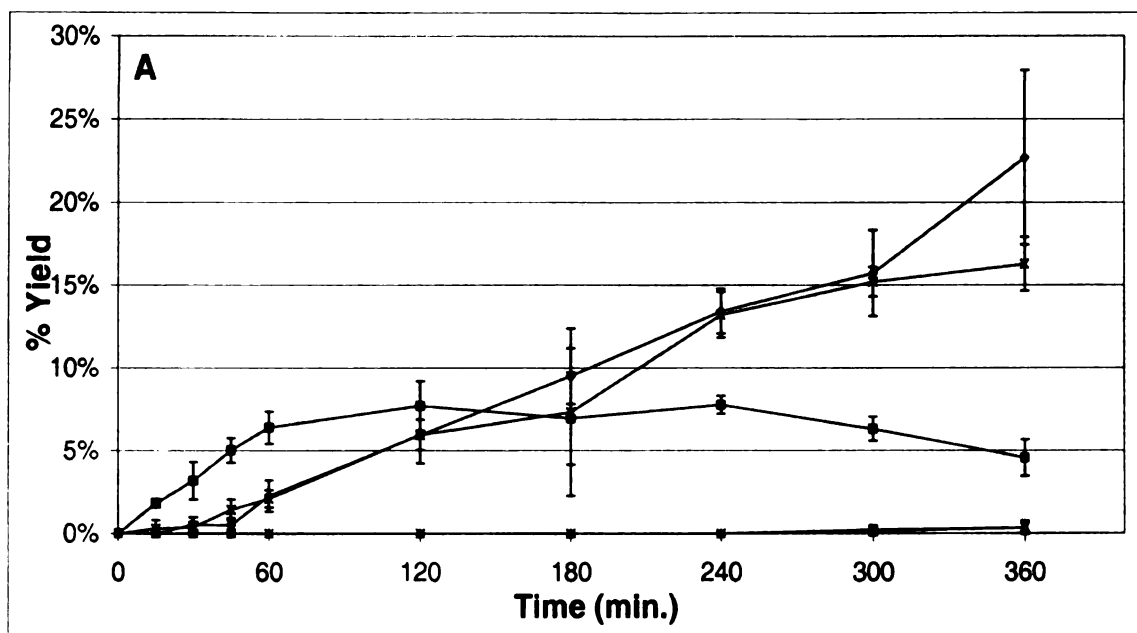


Figure 3.9

### 3.3.2 *Beyond the Boundaries of Box-Behnken Model*

In order to truly verify which set of conditions is optimal, experiments that lie beyond the parameters were repeated for an extended time (24 hrs). This was done to ensure that both 2,5-piperazinedione and piperazine-2-one, the partially reduced cyclic product, react to complete conversion to the desired product, piperazine. It also reflects the realization that piperazine was being destroyed at were otherwise fast conditions, and the fact that amide hydrolysis showed substantial temperature sensitivity. Table 3.2 shows the results at 100% conversion; a lower constant temperature (90°C) and higher catalyst loading (3 g 5% Ru/C) increases product yield from 28 to 37% at 1500 and 1800 psi, respectively (Entries 1 & 3). The change of temperature at 1500 psi H<sub>2</sub>, did not show any increase in piperazine yield, 28%. However, increasing temperature at 1800 psi H<sub>2</sub>, decreases piperazine yield from 37% to 26% (Entries 3 & 4). The conditions at 1800 psi H<sub>2</sub>, 90°C and 3 g catalyst (5% Ru/C) loading have been found to give the highest product yield, 37% (Entry 3).

Figure 3.10 is sample chromatogram series showing the evolution of piperazine formation over time at optimal conditions. Peaks at 4.2 and 9.2 are systematic peaks from the presence of metals in the reactor and changes in the acid gradient in the mobile phase.

Figures 3.11 and 3.12 show the effect of temperature at 1500 psi H<sub>2</sub>, 3 g 5% Ru/C and 1800 psi H<sub>2</sub>, 3 g 5% Ru/C on all product yields. At both pressure levels, the rate of piperazine formation is slower at the lower temperature (90°C). At 1500 psi H<sub>2</sub> and 110°C, the formation of piperazine levels off at ~27% at 12 hrs., but at 90°C, the formation of piperazine is still increasing. This is also true with 1800 psi H<sub>2</sub>. At 90°C, piperazine formation is still increasing at 24 hrs., but at 110°C, the yield of piperazine

starts to decrease at 12 hrs. The formation of ethylenediamine was detected, likely due to piperazine cleaving at elevated temperatures. No yield for ethylenediamine is reported.

It is also interesting to observe the fate of the intermediate products. Glycylglycine forms at the same rate as piperazine at 1500 psi H<sub>2</sub>, 110°C for the first six hrs, but then decreases. It would be reasonable to expect the yield of glycine would start increase at this point, but only 2% glycine formed over the course of 24 hrs. Piperazine-2-one at 1500 H<sub>2</sub>, 110°C, also formed at the same rate as piperazine, but after 4 hrs., the yield dropped from 7% yield to < 1% at 24 hrs. When the temperature was lowered to 90°C, piperazine-2-one formed at a faster rate than glycylglycine for 5 hrs., and leveled off at 7% yield over the 24 hrs. Glycylglycine yield slowly increase to ~12% at 12 hrs. and then leveled off.

At the higher pressure and temperature levels (1800 psi H<sub>2</sub>, 110°C), glycylglycine showed the same trend. At the lower temperature, (1800 psi H<sub>2</sub>, 90°C), glycylglycine quickly formed a maximum yield of 14% at 5.5 hrs. and decreased to ~10% over the 24 hrs.

From these results, we can see the effects of temperature and H<sub>2</sub> pressure on the rate of formation of not only piperazine, but also the intermediate products. Control experiments were run at the intermediate pressure and temperature conditions (1000 psi H<sub>2</sub>, 110°C) to monitor intermediate reactions at a slower reaction rate.

**Table 3.2**

<b>Reaction Conditions</b>				<b>% yield (24 hrs)</b>				
<i>entry</i>	<i>P (psi) H<sub>2</sub></i>	<i>T (°C)</i>	<i>Ru/C (g)</i>	<i>G</i>	<i>GG</i>	<i>EA</i>	<i>P2</i>	<i>P</i>
1 <sup>a</sup>	1500	90	3	<1	9.47	<1	<1	27.8
2	1500	110	3	1.9	5.6	2.4	0	28.1
3 <sup>b</sup>	1800	90	3	1.3	9.9	2.1	0	37.0
4 <sup>a</sup>	1800	110	3	5.2	1.9	1.7	0	26.2

Table 3.2 Percent yield of all products for the reduction of 2,5-piperazinedione at 24 hrs.

All reactions were run at the stated reaction conditions using 0.1M 2,5-piperazinedione (PD); G=glycine, GG=glycylglycine, EA=ethanolamine, P2=piperazine-2-one, P=piperazine

Results are expressed as <sup>a</sup> duplicate, or <sup>b</sup> triplicate measurements

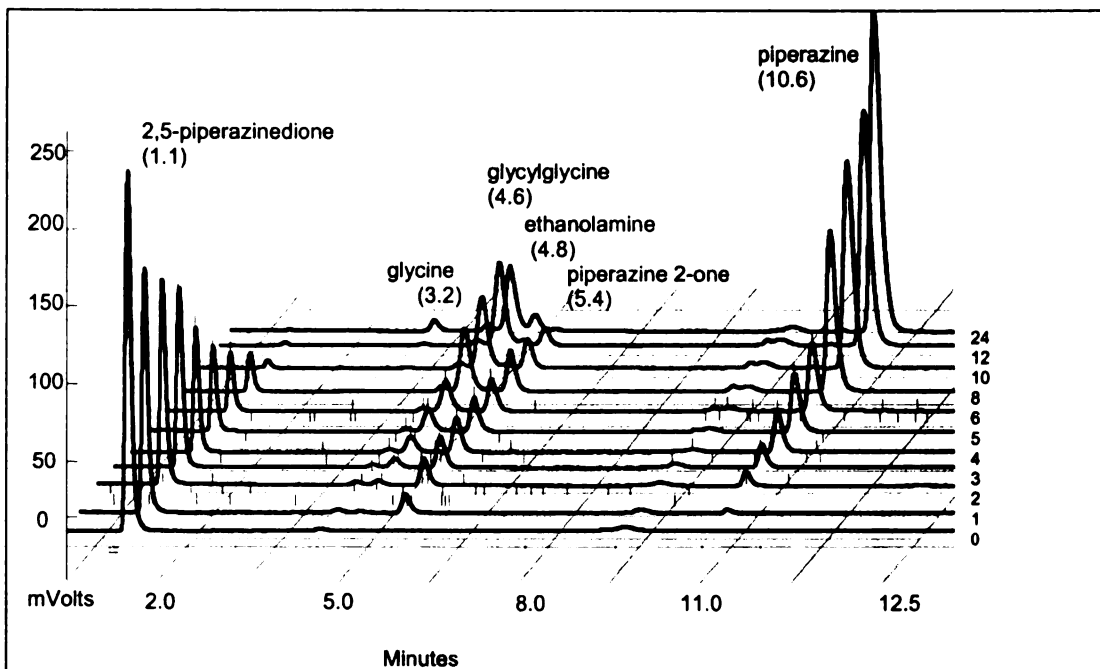


Figure 3.10 Representative chromatogram series of 2,5-piperazinedione hydrogenation to piperazine at 1800 psi H<sub>2</sub>, 90°C, 3 g 5% Ru/C

Retention times (min.) are as follows: 2,5-piperazinedione 1.1, glycine 3.2, glycyglycine 4.6, ethanolamine 4.8, piperazine-2-one 5.4, piperazine 10.6. Peaks at 4.2 and 9.2 min are systematic impurities.

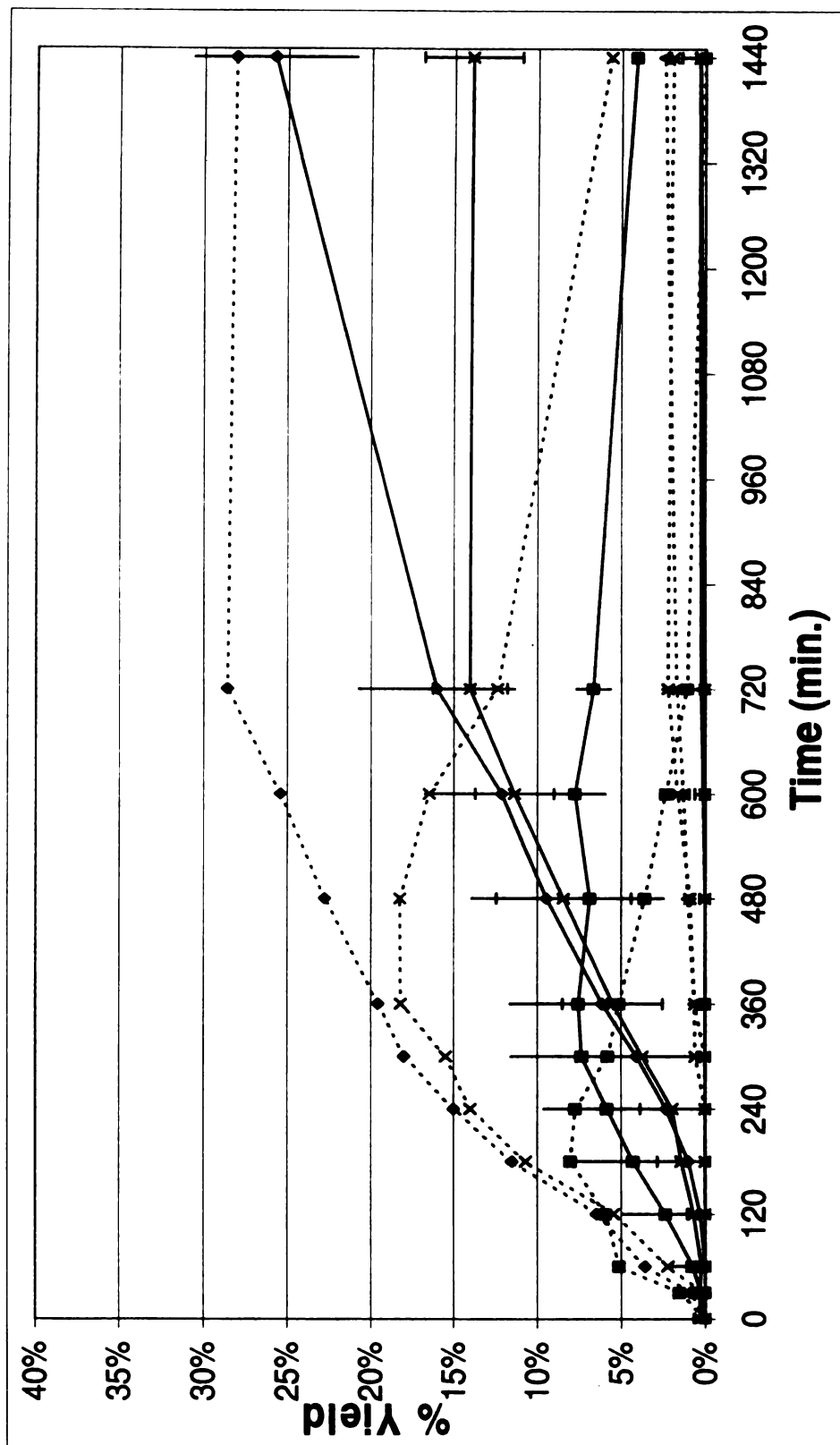


Figure 3.11 Effect of temperature on % yield at 1500 psi H<sub>2</sub>, 3 g 5% Ru/C

Results are expressed as the average of duplicate (90°C) measurements; Error bars correspond to  $\pm 1$  SD. Error bars not observed are smaller than the symbols. ((110°C, n=1)

piperazine (♦), piperazine-2-one (■), glycylglycine (x), glycine (x), ethanolamine (▲); 110°C(-----), 90°C(—)

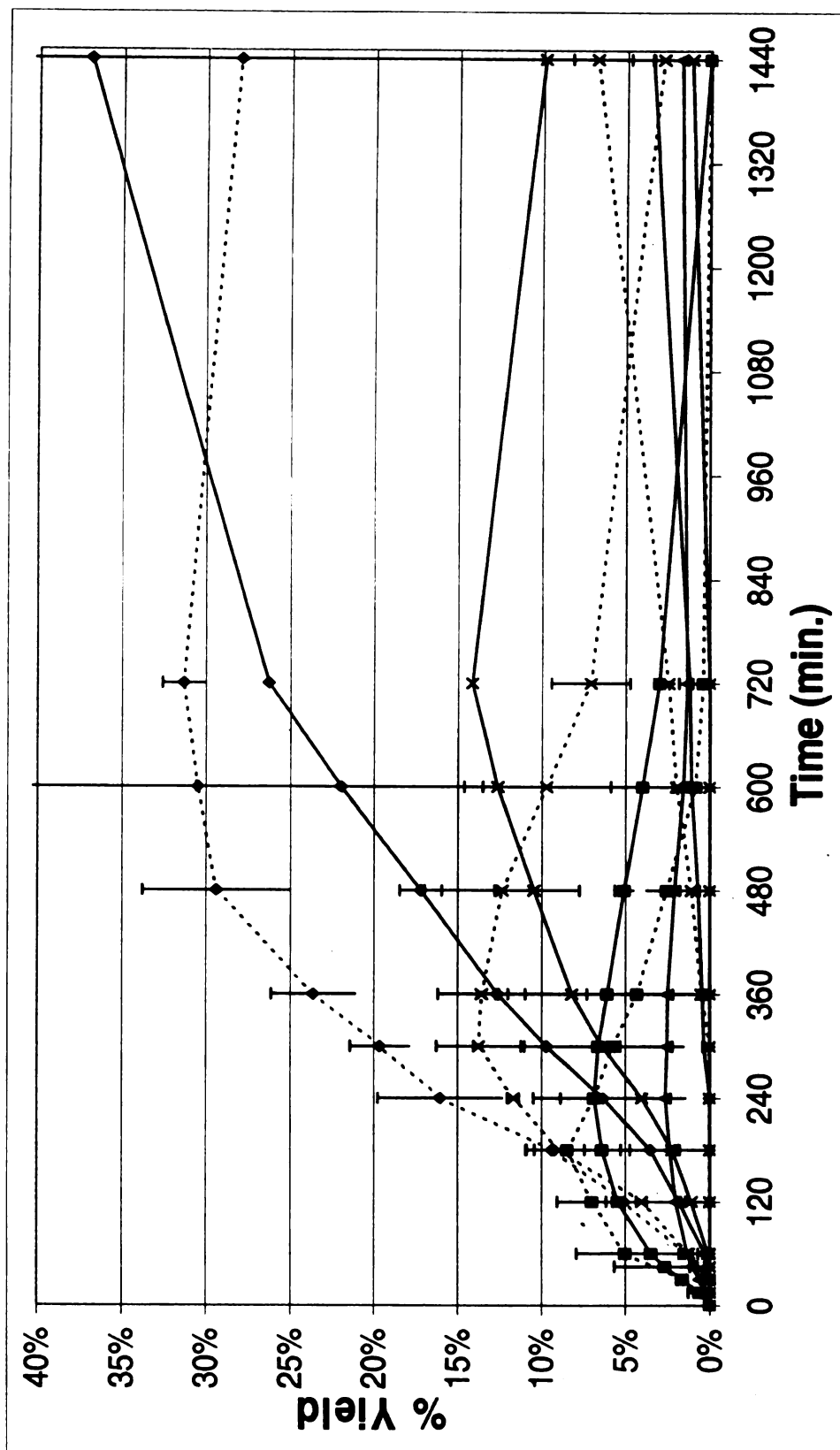


Figure 3.12 Effect of temperature on % yield at 1800 psi H<sub>2</sub>, 3 g 5% Ru/C

Results are expressed as the average of quadruplicate (90°C) and duplicate (110°C) and measurements; Error bars correspond to  $\pm 1$  SD. Error bars not observed are smaller than the symbols.

piperazine (◆), piperazine-2-one (■), glycylglycine (x), ethanolamine (▲); 110°C(-----), 90°C(——)

### 3.3.3 Control Experiments

A series of control experiments was conducted to help verify intermediate product formation, and the dependence of this process on either hydrogen or Ru catalyst (Figure 3.13). Control experiments were run under either of the following conditions; no catalyst or no hydrogen, and using either glycylglycine, piperazine-2-one, normally intermediates, or piperazine as the starting substrate.

In the absence of either hydrogen or Ru catalyst, 2,5-piperazinedione underwent hydrolysis to 2.5% glycylglycine at (1000 psi H<sub>2</sub>, 110°C, 0 g 5% Ru/C) or (1000 psi He, 110°C, 1 g 5% Ru/C) at six hrs. Glycylglycine was the only product formed under each of these conditions. In both cases, 2,5-piperazinedione conversion averaged 20% and overall material balances were >80%.

Control experiments with glycylglycine (1000 psi H<sub>2</sub>, 110°C, 1 g 5% Ru/C) showed hydrolysis to glycine (4% yield), and 8% ethanolamine at six hrs. The conversion of glycylglycine at six hrs was 43%, and the overall material balance was 68%. When the catalyst loading was increased to 3 g 5% Ru/C, glycine and ethanolamine formed at the same rate, with equal yields (12%) at six hrs. The overall glycylglycine conversion was 78%, and reaction material balance was 48%. The formation of ethanolamine is surprising, since acidic conditions are favored for the hydrogenation of amino acids. The pH was monitored over the course of the reactions, starting at 7 and increasing to pH 8.0 or 9.0 at 6 hrs for 1 and 3 g 5% Ru/C, respectively.

Piperazine was run under hydrogenation conditions of 1000 psi H<sub>2</sub>, 110°C, 1 and 3 g 5% Ru/C. No reaction products were detected with 1 g catalyst loading. However, 24% conversion was found, and an overall material balance of 78%. At increased loading, 3 g 5% Ru/C, ethylenediamine (no yield reported) was the only product detected



at six hrs Piperazine conversion was 35%, and overall material balance was 65%. The pH remained constant (pH 11) in both cases.

When piperazine-2-one was reacted under hydrogenation conditions, 1000 psi H<sub>2</sub>, 110°C, 1 g 5% Ru/C, the only products detected were 20.7 % yield piperazine and 8.9 % N-(2-aminoethyl)glycine at six hrs Piperazine-2-one conversion at six hrs was 56%, and overall material balance was 78%. The hydrolysis of piperazine-2-one to N-(2-aminoethyl)glycine was detected in the control experiments only when using piperazine-2-one as the starting material. The pH steadily increased from 8-10 over six hrs.

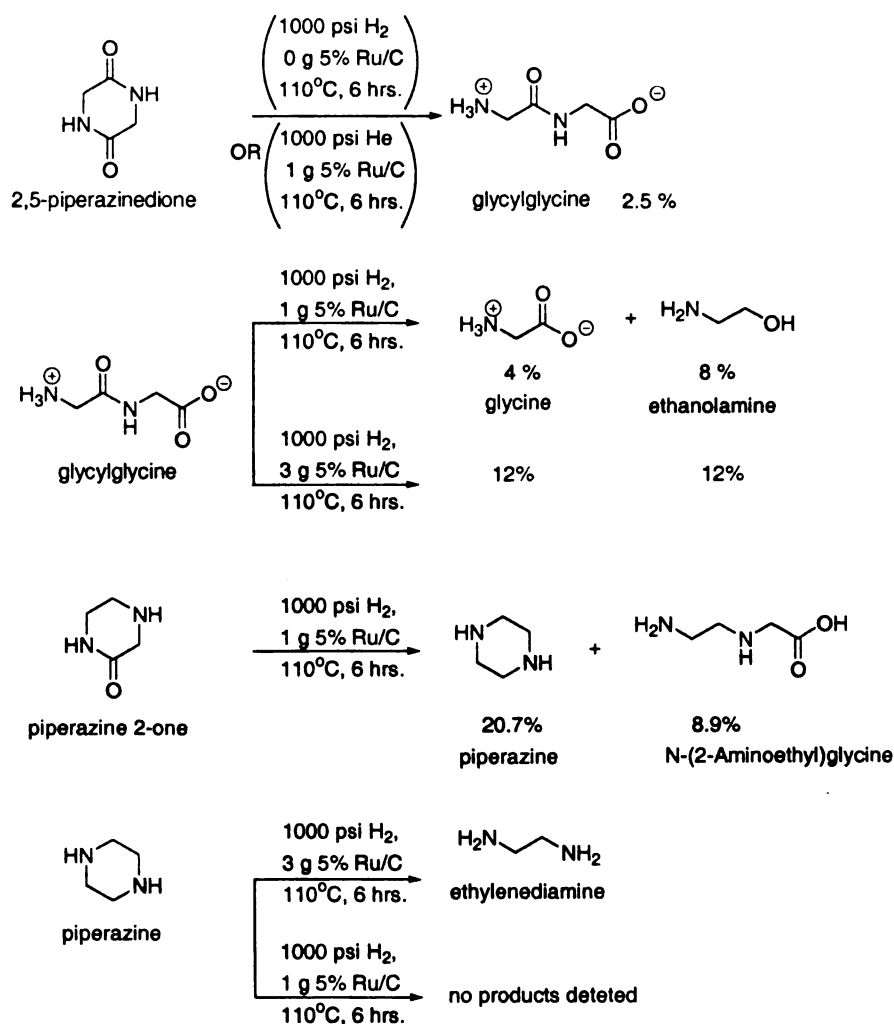


Figure 3.13 Product formation from control experiments

Gas chromatographic analysis of reactions run at optimal conditions did not detect low molecular weight volatiles ( $\text{CH}_4$ ,  $\text{NH}_3$ , etc.). The pH was monitored over the course of all reactions. The evolution of piperazine formation from 2,5-piperazinedione by the increase of pH from 7 to 11, at 1800 psi,  $90^\circ\text{C}$ , 3g Ru/C is shown in Figure 3.14.

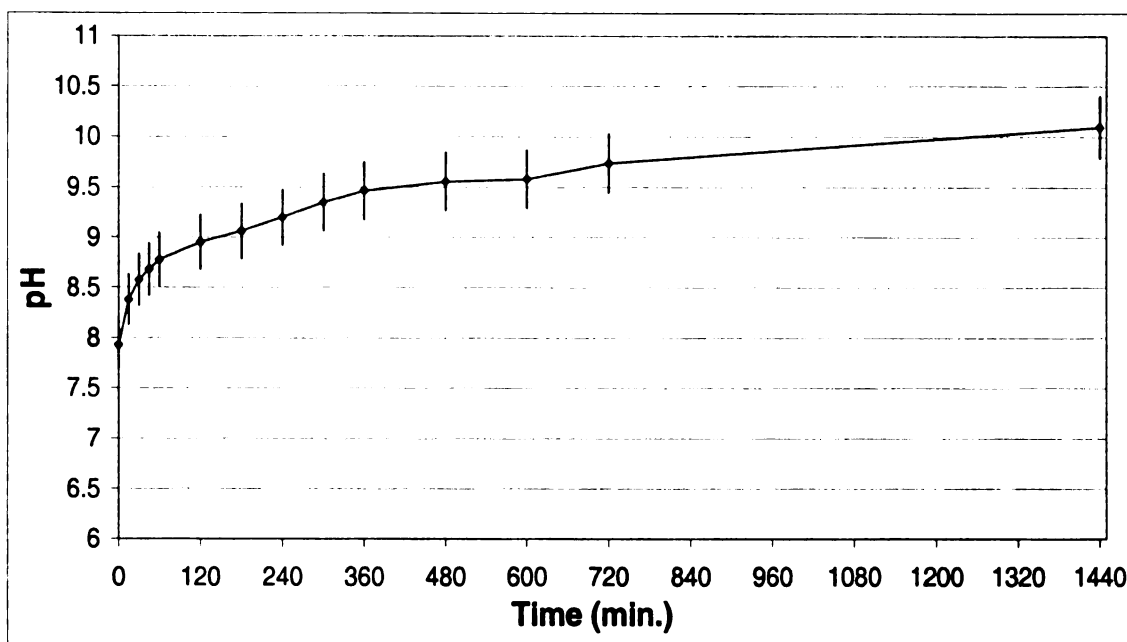


Figure 3.14 Change of pH over time from the conversion of 2,5-piperazinedione to piperazine at 1800 psi,  $90^\circ\text{C}$ , 3g 5% Ru/C

Results are given as the average of triplicate experiments; Error bars correspond to  $\pm$  SD.

#### 3.3.1.4. Preliminary Studies on the Effect of Carbon Support

It is necessary to point out that the overall material balance was not closed. In all the experiments carried out, the initial concentration of the starting material (2,5-piperazinedione, glycylglycine, piperazine-2-one or piperazine) decreased at time zero ( $t=0$ ), or in other words, the nominal % conversion increased. Between the initial recording and  $t=0$ , the reactor was charged with the substrate and heated to the desired

temperature, at which time hydrogen was introduced. It is likely that during this time the substrate adsorbed to the carbon support.

The observed concentration decrease, (or conversion increase), of 2,5-piperazinedione at  $t=0$ , changed with catalyst loading. The conversion at  $t=0$ , for 2,5-piperazinedione (0.1M) is <1 (0.3g Ru/C), 25 (1.0 g Ru/C), and 40% (3.0 g Ru/C) at 1500 psi  $H_2$ , 130°C. At increased catalyst loading (6.0 g Ru/C), the conversion of 2,5-piperazinedione (0.1M) is 40%, at 1500 psi  $H_2$ , 110°C. Figures 3.15 and 3.16 show 2,5-piperazinedione conversion over time of at the different catalyst loadings. At  $t=0$ , the three catalyst loadings increase the apparent initial conversion by 25 and 41%, when ultimately no reaction has yet taken place; thus, % conversion should equal zero.

In Figure 3.16 the level of substrate loading can be compared with catalyst loading. Even when twice the amount of substrate is charged, with equal amount of catalyst, % conversion at  $t=0$  differs by 15%. At equal substrate loading, with 3 and 6 g 5% Ru/C, % conversion at  $t=0$  is practically equal. This suggests that if 2,5-piperazinedione is adsorbing to C, it may be a fully saturated with 3 g 5% Ru/C.

From the control experiments, <1 and 11% conversion at  $t=0$ , was noticed for glycylglycine with 1 and 3 g 5% Ru/C, respectively. At  $t=0$ , % conversion for piperazine-2-one was 18%, and piperazine was 12 and 30% with 1 g and 3 g 5% Ru/C, respectively.

Figure 3.15 The effect of catalyst loading on initial % conversion of 2,5-piperazinedione at 1500 psi H<sub>2</sub>, 130°C, with 0.3, 1, and 3 g 5% Ru/C

Results for catalyst loadings of 1 g Ru/C are expressed at the average of triplicate measurements, and catalyst loadings of 3 g 5% Ru/C are the average of quadruplicate measurements; Error bars correspond to  $\pm 1$  SD. (Catalyst loading of 0.3 g 5% Ru/C, n=1)

0.3 g (—◆—), 1 g (—■—), and 3 g (—▲—) 5% Ru/C

Figure 3.16 The effect of catalyst loading on initial % conversion of 2,5-piperazinedione (0.1 and 0.05M) at 1500 psi H<sub>2</sub>, 110°C, with 3 and 6 g 5% Ru/C

Results for catalyst loadings of 1500 psi H<sub>2</sub>, 110°C, and 3 g 5% Ru/C at 0.1M substrate loading are expressed at the average of quadruplicate measurements; Error bars correspond to  $\pm 1$  SD. (Catalyst loading with 6 g 5% Ru/C with 0.1M substrate loading, n=1, and 3 g 5% Ru/C with 0.05M substrate loading, n=1)

0.3 g 5% Ru/C with 0.1M substrate loading (—◆—), 6 g 5% Ru/C with 0.1M substrate loading (—■—), and 3 g 5% Ru/C with 0.05M substrate loading (—▲—)

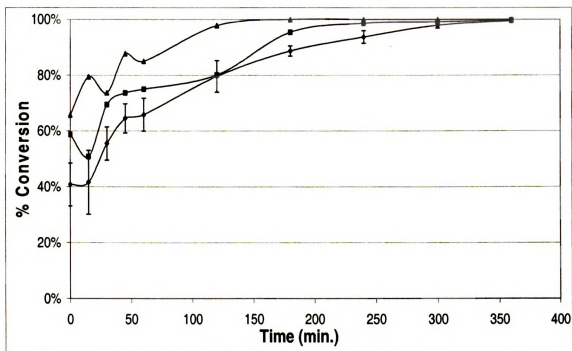
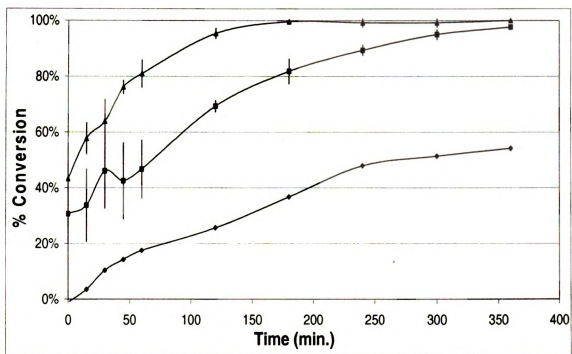


Figure 3.16



From these observations, it was necessary to determine if the starting material, 2,5-piperazinedione, or any of the intermediate products is absorbed within the pore structure of the activated carbon. A series of absorption/desorption experiments were carried out with 2,5-piperazinedione and piperazine.

Under reaction conditions (1800 psi H<sub>2</sub>, 90°C, 3 g 5% Ru/C) 2,5-piperazinedione, on average % conversion at t=0 was 40%. A typical experiment was carried out, with samples only taken at t=0 and t=24 hrs. No starting material recovered from desorption washes, but an additional 0.01 glycine, 0.04 glycyglycine, 0.01 ethanolamine, and 0.90 mmol piperazine were recovered. This increases the overall piperazine yield 10%. Bench top control experiments with equal mixtures of 2,5-piperazinedione and piperazine (0.05M each) with 0.75 g 5% Ru/C (unreduced) was equilibrated overnight at room temperature. Approximately 50% of each absorbed onto the carbon support at equilibrium. Desorption washes recovered 84% 2,5-piperazinedione and 74% piperazine. Individual studies on the remaining compounds were not carried out, but are suggested. Detailed studies on the effect of the carbon support, and perhaps the comparison of other supports for each of the compounds studied in this study should also be carried out. The question of how much trapped material continues to react is undetermined, and supports future research for this portion of the study.

#### *3.3.4 Reaction pathways for 2,5-piperazinedione hydrogenation to piperazine*

Previous studies suggest that amides simply hydrolyze under aqueous conditions,<sup>7</sup> and that the equilibrium between glycyglycine and 2,5-piperazinedione is shifted toward the latter at high temperatures.<sup>36</sup> We have found through a rigorous, systematic study, that 2,5-piperazinedione can be reduced under aqueous catalytic hydrogenation

conditions. It is important to point that, that the reduction of an amide has been achieved under relatively mild and more importantly '*green*' working conditions. The results from this study complement and in some cases may even replace the existing classical approach of amide reductions using organic solvents and costly metal hydrides.

From our results, we observed both hydrolysis and hydrogenation products of 2,5-piperazinedione. In order to understand this competing reaction sequence we must first understand the mechanism. Our results confirm hydrolysis of both 2,5-piperazinedione and glycylglycine under aqueous conditions. In the absence of hydrogen (1000 psi He), at 110°C with 1 g 5% Ru/C, hydrolysis of 2,5-piperazinedione to 20% glycylglycine was detected at 6hrs. At 1000 psi H<sub>2</sub>, 110°C in the absence of catalyst, 20% glycylglycine was the only product detected at six hrs This verifies that the ruthenium catalyst is essential for hydrogenation. This conclusion is also supported by the results found when comparing different levels of catalyst loading.

The level of hydrogen pressure also plays a critical role, with increased hydrogen pressures favoring hydrogenation over hydrolysis, presumably due to increasing hydrogen concentration in aqueous media at increased pressures.<sup>37</sup> At the lower hydrogen pressures, hydrolysis was the primary reaction.

Temperature was also found to play a role in the rate and stability of piperazine formed. At elevated temperature (110°C) the yield of piperazine decreased (See Figure 3.13) and ethylenediamine was detected (no yield recorded). From the control experiments, the cleavage of piperazine to ethylenediamine was the only product detected. The formation of ethylenediamine was observed in previous studies in our laboratory.<sup>32</sup>



In order to gain insight in the mechanism of the hydrogenation of 2,5-piperazinedione, hydrogenation of several amides was modeled via ab initio methods in both gas phase and solution; results are summarized in Figure 3.17. As expected, hydrogenation is more favored in solution. The initial hydrogenation step is slightly harder for amides than acids, but the second step is more favorable for amides than for the corresponding acid. Cyclic piperazinedione was only slightly easier to hydrogenate than the acyclic amide. The dehydration of secondary acyclic amides is favored over C-N cleavage (+6.7 versus +13.1 kcal/mol) to the aldehyde.

The cyclic anhydride, 2,5-piperazinedione, undergoes hydrogenation to piperazine via a route that is shown in Figure 3.18. The formation of piperazine-2-one is believed to be by a Schiff base intermediate which can either undergo hydrogenation further to the final product, piperazine, or hydrolyze to form N-(2-aminoethyl)glycine. The hydrolysis product of piperazine-2-one was not detected over the course of the reaction, but only in the control experiments. It is possible that further C-N hydrolysis of N-(2-aminoethyl)glycine may lead to the trace amount of the ethanolamine detected. It is still undetermined at this point.

Figure 3.19 shows the proposed hydrolysis of 2,5-piperazine to glycylglycine, which can further cleave to glycine. Glycylaminoethanol, N-(2-aminoethyl)glycine and N-(2-aminoethyl)-ethanolamine were not formed at all over the series of reactions carried out.

The result of changes in initial conversion of the starting material at  $t=0$ , may be attributed to the overall low material balance. It is possible the starting material, or intermediate compounds are absorbing in the activated carbon catalyst support. Further

quantitative investigation of each products absorption to the carbon support is necessary to determine exactly how much of the material is adsorbed, and whether adsorbed material remains accessible for reaction. These assessments of overall material availability during the reaction may help solidify the correct mechanistic picture for the formation of piperazine.



### Figure 3.17 Modeling of proposed mechanism for amide hydrogenation in gas phase and in solution

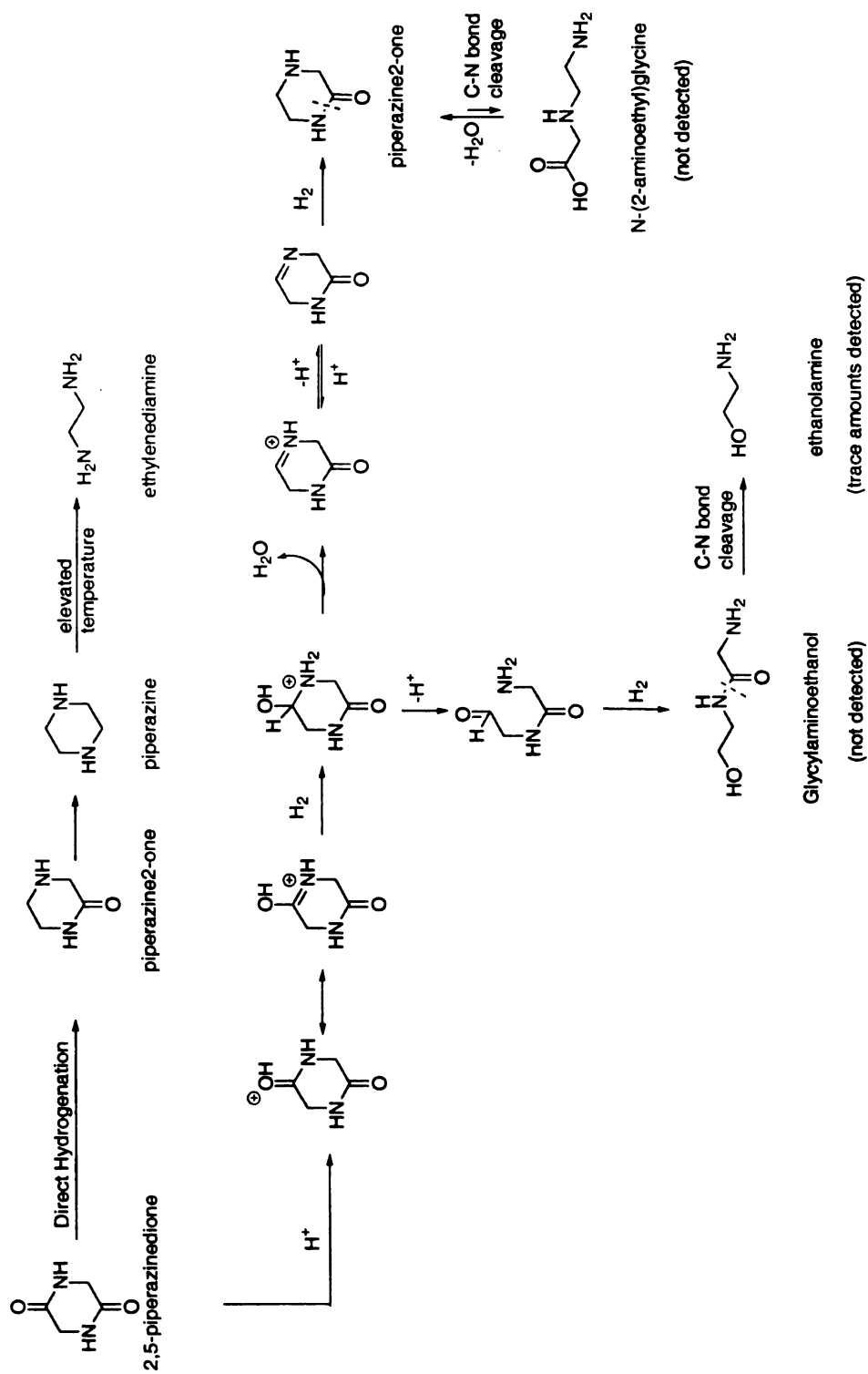


Figure 3.18 Predicted reaction pathways for hydrogenation of 2,5-piperazinedione



## CHAPTER FOUR

### SUMMARY AND CONCLUSIONS

Optimized operating conditions for the hydrogenation of 2,5-piperazinedione to piperazine have been established. Experimental conditions at 1800 psi H<sub>2</sub>, 90°C and 3 g catalyst (5% Ru/C) loading have been found to give the highest piperazine yield, 37%, at 24 hrs. Not only are the hydrogenation product yields of higher than that of hydrolysis, the reaction was completed under '*green*' conditions. One of biggest challenges in this study is overcoming the competing hydrolysis reaction. It has been shown that the hydrogenation takes place as the primary reaction with the formation of the intermediate piperazine-2-one before the hydrolysis product glycylglycine. With the optimized conditions established, a more detailed mechanistic study can be completed.

It is important to note that optimization of the analytical methods continued throughout the course of the hydrogenation experiments. Careful evaluation of the analytical results concluded that all data are, in fact, valid for the hydrogenation experiments. This is based on the use of one single calibration method created and used for all of the data interpretations. More importantly, a portion of the actual substrate charged into the reactor was saved and used for all calculations of the parametric study. Having this "control" sample and accounting for the stability of the desired product, piperazine, all conclusions remain as stated.

## **CHAPTER FIVE**

### **FUTURE RESEARCH**

Some suggestions for future research are listed below:

1. Optimized conditions for the reduction of the cyclic glycine anhydride have been established. These conditions should now be carried out on linear peptides (e.g. glycylglycine, alanylalanine, glycylalanine etc.)
2. Ruthenium catalyst was supplied in its pre-reduced form and needed to be fully reduced (14-16hrs.) before running actual experiments. A brief study on the effect of catalyst reduction time should be carried out in order to make research time more efficient.
3. Only heterogeneous ruthenium catalyst was used for this study. A survey of other metal catalysts (e.g. Re, Rh, Ni, Mo, Pd, Cu) should be sought out (heterogeneous and homogeneous). In addition, synergistic metal effects should be explored.
4. Activated carbon support was used in this study for the metal catalyst. This support was found superior for the catalytic hydrogenation of carboxylic acids in our laboratory. However, initial concentration of the starting material was found to decrease before the reaction conditions started. In addition, overall material balances were not closed. Absorption studies of each of the compounds involved in the reaction should be carried out on the activated carbons. A survey of catalyst supports may also be beneficial and help close the material balance.

5. Continued analytical method development for linear peptides should be carried out for immediate qualitative and quantitative product analysis.



## LIST OF REFERENCES

1. Challis, B. C.; Challis, J. A., *The Chemistry of Amides*. Interscience: New York, 1970; p 731-857.
2. Gaylord, N. G., *Reduction with Complex Metal Hydrides*. Intersciences Publishers, Inc.: New York, 1956; p 544-642.
3. Brown, H. C.; Heim, P., Selective Reductions. 18. Fast Reaction Of Primary, Secondary, And Tertiary Amides With Diborane - Simple, Convenient Procedure For Conversion Of Amides To Corresponding Amines. *Journal Of Organic Chemistry* **1973**, 38, (5), 912-916.
4. Wojcik, B.; Adkins, H., Catalytic hydrogenation of amides to amines. *Journal Of The American Chemical Society* **1934**, 56, (7), 2419-2424.
5. Oeda, H., Catalytic hydrogenation of amides of alpha-hydroxy acids. *Bulletin of the Chemical Society of Japan* **1937**, (12), 121-127.
6. Winans, C. F.; Homer Adkins, Alkylation of Amines as Catalyzed by Nickel. *Journal of the American Chemical Society* **1932**, (54), 306-312.
7. Zabicky, J., *The Chemistry of Amides*. Interscience: New York, 1970.
8. Newman, M. S.; Fukunaga, T., The Reduction Of Amides To Amines Via Nitriles By Lithium Aluminum Hydride. *Journal Of The American Chemical Society* **1960**, 82, (3), 693-696.
9. Brown, H. C.; Heim, P., Diborane As Mild Reducing Agent For Conversion Of Primary Secondary + Tertiary Amides Into Corresponding Amines. *Journal Of The American Chemical Society* **1964**, 86, (17), 3566-&.
10. Kornet, M. J.; Thio, P. A.; Tan, S. I., Borane Reduction Of Amido Esters. *Journal Of Organic Chemistry* **1968**, 33, (9), 3637-&.
11. Umino, N.; Iwakuma, T.; Nobuo Itoh, Sodium Acyloxyborohydride as New Reducing Agents. I. Reduction of Carboxamides to the corresponding Amines. *Tetrahedron Letters* **1976**, (10), 763-766.
12. Zhu, H.-J.; Lu, K.-T.; Sun, G.-R.; He, J.-B.; Li, H.-Q.; Charles U. Pittman, J., Reduction of Amides with NaBH<sub>4</sub> in diglyme at 162C. *New J Chem* **2003**, 27, 409-413.
13. Wann, S. R.; Thorsen, P. T.; Kreevoy, M. M., Reduction Of Carboxylic-Acid Derivatives By Bh<sub>4</sub>- In Acidic Dimethylsulfoxide. *Journal Of Organic Chemistry* **1981**, 46, (12), 2579-2581.

14. Kuehne, M. E.; Shannon, P. J., Reduction Of Amides And Lactams To Amines By Reactions With Phosphorus Oxychloride And Sodium-Borohydride. *Journal Of Organic Chemistry* **1977**, 42, (12), 2082-2087.
15. Satoh, T.; Suzuki, S.; Suzuki, Y.; Miyaji, Y.; Imai, Z., Reduction Of Organic Compounds With Sodium Borohydride-Transition Metal Salt Systems.1. Reduction Of Organic Nitrile, Nitro And Amide Compounds To Primary Amines. *Tetrahedron Letters* **1969**, (52), 4555-&.
16. Raucher, S.; Klein, P., A Convenient Method For The Selective Reduction Of Amides To Amines. *Tetrahedron Letters* **1980**, 21, (42), 4061-4064.
17. Borch, R. F., A New Method for the Reduction of Secondary and Tertiary Amides. *Tetrahedron Letters* **1968**, (1), 61-65.
18. Rahman, A.; Basha, A.; Waheed, N.; Ahmed, S., New Method For Reduction Of Amides To Amines With Sodium-Borohydride. *Tetrahedron Letters* **1976**, (3), 219-222.
19. Kornfeld, E. C., Raney Nickel Hydrogenolysis Of Thioamides - A New Amine Synthesis. *Journal Of Organic Chemistry* **1951**, 16, (1), 131-138.
20. Bazant V; Capka M; Cerny M; Chvalovsky V; Kochloefl K; Kraus M; Malek J, Properties of Sodium-bis-(2-methoxyethoxy)aluminiumhydride. I. Reduction of some Organic Functional Groups. *Tetrahedron Letters* **1968**, (29), 3303-3306.
21. Bhandari, K.; Sharma, V. L.; Chatterjee, S. K., A convenient method for the reduction of amides to their corresponding amines. *Division of process development, Central Drug Research Institute, India* **1990**.
22. Adkins, H.; Wojcik, B., Hydrogenation of amides to amines. *Journal Of The American Chemical Society* **1934**, 56, 247-247.
23. D'Ianni, J. D.; Homer Adkins, Hydrogenation of Hydroxyamides. *Journal of the American Chemical Society* **1939**, (61), 1675-1681.
24. Schneider, H. J.; Adkins, H.; McElvain, S. M., The Hydrogenation Of Amides And Ammonium Salts - The Transalkylation Of Tertiary Amines. *Journal of the American Chemical Society* **1952**, 74, (17), 4287-4290.
25. Sauer, J. C.; Adkins, H., The selective hydrogenation of substituted amides. *Journal Of The American Chemical Society* **1938**, 60, 402-406.
26. Schwoegler, E. J.; Homer Adkins, Preparation of Certain Amines. *Journal of the American Chemical Society* **1939**, (61), 3499-3502.

27. Hirosawa, C.; Wakasa, N.; Fuchikami, T., Hydrogenation of amides by the use of bimetallic catalysts consisting of Group 8 to 10, and Group 6 or 7 metals. *Tetrahedron Letters* **1996**, 37, (37), 6749-6752.
28. Kuwano, R.; Takahashi, M.; Ito, Y., Reduction of amides to amines via catalytic hydrosilylation by a rhodium complex. *Tetrahedron Letters* **1998**, 39, (9), 1017-1020.
29. Igarashi, M.; Fuchikami, T., Transition-metal complex-catalyzed reduction of amides with hydrosilanes: a facile transformation of amides to amines. *Tetrahedron Letters* **2001**, 42, (10), 1945-1947.
30. Jere, F.; Jackson, J.; Miller, D. J., Kinetics of the Aqueous-Phase Hydrogenation of L-Alanine to L-Alaninol. *Industrial Engineering and Chemical Research* **2004**, 43, 3297-3303.
31. Jere, F. T.; Miller, D. J.; Jackson, J. E., Stereoretentive C-H bond activation in the aqueous phase catalytic hydrogenation of amino acids to amino alcohols. *Organic Letters* **2003**, 5, (4), 527-530.
32. Redko, M., Unpublished results. *Michigan State University* **2004-2005**.
33. Steinberg, S.; Bada, J. L., Diketopiperazine Formation During Investigations Of Amino-Acid Racemization In Dipeptides. *Science* **1981**, 213, (4507), 544-545.
34. Steinberg, S. M.; Bada, J. L., Peptide Decomposition In The Neutral Ph-Region Via The Formation Of Diketopiperazines. *Journal Of Organic Chemistry* **1983**, 48, (13), 2295-2298.
35. Radzicka, A.; Wolfenden, R., Rates of uncatalyzed peptide bond hydrolysis in neutral solution and the transition state affinities of proteases. *Journal Of The American Chemical Society* **1996**, 118, (26), 6105-6109.
36. Li, J.; Brill, T. B., Spectroscopy of hydrothermal reactions. 27. Simultaneous determination of hydrolysis rate constants of glycylglycine to glycine and glycylglycine-diketopiperazine equilibrium constants at 310-330 degrees C and 275 bar. *Journal Of Physical Chemistry A* **2003**, 107, (41), 8575-8577.
37. Zhang, Z. G.; Jackson, J. E.; Miller, D. J., Aqueous-phase hydrogenation of lactic acid to propylene glycol. *Applied Catalysis A-General* **2001**, 219, (1-2), 89-98.

MICHIGAN STATE UNIVERSITY LIBRARIES



3 1293 02845 2872